TTI: 0-7064

Texas A&M Transportation Institute

Thick-Lift Paving with Tamper Bar Pavers

Technical Report 0-7064-R1

Cooperative Research Program

TEXAS A&M TRANSPORTATION INSTITUTE
COLLEGE STATION, TEXAS

sponsored by the
Federal Highway Administration and the
Texas Department of Transportation
https://tti.tamu.edu/documents/0-7064-R1.pdf

Technical Report Documentation Page

1. Report No.	2. Government Accession No.	3. Recipient's Catalog No.
FHWA/TX-23/0-7064-R1		

4. Title and Subtitle	5. Report Date
Thick-Lift Paving with Tamper Bar Pavers	Published: November 2022
	6. Performing Organization Code

7. Author(s)	8. Performing Organization Report No.
Bryan Wilson, Moises Saca, and Darlene Goehl	Report 0-7064-R1

9. Performing Organization Name and Address	10. Work Unit No. (TRAIS)
Texas A&M Transportation Institute The Texas A&M University System College Station, Texas 77843-3135	11. Contract or Grant No. Project 0-7064

12. Sponsoring Agency Name and Address	13. Type of Report and Period Covered
Texas Department of Transportation Research and Technology Implementation Office 125 E. 11th Street Austin, Texas 78701-2483	Technical Report: September 2020 to August 2022
	14. Sponsoring Agency Code

15. Supplementary Notes

Project sponsored by the Texas Department of Transportation and the Federal Highway Administration.
Project Title: Use of Tamper Bar Paver to Place Thick Lift Asphalt Concrete Pavement
URL: https://tti.tamu.edu/documents/0-7064-R1.pdf

16. Abstract

This research studied thick-lift asphalt concrete construction using a tamper bar paver. Tamper bar pavers were deployed on three paving projects to place asphalt layers ranging from 6 to 10 inches thick. On each project, test sections were constructed in one and two lifts, evaluating different lift thicknesses, paver screed settings, and rolling patterns. The research team monitored the mat cooldown time; measured mat density throughout compaction; tested the mat after construction with a rolling density meter, 3D Radar, and an inertial roughness profiler; and sampled 172 cores for laboratory testing of air voids and air void uniformity.

The cooldown time of the mat increased by 0.7 hours per additional inch of thickness. Overall mat compaction was acceptable for all test sections. Additional roller passes had the biggest effect on air voids but with diminishing returns. Construction in two lifts produced higher air voids because the bond interface itself had high air voids. Thicker lifts, when compared to the mixture nominal maximum aggregate size, increased the air voids. Thicker lifts also increased vertical segregation, but a single thick lift was still more uniform than two lifts of the same total thickness. The effect of the tamper bar screed itself was not significant, though there were several confounding variables interfering with the analysis. Pavement roughness was expected to increase when placed in a single lift, but the analysis was inconclusive.

Guidelines for thick-lift paving were developed. They provide scenarios for when thick-lift paving is appropriate and give recommendations for paving equipment, compaction practices, concerns about opening to traffic, and managing ride quality.

17. Key Words	18. Distribution Statement
thick-lift, tamper bar paver, tamper bar screed, high-compaction screed, asphaltic concrete, lift thickness, paving, density, air void, roughness	No restrictions. This document is available to the public through NTIS: National Technical Information Service Alexandria, Virginia https://www.ntis.gov

19. Security Classif. (of this report)	20. Security Classif. (of this page)	21. No. of Pages	22. Price
Unclassified	Unclassified	126	

Form DOT F 1700.7 (8-72) Reproduction of completed page authorized

Thick-Lift Paving with Tamper Bar Pavers

by

Bryan Wilson
Associate Research Engineer
Texas A&M Transportation Institute

Moises Saca
Graduate Assistant - Research
Texas A&M Transportation Institute

and

Darlene Goehl
Research Engineer
Texas A&M Transportation Institute

Report 0-7064-R1
Project 0-7064
Project Title: Use of Tamper Bar Paver to Place Thick Lift Asphalt Concrete Pavement

Sponsored by the
Texas Department of Transportation
and the
Federal Highway Administration

Published: November 2022

TEXAS A&M TRANSPORTATION INSTITUTE
College Station, Texas 77843-3135

DISCLAIMER

This research was sponsored by the Texas Department of Transportation (TxDOT) and the Federal Highway Administration (FHWA). The contents of this report reflect the views of the authors, who are responsible for the facts and the accuracy of the data presented herein. The contents do not necessarily reflect the official view or policies of FHWA or TxDOT. This report does not constitute a standard, specification, or regulation.

This report is not intended for construction, bidding, or permit purposes. The engineer in charge of the project was Bryan Wilson, P.E. #126948.

The United States Government and the State of Texas do not endorse products or manufacturers. Trade or manufacturers' names appear herein solely because they are considered essential to the object of this report.

ACKNOWLEDGMENTS

This project was sponsored by TxDOT and FHWA. The authors thank the project manager, Tom Schwerdt, and the project monitoring committee, Ray Brady, Travis Patton, Ryan Barborak, Enad Mahmoud, and Kevin Plumlee. The authors also thank the personnel that helped coordinate, provide equipment for, and construct the test sections. From TxDOT, these were Will Buskell, Shane Cunningham, Shannon Ramos, Jennifer Vorster, and Roger Horst. The contractors were Madden Construction LLC, Reynold's Asphalt Co., and Mario-Sinacola & Sons. Equipment manufacturers and vendors were Kirby-Smith Machinery, Wirtgen Group-Vögele, and Caterpillar Inc. Several Texas A&M Transportation Institute (TTI) employees helped collect data, sample pavement cores, and perform laboratory testing: Jason Huddleston, Lee Gustavus, Wenting Liu, Tony Barbosa, Poura Arabali, and Camilo Jurado.

TABLE OF CONTENTS

LIST OF FIGURES

Page

LIST OF TABLES

Page

CHAPTER 1:
INTRODUCTION

The lift thickness when placing asphalt concrete can have a significant influence on constructability and on the final quality of the pavement layer. As such, the Texas Department of Transportation (TxDOT) has minimum and maximum allowable lift thicknesses for different mixture types and design gradations, which are closely related to the nominal maximum aggregate size (NMAS) of the mixture. The minimum lift thickness is typically 3 times the NMAS, and in Texas, the maximum lift thickness is approximately 4 to 5 times the NMAS (Table 1).

Table 1. TxDOT Maximum Allowable Lift Thickness.

Item Number	Item Title	Mixture Type	Nominal Maximum Aggregate Size (inch)	Maximum Allowed Lift Thickness (inch)	Thickness/ NMAS Ratio
340/341	Dense-graded	A	1.5	6	4.0
		B	1	5	5.0
		C	0.75	4	5.3
344	Superpave	A	1.5	5	3.3
		B	1	4	4.0
		C	0.75	3	4.0

Thick-lift paving is the placement of asphalt concrete in a lift greater than the allowable maximum. For example, the Superpave (SP) Type B mixture in Figure 1 is placed at 10 inches thick, more than twice the allowable 4 inches. With thick-lift paving, a contractor can construct a thick design layer in a single lift instead of two or three separate lifts. This approach can provide the following benefits:

- Streamlines paving operations.
- Eliminates bond interface that could be a potential weak point.
- Saves money by eliminating the mid-layer tack coat.

Still, there are several unique challenges and concerns with thick-lift paving:

- Potential for inadequate and non-uniform compaction.
- Potential for lower ride quality.
- Long cooldown times.
- More critical timing of mix delivery.

Figure 1. Thick-Lift Paving.

A tamper bar paver (i.e., a paver equipped with a tamper bar screed), might address issues of poor compaction and ride quality. Tamper bar screeds are designed to provide greater compaction behind the paver than a typical vibratory screed. Improving initial laydown compaction might improve overall compaction uniformity and reduce roughness introduced by excessive roll-down of the uncompacted mat. Prior to this research, a contractor in the Atlanta District experimented with using a tamper bar paver by placing thick-lifts of SP Type C mixture at 4 to 6 inches thick. Preliminary findings were positive since cores from the test sections had acceptable compaction. Still, further study of tamper bar pavers for thick-lift construction was warranted.

The purpose of this research, therefore, was to determine whether a tamper bar paver could effectively place asphalt concrete in thick lifts and identify the best practices to do so. The research objectives were:

1) Review the literature about the uses of tamper bar pavers, factors that influence compaction quality, and best practices for thick-lift paving.

2) Construct thick-layer test sections in one and two lifts with a tamper bar paver using different screed settings and rolling patterns. Measure the mat cooldown time, compacted air voids content and uniformity, and pavement profile roughness.

3) Statistically analyze the data.

4) Develop guidelines for thick-lift paving and tamper bar pavers, and propose modifications to existing construction specifications.

CHAPTER 2:
BACKGROUND

OVERVIEW

This chapter contains the findings from a literature review on the following topics:

- Tamper bar pavers.
- Compaction and screed mechanics.
- Influential factors of asphalt mixture compaction.
- Practices for thick-lift asphalt concrete paving.

TAMPER BAR PAVERS

For this research, a tamper bar paver is defined as an asphalt paver equipped with a tamper bar screed. A tamper bar screed will achieve higher compaction than a typical vibratory screed, thus reducing the amount of compaction required by rollers. Alternative names for a tamper bar screed include *compaction screed*, *high-compaction screed,* and *high-density screed*.

A detailed diagram of a tamper bar screed is given in Figure 2. The tamper bar, shown in profile in the figure, is a long metal plate with a beveled edge positioned just in front of the screed plate. Driven by an eccentric shaft, the tamper bar has a 2- to 7-mm vertical stroke which helps feed the head of asphalt mixture under the screed and provides pre-compaction. The model shown here, manufactured by Vögele, also has two pressure bars after the screed that provide additional pre-compaction.

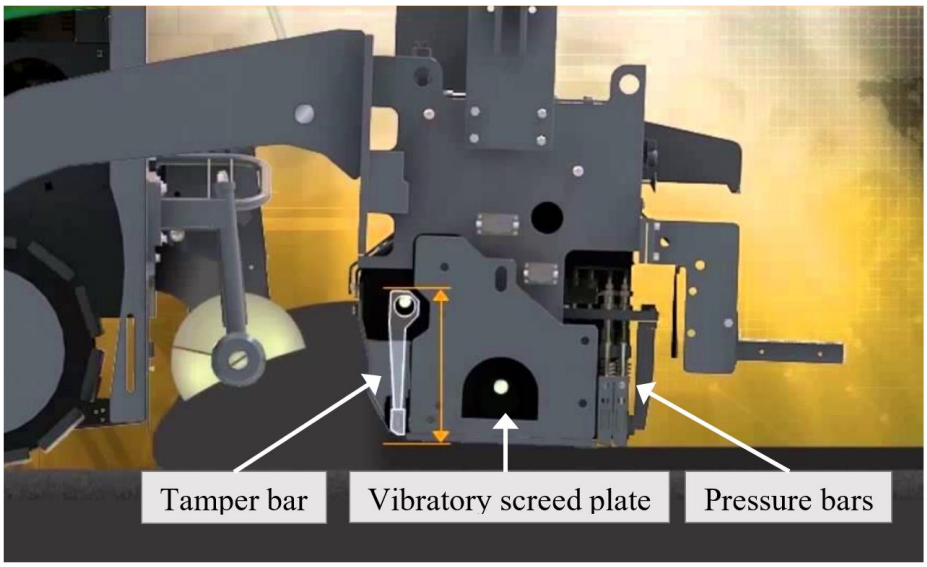

Figure 2. High-Compaction Screed Detail with a Tamper Bar (*1*).

Tamper bar screeds and pavers come in different configurations. The screeds may have one or two tamper bars, zero to two pressure bars, and are integrated with a vibratory or static screed plate. Figure 3 shows three models of tamper bar pavers from Caterpillar, Vögele, and Volvo. These have variable width screeds that can extend from 10 to 30 ft, depending on the model. Variable width screeds can come in front-mount or rear-mount extension designs. Ridged fixed-width screeds are also available though less common.

(a) **(b)**

(c)

Figure 3. Tamper Bar Pavers: (a) Caterpillar, (b) Vögele, and (c) Volvo (*2*–*4*).

Comparison of Screed Types

The International Standard Organization (ISO) provides definitions for construction equipment in a variety of industries. The committee for "road operation machinery and associated equipment" is in the process of revising the definitions for asphalt paver screeds (*5*, *6*). If the changes are accepted, paver screeds would be separated into three categories: vibratory screeds, compaction screeds, and high-compaction screeds. These are compared in Table 2. The categories are distinguished by the presence and number of *compaction devices* built into the screed. Compaction devices are defined here as tamper bars and pressure bars. As previously explained, tamper bars are in front of the screed plate, driven by an eccentric shaft, and have a low to moderate compaction frequency. Pressure bars are hydraulically driven bars after the

screed plate with a high-frequency compaction cycle. What is currently termed a *tamper bar screed* would fall under one of the latter two categories as either a compaction screed or a high-compaction screed.

Table 2. Comparison of Screed Categories (*5, 7, 8*).

Screed Type	Primary Feature (proposed ISO definition)	Weight	Speed	Compaction
Vibratory	Vibratory plate only	Light	35 to 60 fpm	75 to 80%
Compaction	Vibratory plate + One compaction device (typically a tamper bar)	Heavy	15 to 25 fpm	80 to 90%
High-compaction	Vibratory plate + Two or more compaction devices in any combination	Heavy	15 to 25 fpm	> 90%

Applications

Historically, tamper bar screeds were very common but around the 1980's they were replaced with vibratory screed technology (*9, 10*). Vibratory screeds are now the predominant screed choice in North America and Australia. Their lightweight nature makes them more maneuverable and a flexible choice for residential, commercial, and mainline paving. By one account, vibratory screeds generally do not have the weight nor the additional compaction mechanisms for getting adequate density in thick lifts (*5*). Currently, the primary use of tamper bar pavers in North America is for placing roller-compacted concrete (*11, 12*).

Throughout Europe and other developed countries, compaction screeds with tamper bars are the default choice. In Europe, there is a strong incentive to accelerate construction due to very dense population and a roadway network that is less-forgiving to lane closures. Tamper bar pavers allow placement of thicker lifts, multiple lanes, and even different mixture types simultaneously with in-line paving techniques. The heavier, bulkier tamper bar pavers are also used for everyday paving in these countries (*13*). By adjusting the paving speed and screed properties correctly, there is essentially no asphalt lift thickness that cannot be paved.

TxDOT Experience

In 2018, Madden Constructors placed thick single-lift asphalt concrete sections in the Atlanta District using a tamper bar paver (*14*). The mill and inlay project called for 4 inches of SP Type C, and rather than place two 2-inch lifts, the contractor asked to place a single 4-inch lift at no risk to the district. The contractor wanted to save mobilization and traffic closure time, and they also wanted to avoid issues with interface slippage that recently occurred on a similar two-lift project. After demonstrating successful compaction on the first day, the district allowed them to try additional test sections at 5 and 6 inches thick. The results, summarized in Table 3, show that all sections had adequate compaction. This experience was the impetus to fund this research project.

Table 3. Thick-Lift Core Densities.

Core Depth (inch)	Vibratory Passes	Average Density (%)
4	3	93.5
6	3	94.0
5	5	95.8
6	5	95.7

COMPACTION AND SCREED MECHANICS

Compaction is the process by which the volume of air in an asphalt mixture is reduced through external forces. For effective compaction to occur the compaction forces must exceed the forces resisting compaction within the mix (*15*).

Paver screeds are called self-leveling screeds or free-floating screeds. While paving, there is no direct input for the screed height or the mat thickness, but rather the free-floating concept means that the screed height is determined by the equilibrium of the forces acting upon the screed. This screed design helps even out the roughness and bumps in the original surface when placing a new lift. The equilibrium forces are illustrated in Figure 4 and described below:

- **Towing force.** The horizontal force that the tractor exerts on the tow point of the screed as it moves forward. This force is directly related to the speed of the tractor.

- **Resistive force of the head of material.** The force exerted on the screed by the material directly in front of it. This force is directly related to the head (or height) of the material which is itself dependent on other factors like the material feed rate.

- **Weight of the screed.** The vertical force of the weight of the screed, pushing down on the material beneath it. This force remains constant.

- **Frictional force.** The force of friction between the screed plate and the surface of the material being compacted. This force directly opposes the towing force.

- **Resistive vertical force of the material.** The vertical force that the material exerts on the screed as it is being compacted.

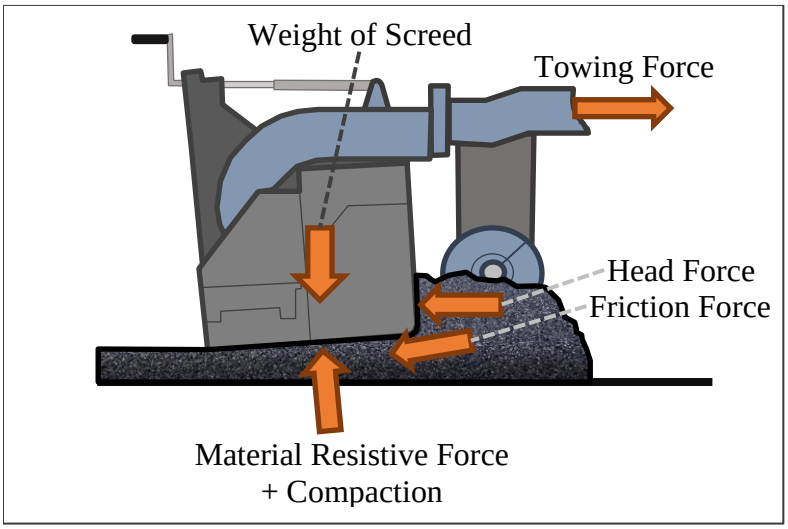

Figure 4. Forces Acting on a Paver Screed.

To change the screed height, the operator will change the angle of the screed (i.e., angle of attack) by adjusting the thickness control screw. This angle will influence the balance of the resistive and frictional forces, thus changing the height at which the forces find equilibrium. Other factors affecting the thickness are the elevation of the tow point, the speed of the paver, and the material feed rate. The tow point elevation changes constantly during paving, and is done so automatically, to keep the angle of attack more consistent despite the up and down vertical movement of the tractor driving over an uneven surface.

Any changes made to adjust the screed height do not take effect immediately. This change will gradually happen over the paving length of at least four times the length of the

towing arm before equilibrium is achieved again (*15–17*). In practice, to ensure a smooth driving experience, any necessary changes in the screed height should be made gradually. The rule of thumb is that a 1-inch change in mat thickness should be achieved over 100 ft of paving.

INFLUENTIAL FACTORS OF ASPHALT MIXTURE COMPACTION

Compaction of asphalt concrete mixture is a critical part of constructing a durable and long-lasting pavement. Better compaction will decrease the air voids content and thus reduce permeability. In this report, the term *air voids content* is shortened to *air voids*. High in-place air voids allow water and air to penetrate into the pavement which can lead to moisture damage, aging, raveling, and cracking (*18*). Several factors affect the final in-place air voids of an asphalt concrete pavement (*19*), including:

- Mixture design.
- Mixture temperature and environmental conditions.
- Construction practices (including lift thickness).
- Supporting layer stiffness.

Mixture Design

The mixture design properties that affect workability are gradation, aggregate properties, asphalt binder content, binder stiffness, and binder additives. The temperature of the mixture is also very important but is discussed in the next section.

Gradation

The mixture gradation, or particle size distribution, is a critical factor in the behavior of the mixture and long-term performance of the in-place pavement material. In this discussion, gradation is defined by the maximum aggregate size, gradation shape, and fines content.

The maximum aggregate size plays a significant role in compactability. All else equal, a mixture with larger aggregates will have higher density (lower air voids) because the aggregate, the densest component in the mixture, will consume a larger percentage of a unit volume. The critical importance of the maximum aggregate size is in its relationship to the constructed lift thickness. This conversation is in the Construction Factors section later in this document.

The particle size distribution plot often includes a theoretical maximum density line (Figure 5). Fine mixtures lie above this line and coarse mixtures below. The closer the gradation is to this line, the higher the density can be achieved (higher compactability). As shown in Figure 6, the finest mixture (i.e., dense-graded [fine]) and coarsest mixture (i.e., gap-graded) had the lowest density after 100 gyrations. Therefore, there is an optimal balance of coarse and fine aggregate to achieve the best compactability. As the amount of coarse aggregate increases, the compaction rate also increases.

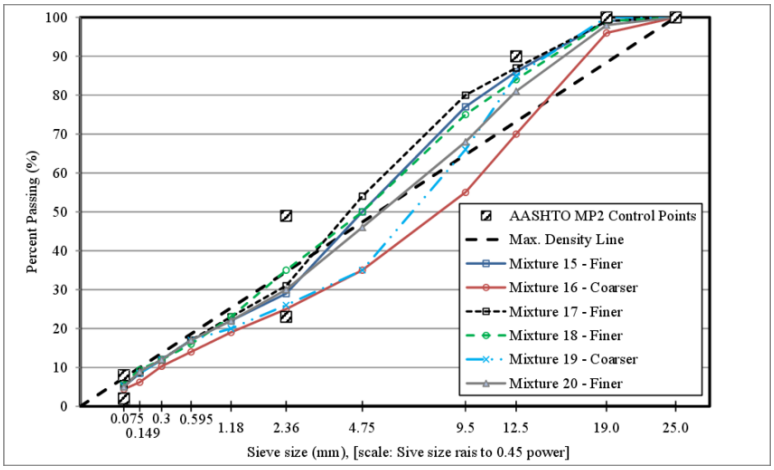

Figure 5. Relationship of Fine and Coarse Mixtures to the Maximum Density Line (*20*).

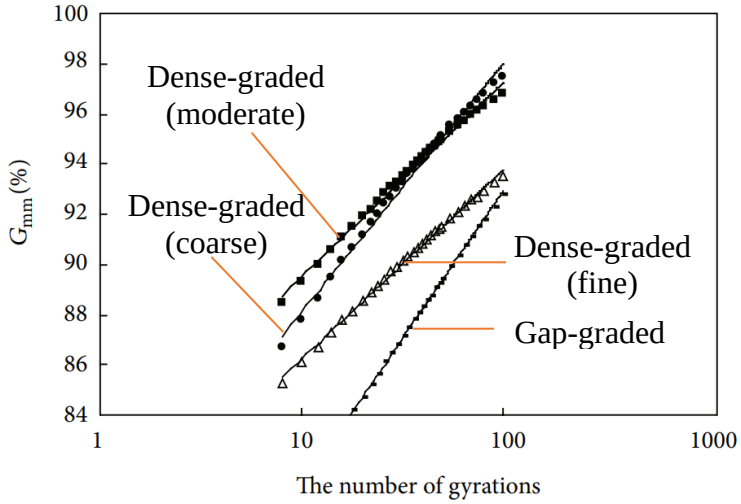

Figure 6. Density of Different Mixture Types throughout Laboratory Compaction. (*21*)

The fines content, percent passing the No. 200 sieve, will also affect compactability. Adding fines up to a certain point has shown to increase the overall density while not affecting

the long-term density as much. This is mainly because the filler is taking some of the space of the voids. Adding an excessive amount of fines greatly increases the mixture surface area, decreasing the available binder film thickness, and will dry out the mixture (*21*, *22*).

Aggregate Properties

Aggregate with higher angularity, whether the aggregate be coarse or fine, will decrease workability and compactability (Figure 7). So, a mixture with crushed stone will be harder to work and compact than a mixture with smooth, rounded river gravel. The specific type and source of aggregate can also play a roll. Softer aggregates (e.g., limestone or dolomite) are more forgiving during compaction than harder aggregates (e.g., granite or trap rock) (*23*, *24*).

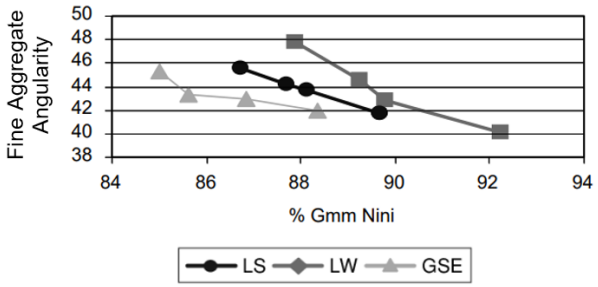

Figure 7. Effect of Fine Aggregate Angularity on Workability (*23*).

Asphalt Binder Content

A mixture with a higher binder content, all else being equal, will be easier to compact (*18*). Not only does the extra binder lubricate and make the mixture more workable, but the binder also fills voids in the aggregate structure. In the mix design process, while the asphalt binder content is not explicitly selected to improve mixture workability, the volumetric design method does optimize the asphalt binder content under a predetermined compaction effort (i.e., number of gyrations). In contrast, the balanced mix design method, based on cracking and rutting performance tests, does not consider workability in any aspect.

Asphalt Binder Grade

The high temperature of the binder performance grade (PG) represents the upper limit at which the binder retains adequate stiffness to resist deformation. This means that at the same temperature a higher PG binder will be more viscous, giving the mix a higher resistance to shear

deformation. Thus, as the PG of a binder increases, the workability of the asphalt mixture decreases.

Additives

Binder modifiers may produce mixtures with different workability behavior, even when the binder PG is the same. Organic and chemical warm mix additives reduce the binder viscosity, and foamed asphalt increases the effective binder volume during mixing. These allow the mixture to be produced, laid, and compacted at lower temperatures. In practice, many contractors maintain the usual production temperatures and instead rely on the additives as a compaction aid to improve the overall compaction quality.

Mixture Temperature and Environmental Conditions

Environmental conditions all relate to the rate of heat loss from the asphalt mixture. Asphalt binder stiffness and viscosity are temperature dependent. As the temperature decreases the binder becomes more viscous, thus decreasing the mixture workability. Breakdown compaction should occur when the mix is hottest, and ideally the breakdown rollers will stay close to the paver and to each other. The effectiveness of the breakdown and intermediate rollers decreases as the temperature gradually lowers, eventually getting to the point where the binder stiffness prevents the mixture from being compacted any further. This temperature is known as the cessation temperature (*24*). In TxDOT specifications, all rolling operations, except a light finish roller, must be completed by the time the mat temperature is 160°F (though the cessation temperature could be higher depending on the mixture properties).

Some mixtures exhibit tender behavior at excessively high temperatures and within an intermediate temperature range known as a "tender zone." Tender behavior is marked by lateral movement of the mixture under the rollers and results in shoving and a cracking pattern known as "checking" (i.e., short tightly spaced transverse cracks). The cause of tenderness is varied and may be related to rounded aggregates, specific gradations, high asphalt binder content, or moisture in the mixture (*25*). In susceptible mixes, the tender zone may start around 240°F and end around 190 to 180°F or even as low as 150°F (*26*). In these cases, the contractor should cease rolling operations until the mat drops below this temperature range.

Environmental factors will affect the cooling rate of the asphalt mat and will determine the amount of time available for compacting. In a synthesis, Hughes et al. (*27*) reported that the most significant factors of cooling are the ground temperature, laydown temperature, air temperature, and mat thickness. Thick-lift asphalt concrete is far less prone to heat loss than thin lifts. Other ambient factors that affect the cooling rate are wind speed and solar radiation (*28*).

Many researchers have developed cooling curves, illustrating the change in mat temperature with time under a set of conditions. The National Asphalt Pavement Association's *Hot Mix Asphalt Paving Handbook* contains curves using three variables: mixture-laydown temperature, base temperature (assumed to be similar to air temperature), and compacted layer thickness (*29*). A more sophisticated and validated mat cooling prediction tool, MultiCool, predicts the mat temperature based on these input parameters and many others. The tool was developed by Timm and Voller based on previous research and software development for Minnesota (*30*) and California (*31*). It is available as an online tool and as a phone app (http://www.eng.auburn.edu/users/timmdav/MultiCool/FinalRelease/Mobile.html). An example output is shown in Figure 8.

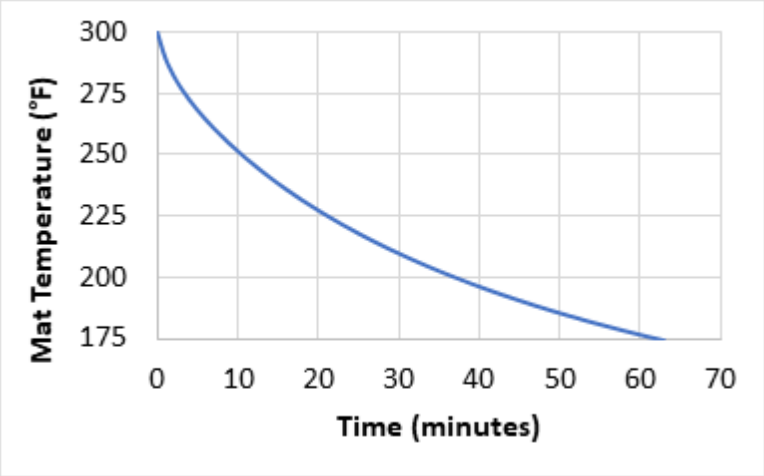

Figure 8. Example Cooling Curve Predicted by MultiCool.

Construction Practices

During construction, the engineer and contractor can improve in-place air voids by selecting an appropriate lift thickness and using the right compaction equipment effectively.

Lift Thickness

The lift thickness during construction has a significant contribution to the ability to achieve adequate compaction. Different studies conducted by Mississippi Department of Transportation (*18*), Florida Department of Transportation (*32*), and Wisconsin Department of Transportation (*33*) evaluated the effect of lift thickness on the in-place density. The results of these studies confirm the findings that compactability improves for thicker lifts through National Cooperative Highway Research Program (NCHRP) Project 9-27 (*34*). This is because (a) the mat maintains a high temperature for a longer time, and (b) the aggregates have more room for reorientation and can slide past each other, making it easier to obtain the desired density.

The effect of lift thickness is closely related to the mixture's NMAS, especially in terms of the minimum allowable lift thickness. Figure 9 illustrates the compaction effort required for different lift thickness-to-NMAS (t/NMAS) ratios. Brown et al. (*27*) recommends using a t/NMAS ratio of at least 3 for fine-graded mixes and at least 4 for coarse grade mixes to have decent compactability. Cooley et al. (*18*) recommends a minimum ratio of 3 for all mixes. Others recommend a minimum ratio of 2 (*29*, *35*). For thicker lifts, the authors note that the compaction effort to achieve maximum density did not increase for a larger t/NMAS ratio of 5. Cooley et al. found that better compaction was achieved as the t/NMAS ratio increased. The largest ratio tested in their research was 6.

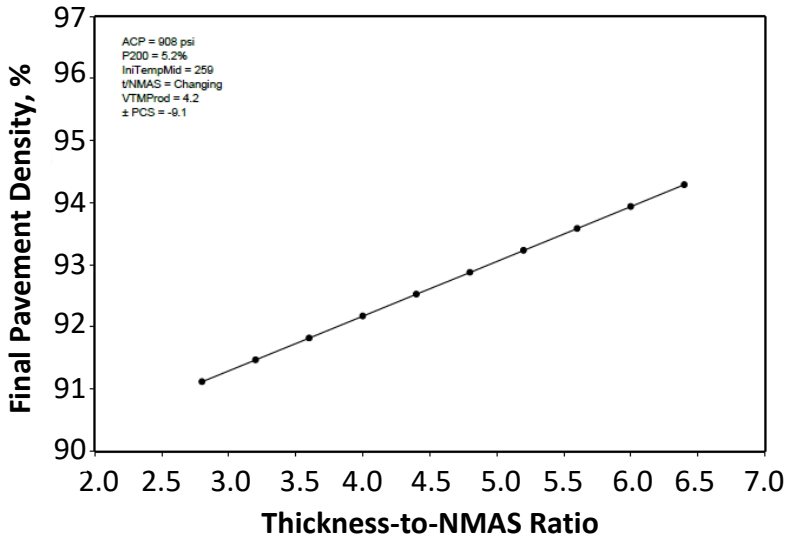

Figure 9. Effect of Lift Thickness-to-NMAS Ratio on Final Pavement Density (*18*).

One concern for placing very thick lifts is with the density uniformity within the layer. Specifically, does compacting excessively thick lifts leave high air voids at the bottom of the lift? Cooley et al. (*18*) tested this hypothesis by measuring the air voids at different strata within thick- and thin-lift cores. For thinner pavements, with t/NMAS ratios generally between 3 and 4, the core air voids from the top half and the bottom half were not statistically different, though there was a consistent trend that the bottom half had lower air voids (i.e., higher density). For thicker pavements, with t/NMAS ratios around 4 to 6, the middle third had the highest density, though it was only statistically different from the top third, which had the highest air voids. There was no relationship between the t/NMAS ratio and the difference in air voids among the strata, suggesting that thick-lift asphalt concrete construction does not create an appreciable air voids gradient.

Compaction Effort

The paver screed and various rollers compact the asphalt concrete by two principal means. First, the equipment applies downward force to the mat surface, and the heavier the equipment and the slower the equipment moves, the more compaction occurs. The second means of compaction is the creation of shear stress within the material by applying vibrating or oscillating force. High shearing stresses help rearrange the aggregates into denser configurations with greater particle interlock. Collectively, these two means (i.e., equipment weight and creation of shear stress) are referred to as "compaction effort" (*36*). The paver screed and the different types of rollers are described as follows:

- **Paver screed**: The screed is responsible for initial compaction and producing a tight, uniform surface texture. A typical vibratory screed achieves 75 to 85 percent density. A heavier screed, especially with additional compaction devices (i.e., tamper bars and pressure bars) can achieve 85 to 95 percent density.

- **Breakdown roller**: This is usually a vibratory steel roller responsible for the most density gain after the screed. In general, higher vibration frequency, lower amplitudes, and lower travel speed is recommended to avoid a rippling effect. High amplitude settings are only recommended for stiff mixes or very thick lifts. For some applications (i.e., thin lifts and open-graded mixes) a static roller is recommended.

- **Intermediate roller**: This roller may be another steel wheel roller or a pneumatic tire roller. The steel wheel roller may again be a vibratory roller, or for some mixes, an oscillatory roller is recommended. Pneumatic tire rollers provide a different type of compaction and are only used on certain mix types. In addition to static compressing force, pneumatic tire rollers also develop a kneading action between the tires that tends to realign aggregates within the mat. The intermediate roller is sometimes omitted altogether if proper compaction is achieved by the breakdown roller.

- **Finish Roller**: Static wheel rollers are almost always used as finish rollers. The finish roller is used last when the asphalt concrete mat is at or beyond its cessation temperature. This roller smooths out light surface defects left from the other rollers.

The contractor must set a rolling pattern on the first day of paving. The pattern consists of the type of rollers, the number of passes for each roller, and the location on the mat of each pass. The pattern is often determined by monitoring the mat density with a nuclear or non-nuclear gage immediately after the paver screed and between each roller pass.

Supporting Layer Stiffness

When contractors fail to achieve adequate density on a project, a frequent response is that the supporting layer was too soft, and, therefore, achieving density was out of the contactor's control. Hughes (*27*) synthesized the findings and observations from four publications that addressed this issue. One study found that subgrade deflections were the second most influential factor in predicting the air voids; however, the deflection data were not collected initially but rather two years after construction, casting doubt on the validity of the findings. Another report suggested that while the sublayer support does play a role, the effect is minor and can be accounted for with proper compaction practices. A laboratory study on the topic found that compaction of the asphalt mixture over stiffer support had higher densities though the effect was marginal. In the last study, no trend between pavement density and subgrade support was found.

PRACTICES FOR THICK-LIFT ASPHALT CONCRETE PAVING

The research team reviewed asphalt concrete design and construction specifications for 19 state departments of transportation, the Asphalt Institute, and the Australian transportation

body Austroads (*37–57*). Often different lift thicknesses would be prescribed depending on the mixture type and the location of the layer within the pavement. The detailed findings are tabulated in Appendix B.

The allowable maximum lift thicknesses for the 19 states and Australia are shown in Figure 10. The lift thicknesses ranged from 1.5 inches (a 0.375-inch-mixture in New Mexico) to 7.75 inches (a 2-inch base course mixture in Ohio). Base courses in Arizona and Louisiana do not have lift-thickness maximums, and California, Illinois, Massachusetts, and Minnesota do not have any maximum lift thickness requirements.

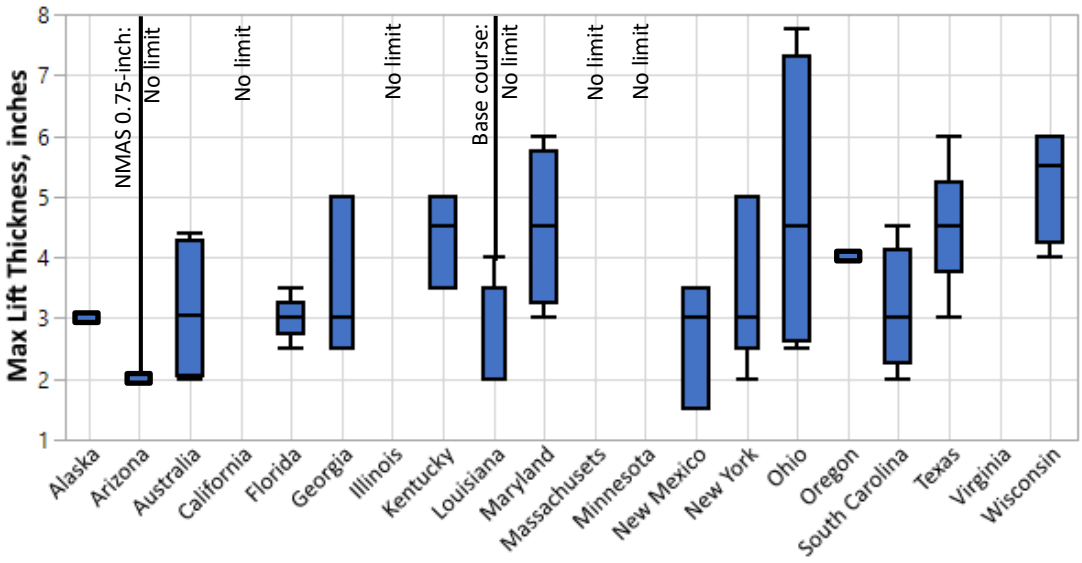

Figure 10. Range of Allowed Maximum Lift Thicknesses.

Figure 11 shows the allowed t/NMAS ratios for each agency. The t/NMAS ratios typically ranged from 3.0 to 6.0. Texas goes as high as 5.3 with their Item 341 Type C mixture. Wisconsin and South Carolina allow a ratio of 8.0, Oregon goes to 10.8, and Arizona, California, Illinois, Louisiana, Massachusetts, and Minnesota have no limits on some or all of their mixtures. Most agencies provided additional guidance for laydown and compaction procedures of thick-lift construction, including allowing a lower mixture, pavement, or ambient temperature for laydown.

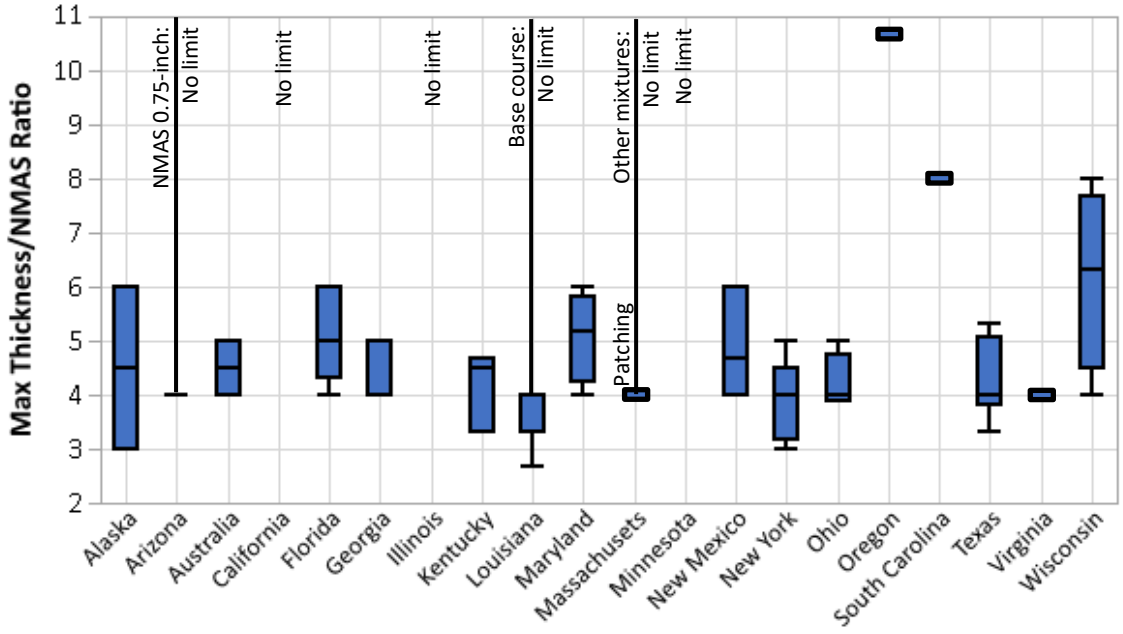

Figure 11. Range of Allowed Maximum t/NMAS Ratios.

SUMMARY

This literature review focused on the following topics:

- Tamper bar pavers: equipment overview, typical applications, and uses for thick-lift construction.
- Compaction and screed mechanics.
- Influential factors of asphalt mixture compaction.
- Practices for thick-lift asphalt concrete paving.

Key findings include:

- While not common in the United States, tamper bar pavers are the go-to option in Europe and other countries.
- Tamper bar screeds reportedly achieve a higher compaction than a typical vibratory screed, though the researchers did not find published data to support the statement.
- A tamper bar paver successfully placed 6 inches of asphalt concrete in a demonstration project in the Atlanta District.

- A review of screed mechanics and laydown operations will help the research team as they design the section layout for testing.

- Mixture workability is heavily governed by gradation, aggregate properties, asphalt binder content, and temperature.

- Constructing a thicker lift improves density, both because temperature is maintained and because there is more room for aggregate to rearrange.

- Not all states have maximum lift thickness limits. Of those that did, the t/NMAS ratios were between 3.3 to 6.0.

- Agencies' specifications are often more lenient on temperature when placing thick lifts and may stipulate different compaction methods.

Items not found in the literature review were:

- Substantial evidence that tamper bar pavers are required for thick-lift construction.

- Substantial evidence that tamper bar pavers reduce breakdown and intermediate rolling operations and reduce overall project costs.

CHAPTER 3:
METHODOLOGY

OVERVIEW

Tamper bar pavers were deployed on three paving projects to place thick asphalt layers ranging from 6 to 10 inches thick. On each project, test sections were constructed in one or two lifts, evaluating different lift thicknesses, paver screed settings, and rolling patterns. The research team monitored the asphalt cooldown time after laydown and the mat density throughout compaction. After construction, the in-situ pavement density was tested with a PaveScan rolling density meter (RDM) and 3D Radar. Cores were sampled for laboratory testing including computed tomography (CT) scanning for air voids uniformity, traditional bulk air voids testing, and measuring rutting and cracking characteristics. Each project was profiled to measure ride quality.

This chapter describes test section construction (consisting of project location, test section layouts, and construction procedures), field and laboratory testing, and statistical analyses. In this report, the term *air voids content* is shortened to *air voids*.

TEST SECTION CONSTRUCTION

Four sets of test sections were constructed on three different projects in the Tyler, Atlanta, and Dallas districts, as summarized in Table 4. Test sections within each project were constructed end-to-end. The Tyler and Atlanta district projects were constructed by the same contractor using the same SP Type C mixture. The contractor used a rented Vögele-brand tamper bar paver. Two sets of test sections were built on the Dallas District project by the same contractor with a SP Type B mixture. This contactor owned a Caterpillar-brand tamper bar paver.

Table 4. Test Sections.

District	Route	Mixture	Thickness	Construction Type
Tyler	US 259	SP Type C	6-inch	Mill–inlay
Atlanta	US 59	SP Type C	6-inch	Mill–inlay
Dallas	SH 121–Detour	SP Type B	10-inch	New construction
Dallas	SH 121–Shoulder	SP Type B	8-inch	New construction

In all sets of test sections, there are sections built with the tamper bar enabled and with the bar disabled, using the same paver and screed available to the contractor. This is not the same as comparing two different screeds. A tamper bar screed is larger and heavier than a typical vibratory screed, and the additional weight will add to the compaction effort. So, the results of the vibratory-only sections cannot be interpreted as thick-lift paving with a typical smaller screed. Another common observation was that there was high variability in the actual number of breakdown roller passes applied within a test section. The compaction process naturally has areas of overlap, and due to operator error, there were also areas with fewer passes than prescribed.

TYL-US 259

The first test sections were constructed in the Tyler District, Rusk County, on US 259 through the small town of Mt. Enterprise (Figure 12). The roadway is a four-lane, rural principal arterial with average annual daily traffic (AADT) of 6,800 and 38.4 percent trucks. The roadway intersects with US 84 at a signalized intersection.

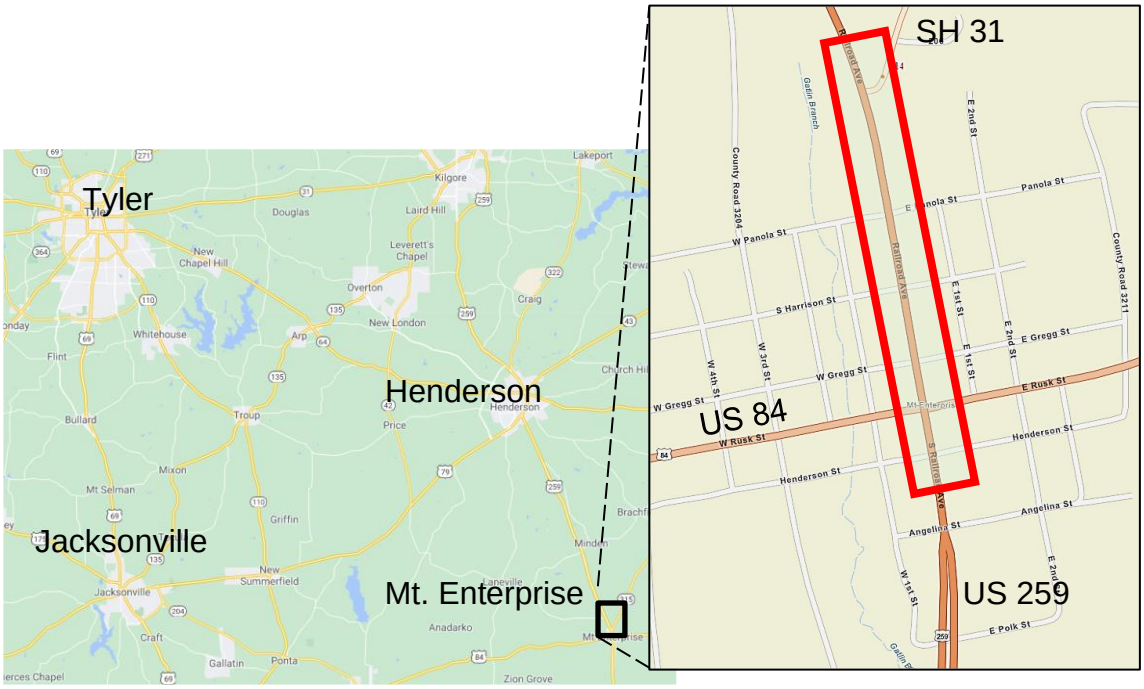

Figure 12. TYL-US 259 Project Location.

The existing pavement was 10 inches thick and had some rutting and fatigue cracking, especially in the inside through lanes. A ground-penetrating radar survey revealed subsurface stripping.

The rehabilitation plan was to mill out 6 inches of pavement on the through lanes and inlay with SP Type C. In the inside lanes, the intersection and intersection approaches were milled deeper to 8 inches to remove the stripped pavement layer. The center turn lane and shoulders were not milled or inlayed. The pavement was then resurfaced with a seal coat from edge to edge.

The test section details are in Table 5, and the layout is shown in Figure 13. All test sections were built in the inside through lanes between SH 315 and Henderson St. Four sections were built with the tamper bar enabled and four with the tamper bar disabled (only the vibratory screed enabled). Single lift and multiple lift sections were paved. Sections were compacted with either three or five vibratory breakdown roller passes, where one pass is defined as down-and-back. In practice, however, the roller operator did not consistently apply a set number of passes uniformly across the full mat.

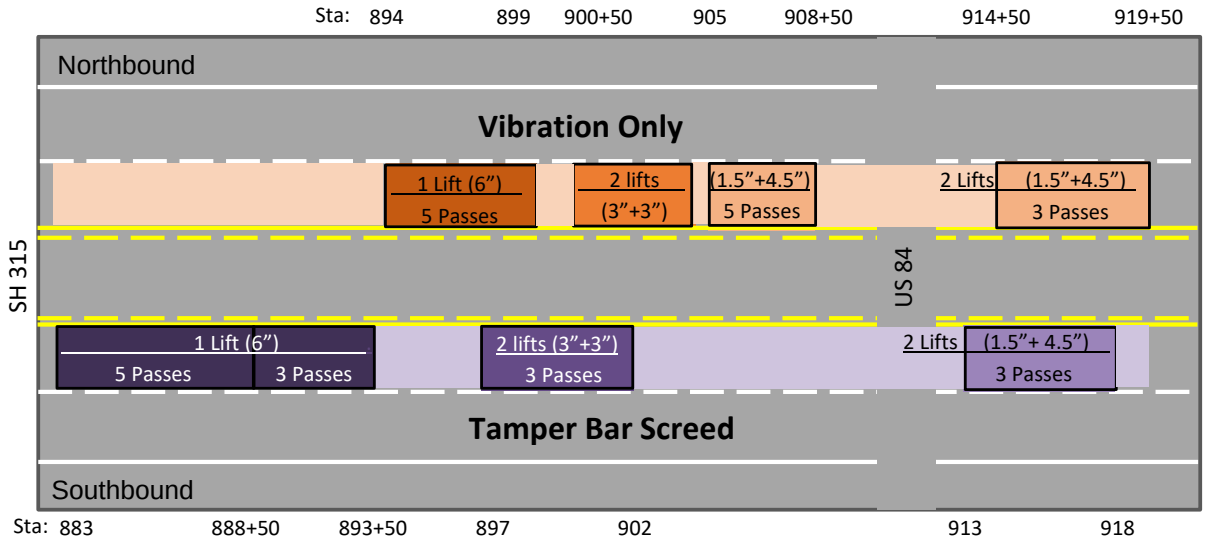

Figure 13. TYL-US 259 Test Section Layout.

Table 5. TYL-SH 259 Test Section Details.

Lifts	Screed Setting*	Breakdown Rolling Passes**
Single 6"	Tamper Bar	3 vibe
Single 6"	Tamper Bar	5 vibe
Single 6"	Vibratory	5 vibe
3" + 3"	Tamper Bar	3 vibe
3" + 3"	Vibratory	3 vibe
1.5"+4.5"	Tamper Bar	3 vibe
1.5"+4.5"	Vibratory	3 vibe
1.5"+4.5"	Vibratory	5 vibe

** Tamper bar: tamper bar at 60 percent and 7mm stroke, vibratory unknown. Vibratory: tamper bar disabled, vibratory unknown.*
*** High variation in actual rolling pattern.*

Paving took place on July 13 and 14, 2020, by Madden Construction. The research project rented a Vögele tamper bar paver, model Super 2000-3i, with an AB 600TV screed. The contractor had experience using the same machine on projects two years prior. Figure 14 shows the equipment used by the contractor to lay and compact the asphalt.

(a)

(b)

(c)

Figure 14. TYL-US 259 and ATL-US 59 Construction Equipment: (a) Tamper Bar Paver, (b) Breakdown Steel-Wheel Roller (HAMM), (c) Breakdown Steel-Wheel Roller (Caterpillar).

ATL-US 59

The next test sections were constructed in the Atlanta District, Panola County, on US 59 just north of Carthage (Figure 15). The roadway is a divided four-lane, rural principal arterial with an AADT of 10,610 and 28.9 percent trucks.

Specific locations were marked for patch repair. The patch design was a 4-inch mill and inlay with SP Type C. For this study, milling on three of the patches was increased to 6 inches and were used exclusively for the test sections. Again, Madden Construction was the contractor, and the mix design for patching was the same as on TYL-US 259.

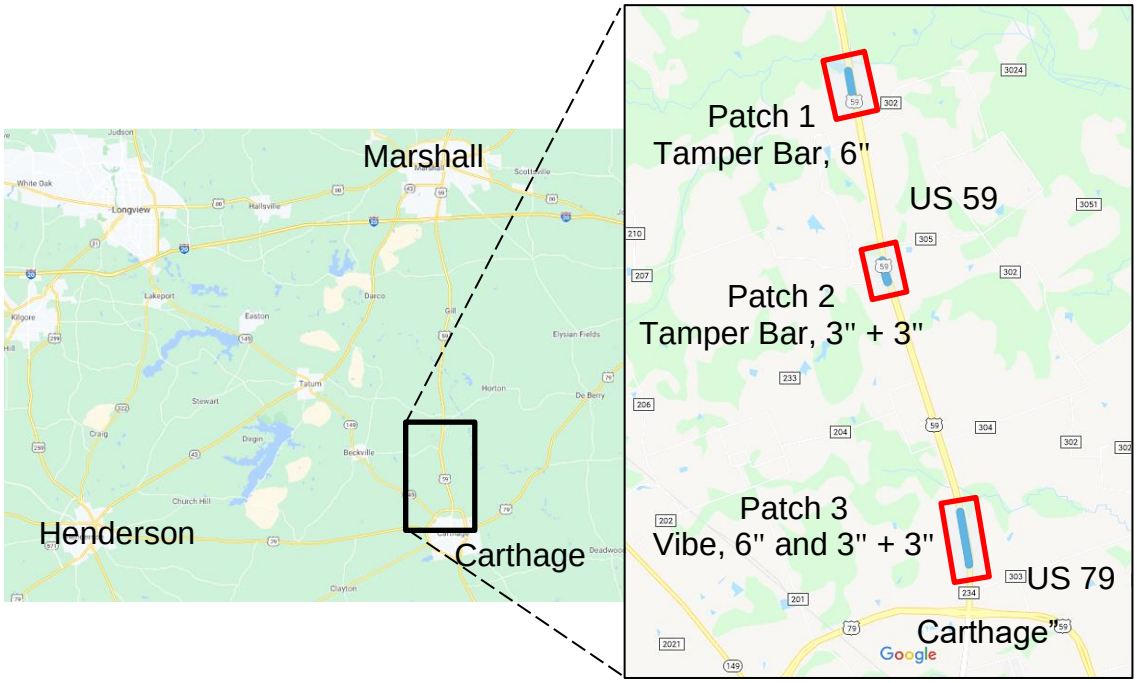

Figure 15. ALT-US 59 Project Location.

Paving took place on July 27 and 28, 2020. The contractor used the same Vögele tamper bar paver and other paving equipment as used on the TYL-US 259 job, except that there were two Caterpillar breakdown rollers instead of one Caterpillar and one HAMM roller.

All test sections were built in the southbound outside lane between Irons Bayou and US 79. The test section details are given in Table 6, and the layout is shown in Figure 16. A full factorial test layout was done using the screed with and without the tamper bar enabled, one 6-inch lift and two 3-inch lifts, and three and five vibratory breakdown roller passes. The sections were between 400 and 375 ft long.

Table 6. ATL-US 59 Test Section Details.

Lifts	Screed Setting*	Breakdown Rolling Passes
Single 6"	Tamper Bar	3 vibe
Single 6"	Tamper Bar	5 vibe
Single 6"	Vibratory	3 vibe
Single 6"	Vibratory	5 vibe
3" + 3"	Tamper Bar	3 vibe
3" + 3"	Tamper Bar	5 vibe
3" + 3"	Vibratory	3 vibe
3" + 3"	Vibratory	5 vibe

** Tamper bar: tamper bar at 60 percent and 7mm stroke, vibratory unknown. Vibratory: tamper bar disabled, vibratory unknown.*

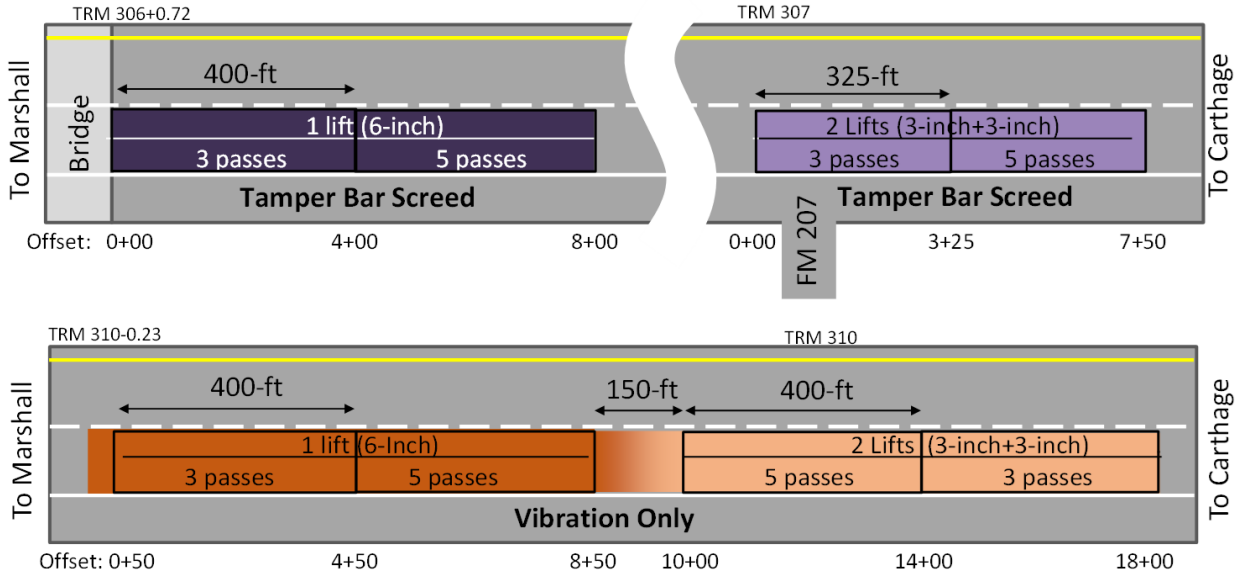

Figure 16. ATL-US 59 Test Section Layout.

DAL-SH 121

The final two test sections were both constructed in the Dallas District, Collin County, on SH 121, project CSJ: 0549-03-024. The roadway is mostly an undivided two-lane (super 2), rural principal arterial with an AADT of 10,500 and 12 percent trucks. The corridor is being expanded to a divided four-lane road. Construction of test sections was done in two locations: a 10-inch

thick intermediate layer on a detour section and an 8-inch thick intermediate layer on a mainline shoulder section.

Detour

The temporary detour pavement construction was just south of the intersection with SH 160, going from the present southbound lanes to the northbound lanes, crossing the median of the divided highway (Figure 17).

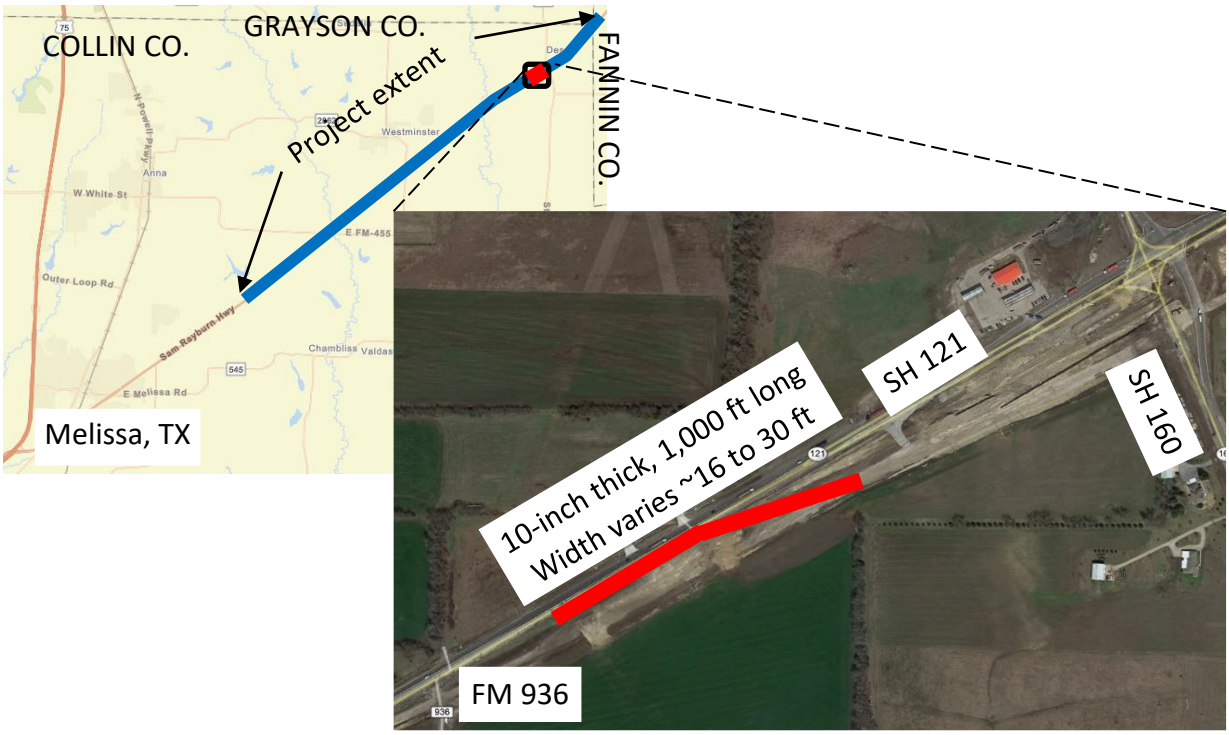

Figure 17. DAL-SH 121 Detour Project Location.

The detour pavement, designed to traverse natural subgrade, was thick full-depth asphalt concrete. The bottom layer was 10 inches of SP Type B, followed by a 2-inch layer of SP Type C, both TxDOT Item 344. The test sections were constructed with the SP Type B layer and tested and sampled before the surface layer was paved.

Four test sections were constructed, as detailed in Table 7 and illustrated in Figure 18. In all test sections, the breakdown roller operator was told to apply five breakdown passes (instead of the usual two) ahead of the pneumatic roller. The drum setting for the first breakdown pass was always static, and the others were vibratory. The roller operator was not always consistent and would sometimes do the usual three passes or overlap in areas with seven roller passes.

Table 7. DAL-SH 121 Detour Test Section Details.

Lifts	Screed Setting*	Breakdown Rolling Passes**
Single 10"	Tamper Bar	1 static, 4 vibe
Single 10"	Vibratory	1 static, 4 vibe
5" + 5"	Tamper Bar	1 static, 4 vibe
5" + 5"	Vibratory	1 static, 4 vibe

** Tamper bar: tamper bar at 1,600 RPM and max stroke, vibratory at 1,200 RPM. Vibratory: tamper bar disabled, vibratory at 3,000 RPM.*
*** High variability in actual rolling passes.*

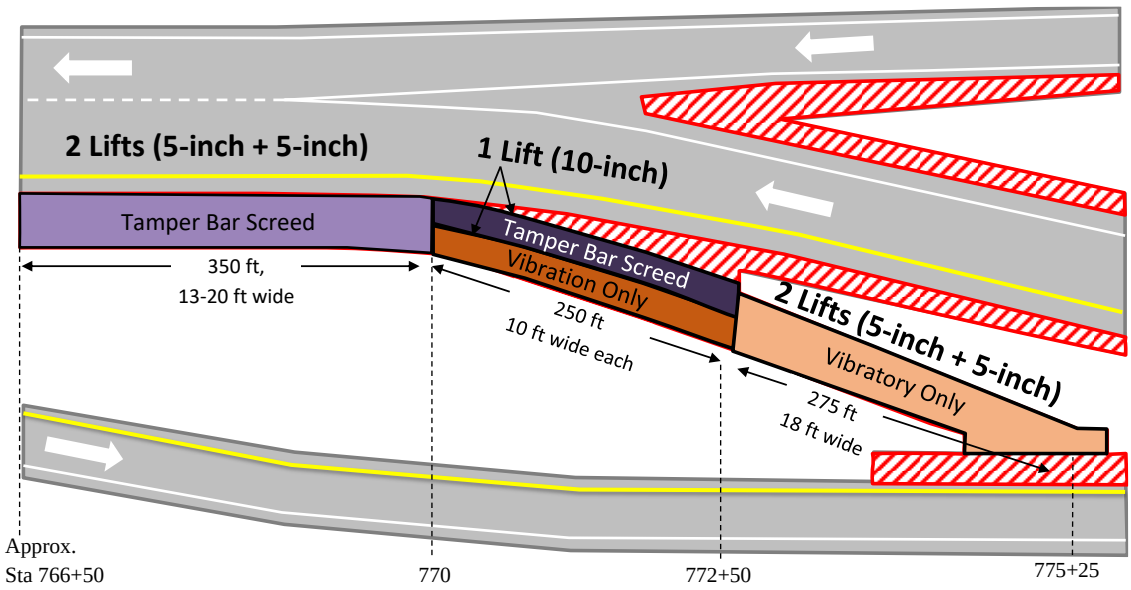

Figure 18. DAL-SH 121 Detour Test Section Layout.

An equipment representative noted that the tamper bar installed on the paver was significantly worn down. A new bar has a rectangular profile 14 mm wide, but the leading edge of this bar had worn down to a curve with a footprint about 5 mm wide. The tamper bar design and settings should ensure the bar impacts the mat twice in each location, but with a narrower bar width most locations will be impacted once, though the impact stress would be higher.

Paving took place on June 11 and June 12, 2021. The prime contractor was Mario Sinacola & Sons, and the paving subcontractor was Reynolds Asphalt. Reynolds Asphalt owns and operates two Caterpillar tamper bar pavers, model AP1055F. Figure 19 shows the equipment

used by the contractor to lay and compact the pavement. The same equipment was used in the shoulder test sections.

(a) **(b)**

(c) **(d)**

Figure 19. DAL-SH 121 Construction Equipment: (a) Tamper Bar Paver, (b) Breakdown Steel-Wheel Roller, (c) Intermediate Pneumatic Roller, (d) Finish Roller.

The weather and site conditions were less than ideal for construction. The area had experienced on-and-off rainfall for several weeks. Despite allowing the area to dry for a few days, the natural subgrade in the median was still very soft, deflecting and shoving under construction traffic and creating ruts up to 10 inches deep (Figure 20). The subgrade was soft everywhere, but the worst was in the middle of the east-most test section (two lifts of 5 inches with a vibratory screed). The first day of paving, the contractor completed both single 10-inch lift sections and the bottom 5-inch lift in the two-lift sections. The next morning, a brief but intense storm dropped 1 inch of rain in 40 minutes. In the early afternoon, by the time paving of

the second 5-inch lift started, the surface had mostly dried out, but some residual moisture remained. It is unknown how the rainfall may have impacted stockpiles and mixture production.

Figure 20. DAL-SH 121 Detour, Soft Subgrade Rutting under Construction Traffic.

Mainline Shoulder

Once the detour sections were completed as a proof of concept, a location was identified on the mainline which would have more consistency in the subgrade and overall better paving conditions. Test sections were located in the shoulder, which was not subject to ride quality verification, in the southbound direction between CR 635 and FM 1002, north of SH 160 (Figure 21).

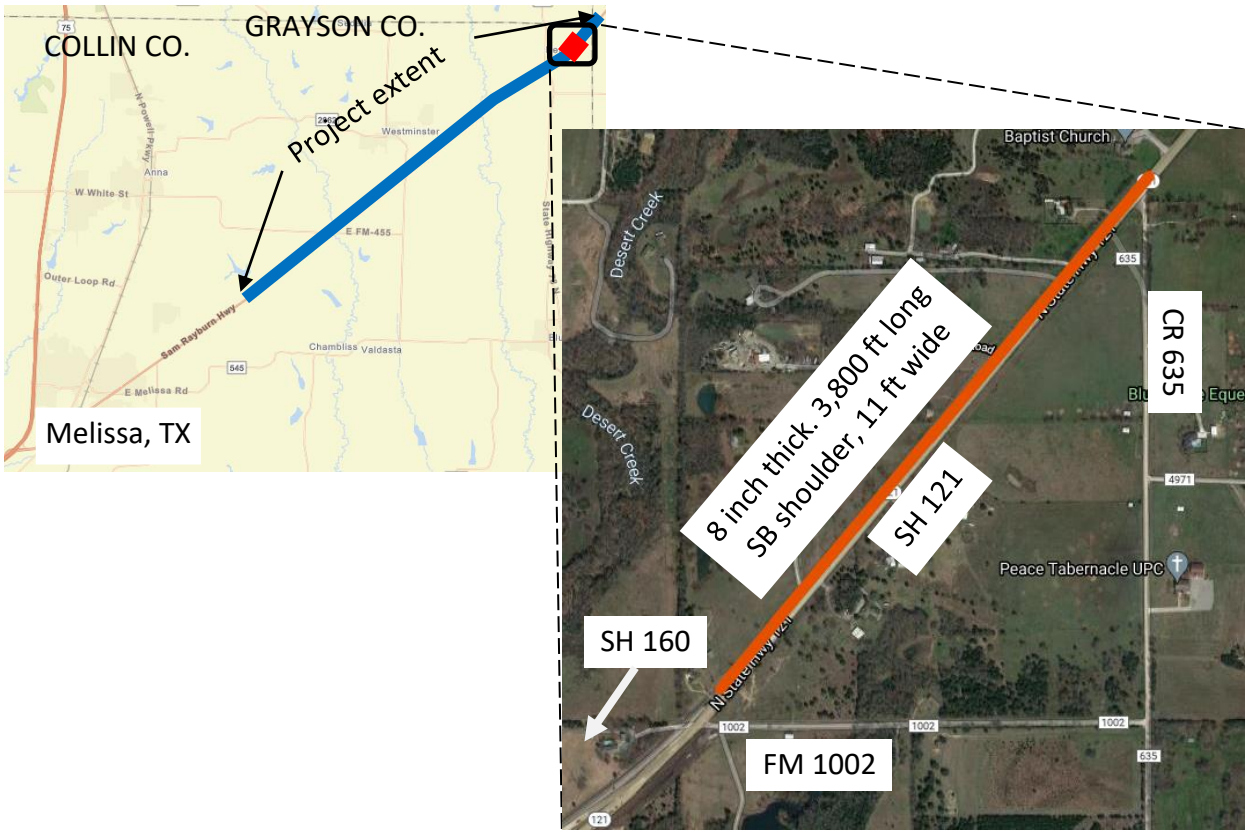

Figure 21. DAL-SH 121 Shoulder Project Location.

The shoulder pavement was all new construction. The pavement design was a 10-inch lime-treated subgrade and an 8-inch hot mix asphalt (HMA) layer of SP Type B surfaced with a 2-inch layer of SP Type C, both TxDOT Item 344. The test sections were constructed in the SP Type B layer and were tested and sampled before the surface layer was paved.

Eight test sections were constructed as detailed in Table 8 and illustrated in Figure 22.

Table 8. DAL-SH 121 Shoulder Test Section Details.

Lifts	Screed Setting*	Breakdown Rolling Passes
Single 8"	Tamper Bar	4 vibe
Single 8"	Tamper Bar	6 vibe
Single 8"	Vibratory	4 vibe
Single 8"	Vibratory	6 vibe
4" + 4"	Tamper Bar	4 vibe
4" + 4"	Tamper Bar	6 vibe
4" + 4"	Vibratory	4 vibe
4" + 4"	Vibratory	6 vibe

** Tamper bar: tamper bar at 1,800 RPM and max stroke, vibratory at 3,000 RPM. Vibratory: tamper bar disabled, vibratory at 3,000 RPM.*

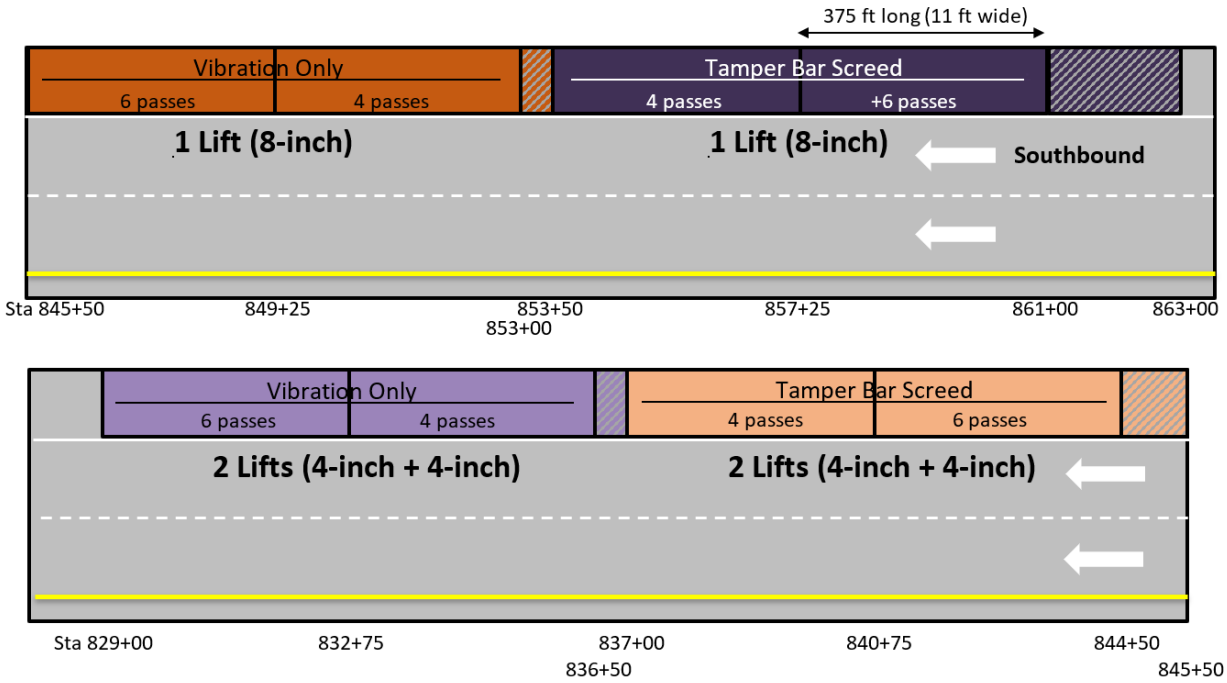

Figure 22. DAL-SH 121 Shoulder Test Section Layout.

Paving took place on October 20, 2021. The same equipment that was used previously was used for these test sections. Both the screed settings and the rolling patterns were different in this set of testing than for the detour section, as noted in Table 9. The breakdown roller was more consistent than when paving the detour, achieving the desired number of passes. However, the operator inadvertently introduced an undesirable rolling technique while trying to satisfy the

prescribed rolling pattern. When reversing directions, the roller operator often performed straight stops rather than turning toward the center of the mat, which introduced more roughness in the finished mat. Also, the operator focused compaction on the center of the mat and made less effort to roll the unconfined mat edges.

FIELD AND LABORATORY TESTING

Several tests were performed on the test sections during construction, on the finished mat, and with sampled cores in the laboratory. Table 9 summarizes the measurement from each test and each is discussed in detail in this section.

Table 9. Field and Laboratory Measurement Descriptions.

Measurement	Description
Cooldown Time	• The time it takes after laydown for the mat temperature to decrease to 160°F. • Measurements taken at various depths in the mat.
Air Voids During Construction	• During construction with pavement quality indicator (PQI)density gauge after screed and between roller passes.
Air Voids from Cores	• CT scan of cores to assess air void (AV) content gradient. • Traditional bulk AV content of full sample. • Traditional bulk AV content of 2-inch segments.
Air Voids from Radar	• Full-coverage scanning with the PaveScan RDM and calibrated to predict AV content.
Reflection Amplitude	• Full-coverage scanning with 3D Radar. • Evaluated at the bottom of layer, mid-layer, and near the surface.
Stiffness	• Modulus of resilience of cores (2-inch segments).
Cracking Resistance	• Cracking index of cores from the indirect tensile asphalt cracking test (IDEAL-CT) (2-inch segments).
Profile Roughness	• International roughness index from profiling.

Mat Cooldown Time

On at least one location per project, a temperature probe (Figure 23) was inserted into the loose mat just before compaction. The probe has thermocouple sensors spaced every one or two

inches of depth. An infrared (IR) sensor and an IR camera were used to measure the surface temperature. Mat temperature was measured for several hours until the mat cooled down.

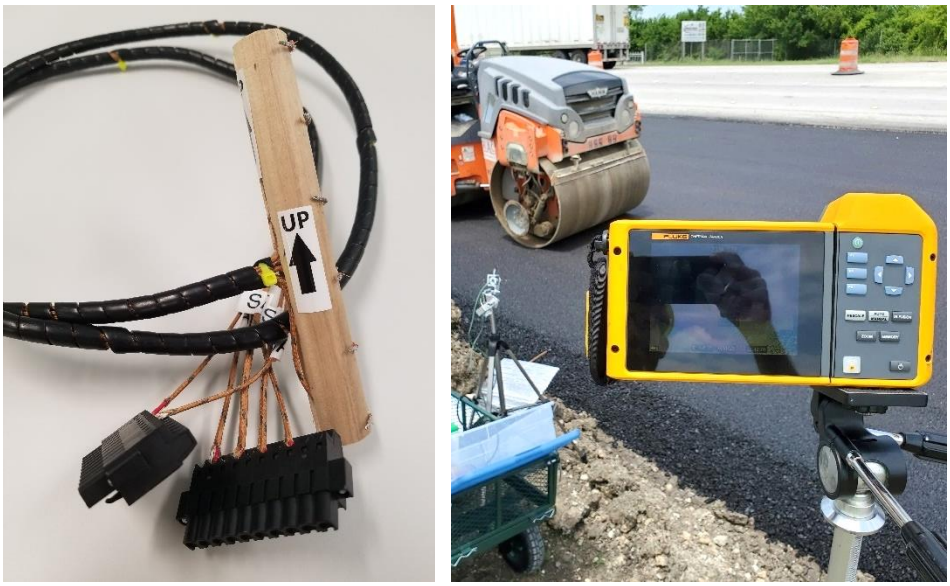

Figure 23. Temperature Probe, Installation Site, and IR Camera.

Air Voids During Construction

A PQI is a non-destructive density tester. The team used a PQI to test the mat density immediately after the paver screed and between breakdown roller passes (Figure 24). Another measurement was made following intermediate and finish rolling. In most cases, three locations were tested with the PQI within each section. In later sections, the team only measured the initial, uncompacted condition and the final density.

Figure 24. Pavement Quality Indicator.

The lead breakdown roller was equipped with a compaction monitoring system consisting of GPS, infrared thermal sensors, and an accelerometer mounted just outside the axel of the vibratory drum. The system collected the roller position throughout testing so the team could verify the number of breakdown roller passes that it made and whether the drum was set to vibrate or not.

Full-Coverage Radar Testing

After compaction, the mat was tested by two advanced radar systems: a PaveScan RDM and a 3D Radar system (Figure 25). The RDM is a three-channel system equipped with high-frequency 2.5 GHz antennas. After calibration, the system can predict air voids at 6-inch intervals along each antenna profile. On each project, the team used at least nine cores for calibration for both single-lift and two-lift sections. They collected three profiling passes on each section down the left, center, and right sides of the mat. While the high-frequency antenna provides excellent near-surface resolution and accuracy, the measurement is only based on the upper 0.5 inches. Variation deeper in the mat is only accounted for through core calibration.

Figure 25. Rolling Density Meter and 3D Radar.

The 3D Radar by Kontur uses an array of step-frequency continuous waveform antennas capable of measuring frequencies from 50 MHz to 2.0 GHz. By using a range of frequencies, the system generates high-resolution data throughout the pavement depth. This system is ideal for detecting anomalies within the layer and across the width of the pavement like a poorly compacted lift interface. Two passes were made on each project down the left and right sides of the mat.

To process the 3D Radar data, Examiner 3.5 software was used to filter out background noise and enhance features of interest. Data processing was performed with the following steps:

- Interference suppression to minimize the effect of external radiation sources like cell phone antenna towers and base stations.
- Background removal to account for faint reverberations of high-amplitude early signals emitted by the radar antennas.
- Inverse Fast Fourier Transform to convert the reflection data from the frequency domain back into the time domain.
- Apply time-ground mode to account for variable antenna height due to bouncing.
- Increase contrast to improve data visualization for identifying the mid-layer interface.
- Data trimming after 15 nanoseconds (about 2.5 ft below the surface).

Multiple 3D interfaces within the mat were semi-automatically traced within each section. The interface between the bottom of the layer and the existing pavement or subgrade was easily traceable with the automated tools. A "reference" interface was created as a horizontal plane 2.5 inches below the pavement surface. Finally, a mid-depth interface was defined for both single-lift and two-lift test sections. For single-lift sections, the mid-depth interface was a horizontal plane at the middle of the lift. For two-lift sections, the interface was traced with a combination of automated and manual techniques. Example data of a single-lift and a two-lift section side-by-side are shown in Figure 26. The figure shows mid-depth reflection amplitudes in top-down view and also illustrates the lift interfaces in a cross-section view.

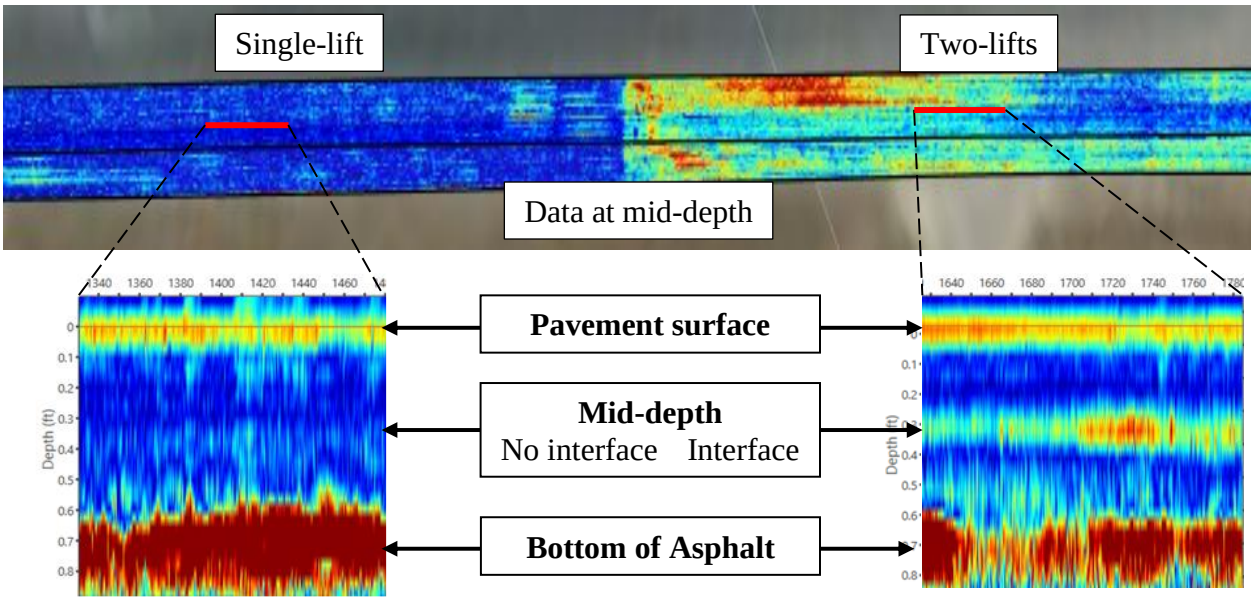

Figure 26. 3D Radar Data at Mid-depth and Interfaces.

Roughness

Each project, except for DAL-SH 121 Detour, was tested with an inertial roughness profiler (Figure 27). The operator, a testing subcontractor, made three runs over all test sections. In post-processing, the profile data were separated into segments and the international roughness index calculated for each test section.

Figure 27. Inertial Roughness Profiler.

Core Sampling and Testing

The team sampled six cores from each test section. The cores were tested with a CT scanner in the lab to capture the air voids gradient and were then tested for overall air voids using the bulk saturated surface-dry (SSD) method. These steps are shown in Figure 28. The CT scan data for each core were calibrated based on the measured overall air voids. Consequently, the correlation between the CT scan and the bulk SSD air voids was very strong (Figure 29).

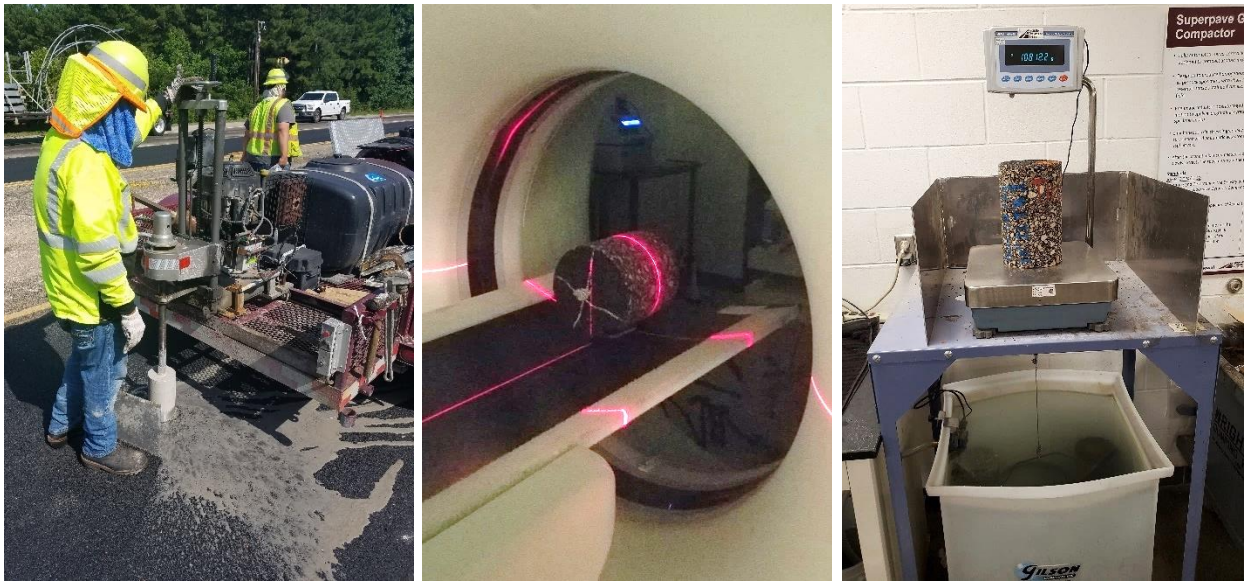

Figure 28. Core Sampling, CT Scanner, and SSD Bulk Testing Equipment.

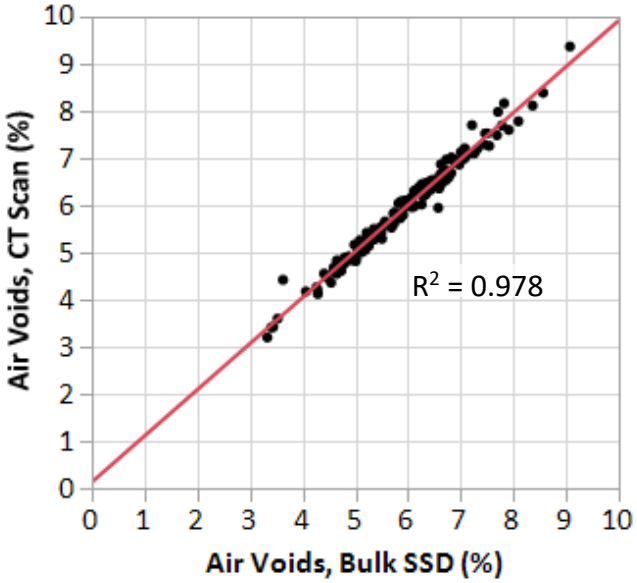

Figure 29. Correlation between Bulk SSD and CT Scan Measured Air Voids.

A subset of cores was used to evaluate the relationship of air voids to mixture stiffness and cracking resistance. This effort was a minor part of the project and did not influence the development of the research recommendations. As such, it is not included in the body of the report but is discussed in Appendix C.

STATISTICAL ANALYSIS

Several statistical analyses were performed to determine the effects of main research predictor variables (e.g., lift thickness, screed setting, and roller passes) on the response variables (e.g., cooldown time, overall air voids, and roughness). The complete list of response variables and predictor variables is given in Table 10. Each analysis used a certain combination of predictor variables and variable interactions as appropriate with the analysis goals. Analyses were done using the statistical software JMP, generally through multivariate analysis of variance (MANOVA) or multivariate analysis of covariance (MANCOVA) and stepwise regression. Details of how each analysis was formulated and definitions of the response variable, predictor variables, data set, and sample size are contained in Appendix D.

Table 10. All Response and Predictor Variables.

Response Variables	Predictor Variables and Levels/Ranges

• Cooldown time (time until 160°F [hr]).
• Air voids from PQI (%).
• Air voids from cores:
  - Overall (%).
  - By lift (%).
  - Ratio at bottom to overall.
• Air voids from PaveScan RDM (%).
• Reflection amplitude at mid-depth from 3D Radar.
• International roughness index.
	• Project (TYL-SH 259, ATL-US 59, DAL-SH 121 Detour/Shoulder).
	• Layer thickness (4.5 to 10 inches).
	• Lift thickness (3 to 10 inches).
	• Lift (top, bottom).
	• Number of lifts (1, 2).
	• Lift t/NMAS (4.7 to 13.7).
	• Screed setting (tamper bar, vibe only).
	• Breakdown roller passes (3 to 6).
	• Laydown temperature (301 to 323°F).
	• Thermal sensor location (surface, top, middle, bottom).

SUMMARY

Four sets of test sections were constructed, comprising 28 unique test sections. The project locations, test section layouts, and construction procedures for each test project were documented. Some problems that were encountered during construction were management of the rolling operations for consistency, an excessively worn-out tamper bar on the DAL-SH 121 projects, and inconsistent subgrade support on the DAL-SH 121 detour sections.

Testing in the field comprised measuring mat cooldown time, monitoring mat air voids during construction, full-coverage mat testing with the PaveScan RDM and 3D Radar, and roughness profiling. Over 170 cores were sampled and tested in the laboratory for air voids with a CT scanner and traditional bulk SSD testing.

Several statistical analyses were performed to determine the effects of main research predictor variables on the response variables like cooldown time, overall air voids, and roughness.

CHAPTER 4:
RESULTS

OVERVIEW

This chapter presents the results of testing and statistical analyses. As discussed, several aspects of thick-lift paving were assessed:

- Mat cooldown time.
- Air voids of the mat during construction.
- Air voids of cores (overall, by lift, and uniformity).
- Air voids from the PaveScan RDM.
- Reflection amplitude from the 3D Radar.
- Profile roughness.

The chapter is organized into sections based on these studies. The summary results are provided here, and detailed statistical results are in Appendix E.

MAT COOLDOWN TIME

An example of mat temperature data after compaction, from the TYL-US 259 project, with a single 6-inch lift is shown in Figure 30. The plot shows the temperature of the surface measured from an infrared sensor, the temperatures within the lift at three depths, and the initial temperature of the mat, which was extrapolated from the middle-of-the-lift data. The red line at 160°F is the specified temperature when the mat can be open to traffic. On this project, the initial temperature was just over 300°F. The surface of the mat cooled down to 160°F after 6.5 hours. The middle of the mat, however, 3-inches down, retained heat much longer and didn't reach 160°F until 7.6 hours.

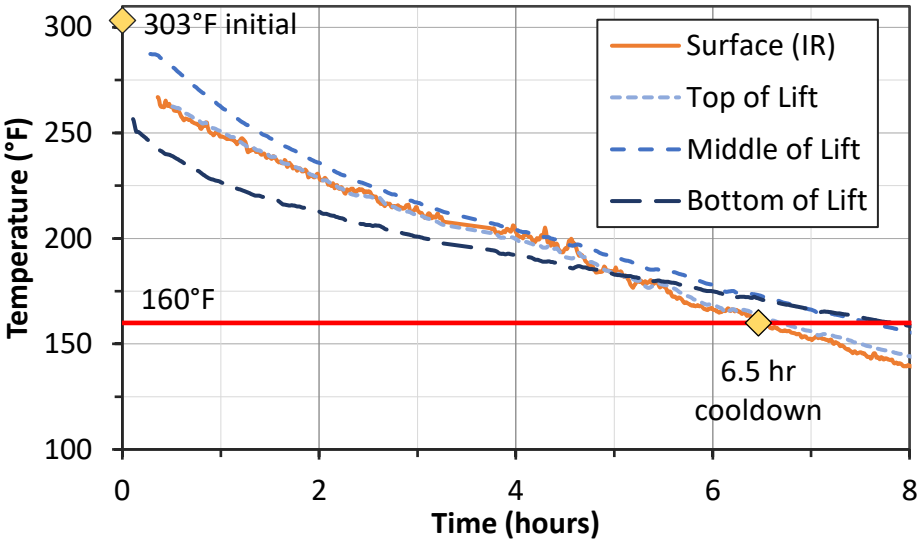

Figure 30. Mat Temperature versus Time.

The cooldown times at the surface and middle of the lift for each project and at different lift thicknesses are summarized in Figure 31, and the statistical results are in Table 11. Cooldown times ranged from 4.8 hours on the thinnest section when measured on the surface to 9.3 hours on the thickest section when measured inside the mat. The variables *Sensor location*, *Lift thickness*, and *Project* were all statistically significant. The cooldown time on and near the surface was faster than in the middle or bottom of the lift by about 1.8 hours. Thicker lifts also took longer to cooldown, with a general trend of each inch adding 0.7 hours of cooldown time. The initial *Laydown temperature* variable was not statistically significant. This suggests that moderate changes in the initial mixture temperature (e.g., using warm mix additives) do not have a dramatic effect on the cooldown time.

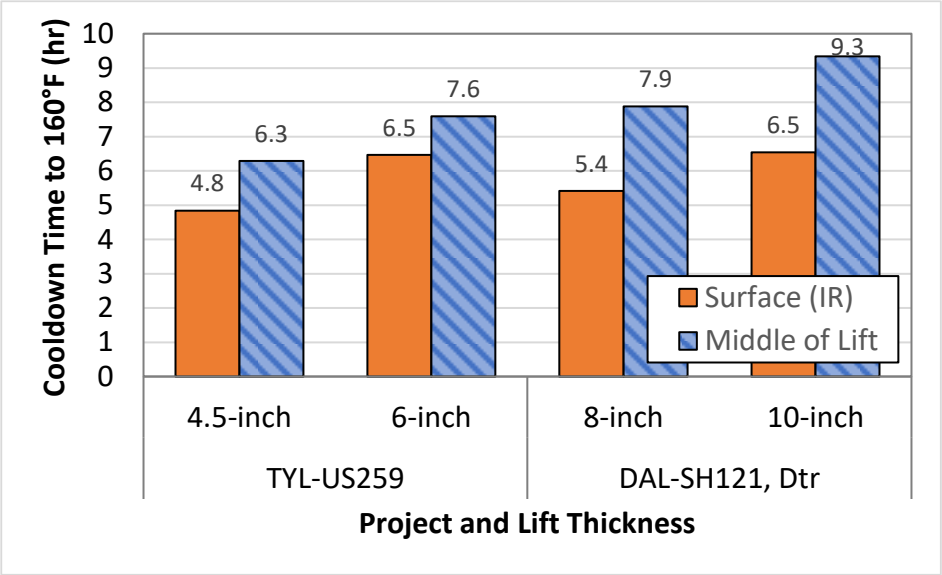

Figure 31. Cooldown Time Results.

Table 11. Statistical Results of Cooldown Time Analysis.

Predictor Variable	*p*-value	−log(*p*-value)	Significant
Sensor location	0.0011	2.9	Y
Lift thickness	0.0024	2.6	Y
Project	0.0151	1.8	Y
Laydown temperature	> 0.390	0.892	N (exclude)

AIR VOIDS DURING CONSTRUCTION

This analysis focused on the air voids, measured by the PQI, behind the screed and throughout the compaction process. The predicted versus actual air voids are shown in Figure 32. The overall model was highly significant (*p*-value < 0.0001) and had a high adjusted R^2-value of 0.85. The statistical results for each predictor variable are shown in Table 12. The *Number of passes* was clearly the most significant factor. *Lift thickness* had a significant effect, through practically, the effect was minimal. For example, compacting on a single 8-inch lift decreases the air voids by about 0.5 percent more than compacting on a 4-inch lift. The screed setting was not statistically significant.

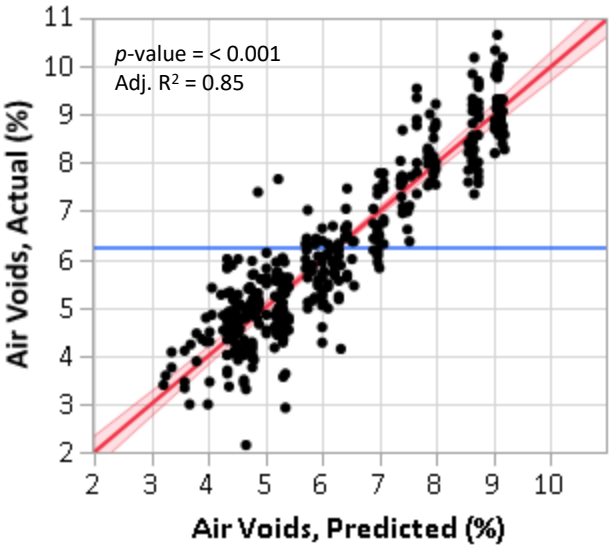

Figure 32. Predicted vs Actual Air Voids (PQI).

Table 12. Statistical Results of Air Voids During Construction Analysis.

Predictor Variable	*p*-value	−log(*p*-value)	Significant
log(Breakdown Roller Passes + 1)	< 0.0001	169	Y
Project	< 0.0001	36.7	Y
Lift Thickness	< 0.0001	6.87	Y
Screed Setting	0.1282	0.892	N (include)
Lift	0.6768	0.170	N (excluded)

An alternative non-linear model result is shown in Figure 33. The graph shows that the mat air voids directly behind the screed were 8.6 percent on average, then quickly reduced 2 percent after one pass of the roller. The second pass reduced air voids by just over 1 percent with diminishing returns until only 0.1 percent change in density was achieved after the sixth roller pass.

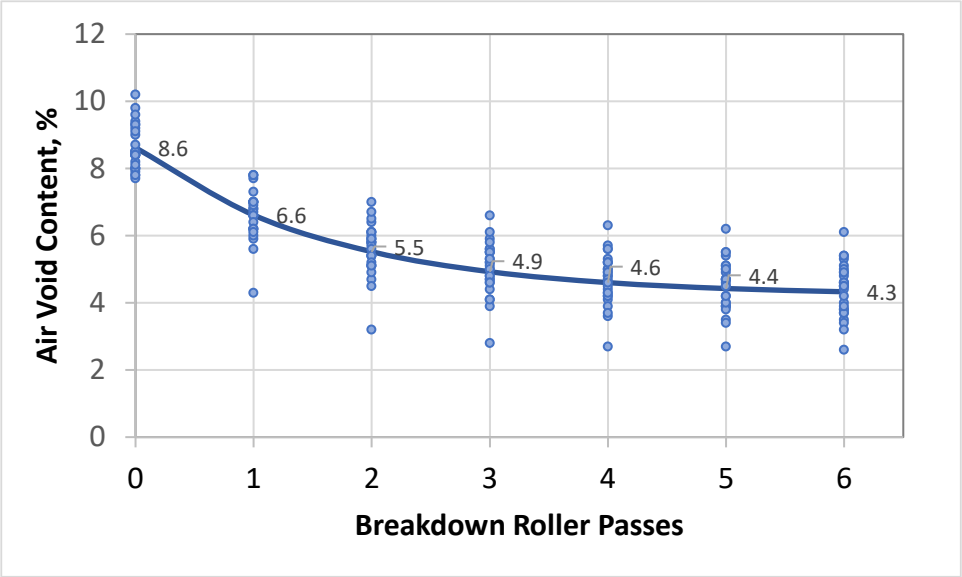

Figure 33. Air Voids Versus Roller Passes

As found previously, the screed setting did not have a statistically significant impact on the air voids behind the screed. The average air voids were 8.8 and 8.7 percent, and the *p*-value was 0.47. Even the interaction term of *Project* and *Screed Setting* was insignificant, meaning the screed did not influence any of the projects constructed (see Table 13 and Figure 34). The researchers suspect that if the tamper bar screed on SH 121 were in a better condition, there might have been a more noticeable effect of the screed settings.

Table 13. Statistical Results of Air Voids during Construction Analysis (Non-linear).

Predictor Variable	*p*-value	−log(*p*-value)	Significant
Project	0.0001	3.97	Y
Lift Thickness	0.0060	2.23	Y
Screed Setting	0.4725	0.3260	N (include)

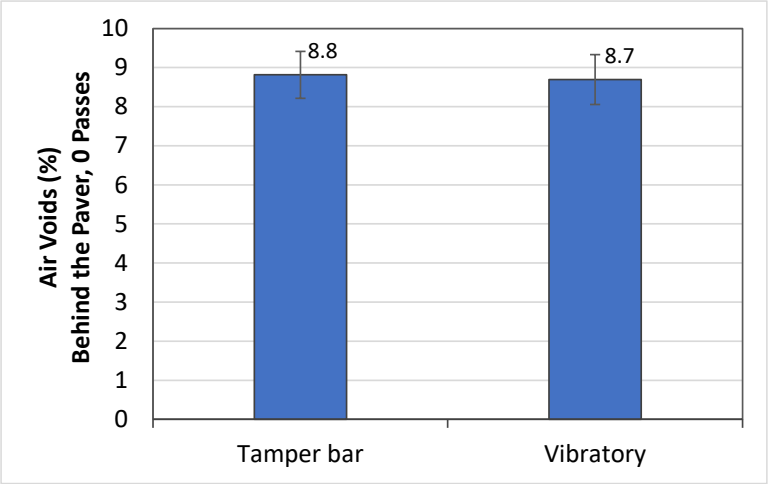

Figure 34. Effect of Screed Type on PQI Air Voids (None).

AIR VOIDS FROM CORES

This section describes the results of the overall air voids, air voids by lift, and air voids uniformity. These data were all derived from the sampled cores through either CT scanning or measurements using the bulk SSD method.

Overall Air Voids

The predicted versus actual overall air voids are shown in Figure 35. The overall model had statistical significance (*p*-value < 0.001); however, the data also had a high degree of scatter as noted by the low adjusted R^2 value of 0.37. The statistical results for each predictor variable are shown in Table 14, and each of the five modeled main effects are illustrated in Figure 36.

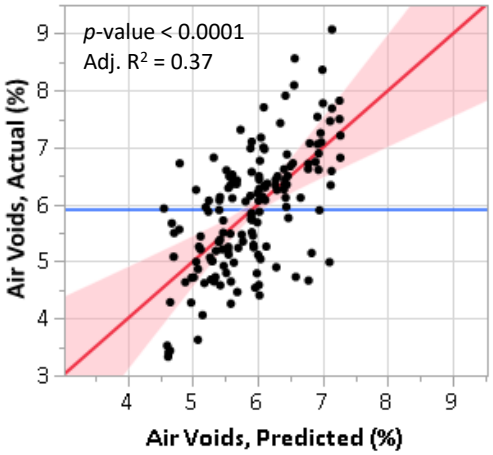

Figure 35. Predicted versus Actual Air Voids (Overall).

Table 14. Statistical Results of Air Voids (Overall) Analysis.

Predictor Variable	*p*-value	−log(*p*-value)	Significant
Breakdown roller passes	< 0.0001	8.6	Y
Project {ATL-US 59–DAL-SH 121 Shldr}	< 0.0001	5.1	Y
Number of lifts * Roller passes	< 0.0001	4.4	Y
t/NMAS * Project {DAL-SH 121 Dtr–TYL-SH 259}	< 0.0001	4.2	Y
Roller passes * t/NMAS	0.0004	9.4	Y
Roller passes * Project {ATL-US 59–DAL-SH 121 Shldr}	0.0008	9.1	Y
Screed setting	0.0008	3.1	Y
t/NMAS	0.012	1.9	Y
Number of lifts * Project {ATL-US 59–DAL-SH 121 Shldr}	0.014	1.9	Y
Number of lifts	0.014	1.8	Y
Project {DAL-SH 121 Dtr–TYL-SH 259}	0.051	1.3	N, included
Project {DAL-SH 121 Dtr and TYL-SH 259–ATL-US 59 and DAL-SH 121 Shldr}	0.144	0.84	N, included

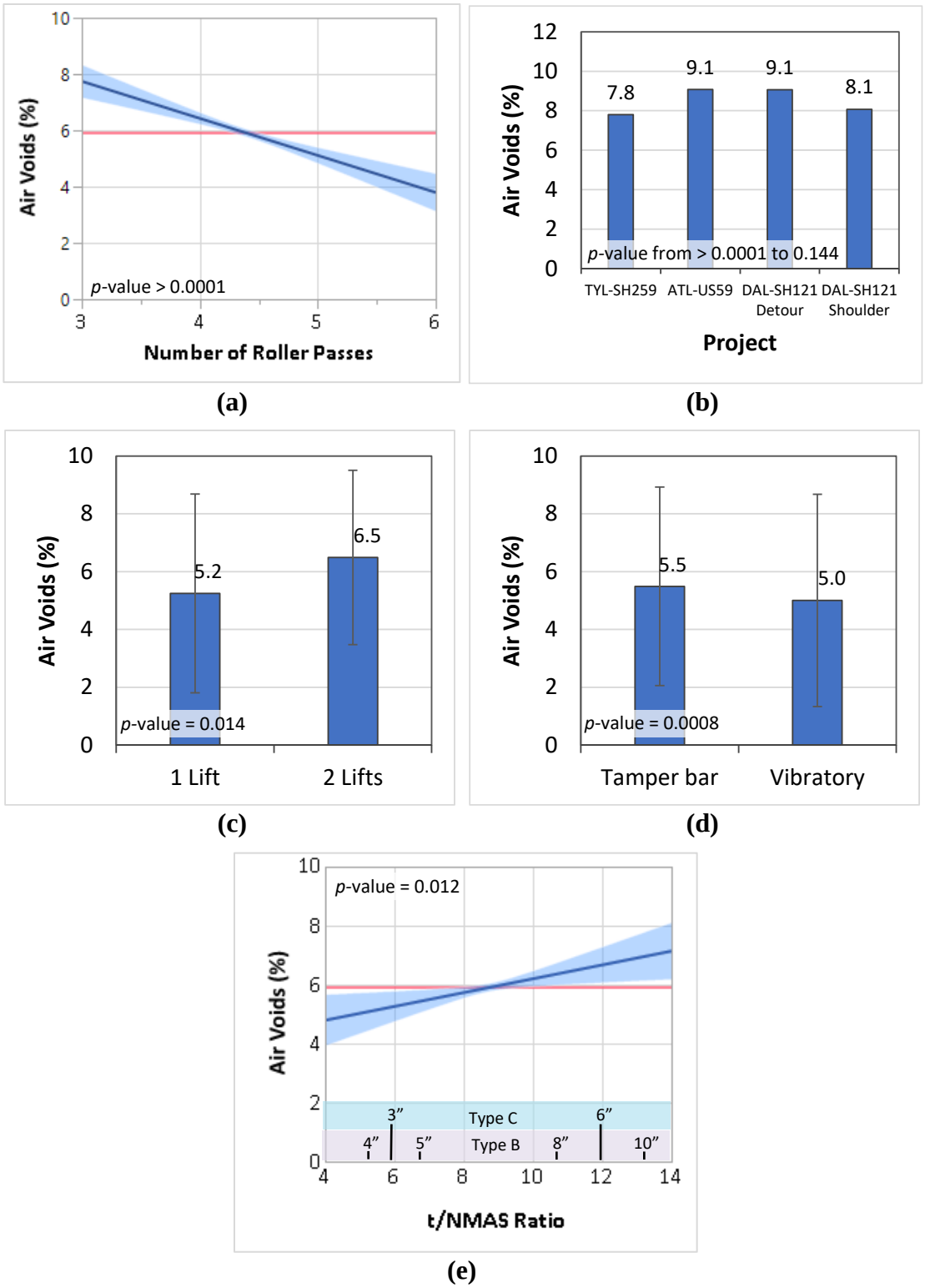

Figure 36. Air Voids versus Main Effects: (a) Number of Roller Passes, (b) Project, (c) Number of Lifts, (d) Screed Setting, and (e) t/NMAS ratio.

The most significant predictor variable was *Breakdown roller passes*. The rolling process had more impact on the final air voids than anything else involved in the laydown process, the mixture properties, or the lift thickness. The leverage plot shows the significance of the factor based on the slope of the trend line and that the confidence bands around the line (shaded red) are far from the horizontal blue line. The graph suggests that adding an extra roller pass decreases the air voids by over 1 percent. The effect of roller passes, however, is likely non-linear, as seen in the previous analysis with PQI air voids, and the impact of sequential passes has diminishing returns.

During testing, the researchers tracked the path of the breakdown roller on each day of paving with GPS. They observed that, on some projects, there was considerable variation between the rolling pattern prescribed in the research plan and the actual rolling pattern. Also, the degree of compaction had high variation across the mat transversely, especially near an unconfined edge (lower compaction) or where the rolling pattern overlapped (higher compaction). Given the significance of the roller pattern effect, the researchers theorize that much of the randomness in the data is directly attributed to variability in the rolling pattern and variability across the mat transversely. It might be possible to correct this error if the actual number of roller passes over each core location could be determined.

The *Project* variable was the next most significant factor. In the stepwise model-building tool, categorical variables with more than two categories are broken up into n-1 parameters, and the significance of each parameter is calculated separately. In this data set, the difference between the ATL-US 59 and the DAL-SH 121 Shoulder projects was the most statistically significant when considering the effects of all other parameters. There are also significant interactions between each of the main effects and one or more projects. In total, 6 of the 12 model parameters include the *Project* variable. This means there were different types and degrees of influence at the project level that were not accounted for by the primary study factors. These influences are wide ranging and could include:

- Contractor.
- Paver model and manufacturer.
- Condition of the tamper bar.
- Method of adjusting screed settings.

- Asphalt mix designs.
- Supporting substrate.
- Edge confinement.

Even when these variables were known, it was not appropriate to include each of them separately in the model. Consequently, the *Project* factor serves as a catch-all for these uncontrolled variables.

The *Number of Lifts* factor shows that pavement placed in a single lift had lower air voids than pavement placed in two lifts. On average, single-lift cores had air voids that were 1.3 percent lower than the two-lift cores. This is because the bond interface in two-lift cores was higher than the air voids in the middle of the lift, as is clearly evident in the CT scan data in Figure 37. On average, the air voids at the bond interface is 14.5 percent, compared to 4.2 percent air voids at the center of a single-lift layer (Figure 38).

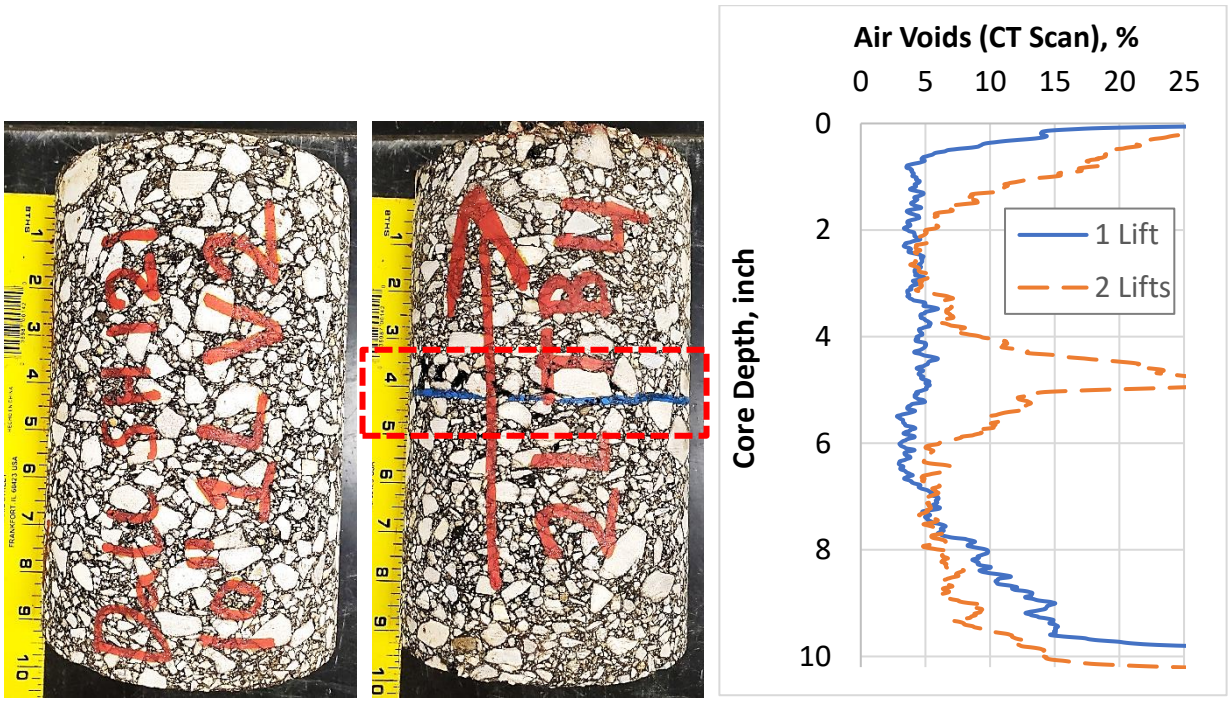

(a) **(b)** **(c)**

Figure 37. Example Cores: (a) Single Lift, (b) Two-Lift, and (c) CT Scan Results.

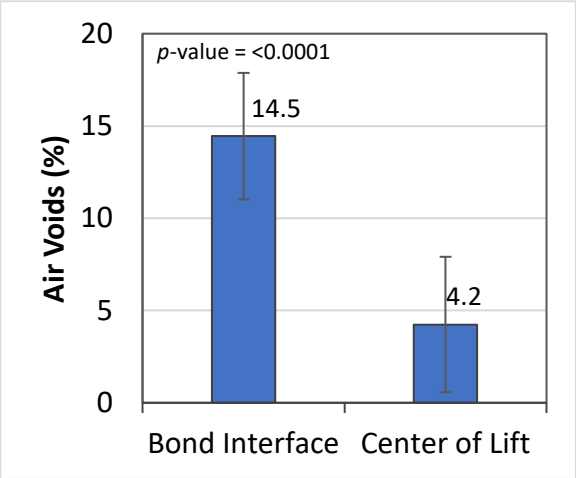

Figure 38. Comparison of Air Voids at Bond Interface and Center of Lift.

The effect of the *Screed Setting* factor indicated that the vibratory-only setting on the paver screed resulted in more compaction than the tamper bar screed setting. The difference was only 0.5 percent air voids, but it was statistically significant. The researchers question the validity of this finding because of two reasons. First, due to miscommunication with the contractor, the screed settings were inconsistent among the different construction projects. On the DAL-SH 121 Detour project, when the tamper bar was enabled, the vibratory action was set to 1,200 RPMs, but when the tamper bar was turned off, the vibration was increased to 3,000 RPMs. The specific effect of the tamper bar, therefore, was confounded by the change in the vibratory setting. Then, on the DAL-SH 121 Shoulder project, the vibratory screed was maintained at 3,000 RPMs in both cases. On the TYL and ATL projects, the vibratory screed setting was unknown, both when the tamper bar was enabled and disabled. The second issue is that the tamper bar screed on the DAL projects was significantly worn. A new tamper bar has a rectangular profile 14 mm wide, but the leading edge of this bar had worn down to a curve with a footprint about 5 mm wide.

Finally, the effect of the *t/NMAS Ratio* factor showed that an increase in the ratio (i.e. thicker lift for a given mix type) increases the overall air voids slightly. On average, an increase of the t/NMAS ratio by two will increase air voids by 1 percent. This finding is contrary to results in the literature that studied this same factor in a laboratory setting. However, evaluating the main effect of t/NMAS in the analysis of overall air voids is misleading because the effect gets confounded with the effect of the number of lifts. Samples with the lowest t/NMAS ratios

were also placed in two lifts, which tends to increase the air voids. The next analysis of air voids by lift is an attempt to clarify the influence of the t/NMAS ratio factor.

Air Voids by Lift

The results from analyzing air voids by lift is shown in Figure 39 and Table 15. While the model did contain some significant factors (*Roller Passes* and *Screed Setting*), the R^2 value of the model is very low, indicating that there is another factor, not in the model, that has a significant effect and/or that there is high variability inherent to the data. The effect of *Lift t/NMAS* was not significant in the model. Therefore, from the core lift data set, the researchers did not observe any effect of the *lift t/NMAS* (or *lift thickness* alone) on air voids.

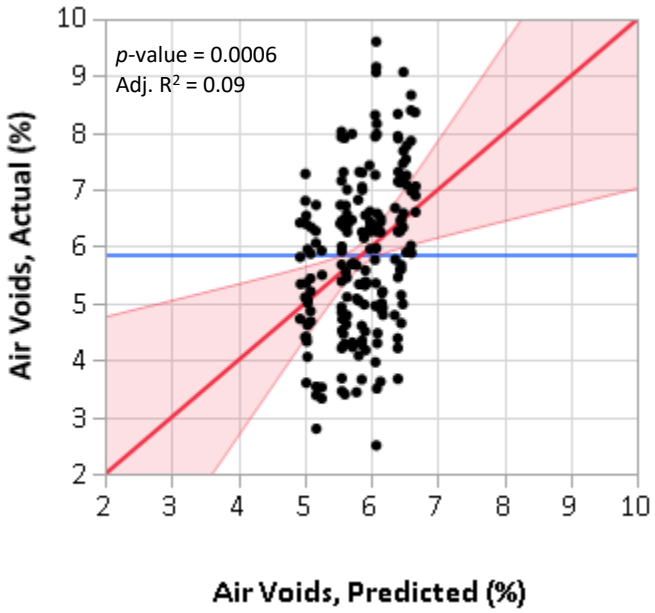

Figure 39. Predicted versus Actual Air Voids (by Lift).

Table 15. Statistical Results of Air Voids (by Lift) Analysis.

Predictor Variable	*p*-value	−log(*p*-value)	Significant
Roller passes	0.0001	4.0	Y
Screed setting	0.0014	2.1	Y
Project	0.2886	0.5	N (include)
Lift t/NMAS	0.6953	0.2	N (include)

The difference in compaction between the top lift and bottom lift was analyzed separately with a paired t-test. The air voids of the bottom lift were subtracted from the top lift for all two-layer cores, and this difference for all paired data was compared to zero. The distribution of all the differences is shown in Figure 40. On average, the top lift has less compaction and 1.8 percent higher air voids than the bottom lift. The difference from zero was statistically significant (*p*-value < 0.0001). The difference is likely due to the high air voids at the interface. The researchers theorize that, though compacting against a stiffer layer could help compaction, it actually becomes harder to compact the interface itself because it is difficult for finer aggregate to reposition into the voids within the coarse aggregate at the interface.

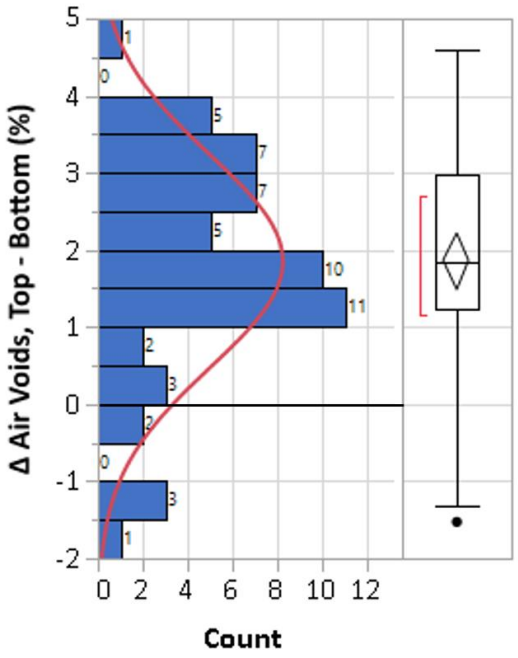

Figure 40. Paired Difference between Top Lift and Bottom Lift Air Voids.

Air Voids Uniformity

One concern about placing thick lifts is whether the contractor can achieve adequate compaction at the bottom of the lift. The air voids uniformity analysis compared the air voids at the bottom 0.5 inch with the overall air voids to calculate a ratio. For example, a ratio of 2 means that the bottom air voids are twice as high as the overall air voids.

The result of the air voids uniformity analysis is in Table 16. *Lift thickness* was the most significant variable that affected the uniformity of air voids within a lift. The relationship is illustrated in the leverage plot in Figure 41. As the lift thickness increases, the ratio of bottom air voids to overall air voids increases. This is confirmation that thicker lifts are more difficult to compact uniformly, even if overall compaction is improved. At 10 inches, the ratio is over 2, and as the lift approaches 2 inches (which was outside the scope of testing in this project), the ratio is expected to go to 1.

Table 16. Statistical Results of Air Voids Uniformity Analysis.

Predictor Variable	*p*-value	−log(*p*-value)	Significant
Lift Thickness	< 0.0001	16.9	Y
Project	< 0.0001	7.4	Y
Lift	< 0.0001	5.5	Y
Project * Lift	< 0.0001	5.1	Y
Project * Lift Thickness	< 0.0001	5.0	Y
Screed Setting	0.49	0.3	N, excluded
Breakdown Roller Passes	0.90	0.04	N, excluded

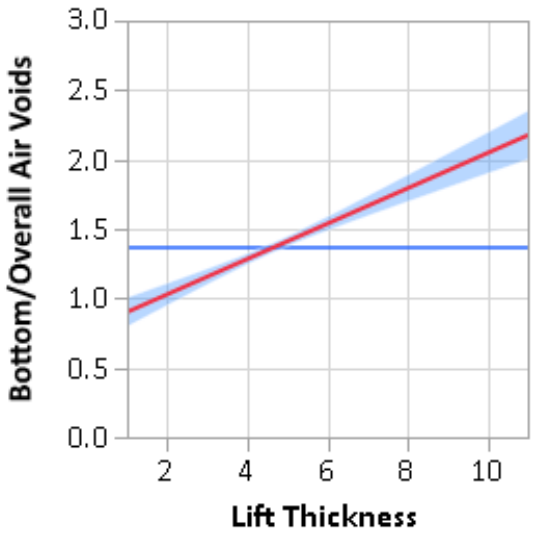

Figure 41. Ratio of Bottom to Overall Air Voids versus Lift Thickness.

The *Project* factor and related interactions were significant. This finding has little practical interest, but including the factor and interactions in the model helps define the actual effect of other factors. The *Lift* factor, whether the lift was the bottom or the top, was significant. Lifts on the top had an average ratio of 1.4 (less uniformity), and bottom lifts had ratios of 1.2, but the difference is not practically significant.

The factors *Screed setting* and *Roller passes* were not significant. This means that additional compaction effort did not mitigate the effect of non-uniformity with increased lift thickness. If one decides to pave thick, they should accept that the lift will have higher air voids at the bottom of the lift, regardless of the rolling pattern or paving equipment used.

AIR VOIDS FROM THE PAVESCAN RDM

Example PaveScan RDM calibrations for DAL-SH 121, comparing the measured dielectric value to actual air voids, are shown in Figure 42. These equations are used to predict air voids through the tested mat. The detour and shoulder sections used the same prediction equations. For this project, the R^2 values for both calibrations were over 0.65. The calibration for the two-lift section predicted higher air voids. A similar trend was noted on the ATL-US 59 calibrations; however, on TYL-SH 259, the single-lift and two-lift sections had nearly the same calibration.

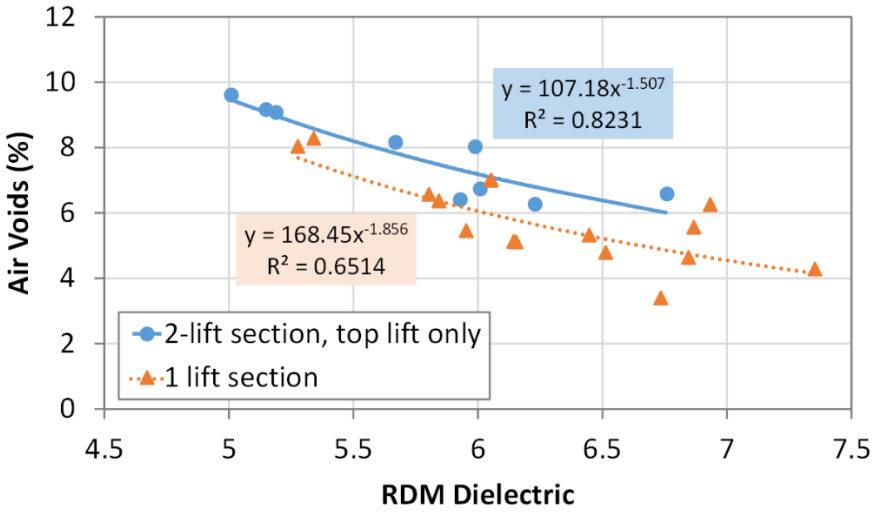

Figure 42. PaveScan RDM Calibration for DAL-SH 121 Detour/Shoulder.

The overall distribution of air voids on each project is given in Figure 43. The average air voids range from 6.1 to 7.4 percent. This figure does not distinguish among the sections within each project, though a simple observation of the distributions show that data from the DAL-SH 121 Shldr and ATL-US 59 projects clearly fell into two groupings.

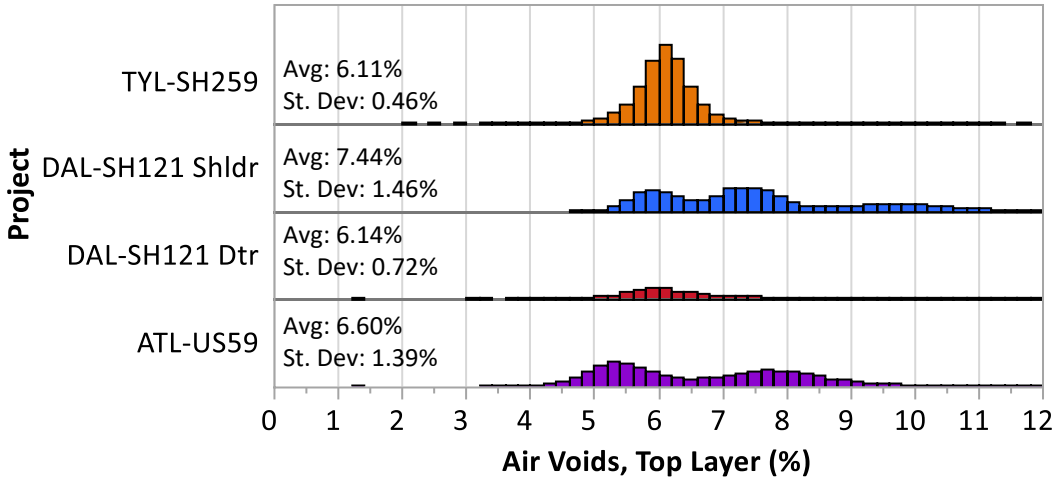

Figure 43. Air Voids in Each Project.

The predicted versus actual air voids are shown in Figure 44. The overall model was statistically significant (*p*-value < 0.001) and had a low adjusted R^2 value of 0.43. While not shown here, a model of the dielectric values (rather than the predicted air voids) had an R^2 value of 0.68, suggesting that some of the error is attributable to the air void calibrations themselves.

The statistical results for each predictor variable are shown in Table 17, and each of the four modeled main effects are illustrated in Figure 44. The most significant factor was *Lift t/NMAS* ratio. As the ratio increased (i.e., lift thickness increases), the voids decreased. *Roller passes* and *Screed setting* were significant but were not practically significant.

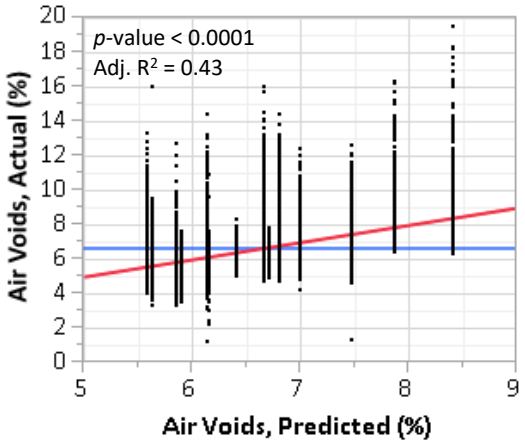

Figure 44. Predicted versus Actual Air Voids (PaveScan RDM, Top Lift).

Table 17. Statistical Results of Air Voids Analysis_PaveScan RDM.

Predictor Variable	*p*-value	−log(*p*-value)	Significant
Lift t/NMAS	< 0.0001	14600	Y
Project	< 0.0001	3880	Y
Roller passes	< 0.0001	640	Y
Lift t/NMAS * Roller passes	< 0.0001	487	Y
Screed setting	< 0.0001	6.7	Y

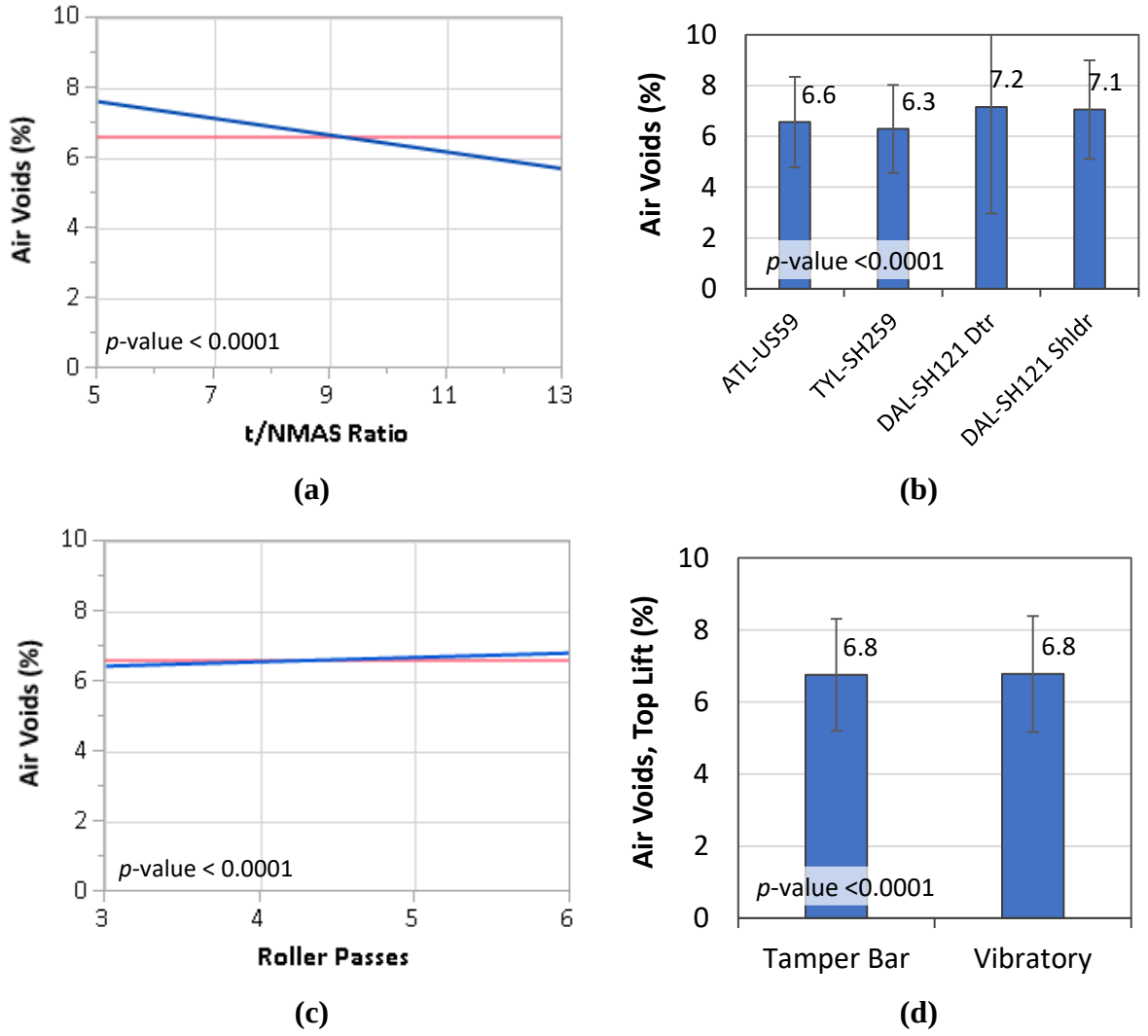

Figure 45. Air Voids (Top Lift) versus Main Effects: (a) t/NMAS Ratio, (b) Project, (c) Number of Roller Passes, and (d) Screed Setting.

REFLECTION AMPLITUDE FROM THE 3D RADAR

The 3D radar produced a wealth of data ranging the full pavement width and from the surface through the bottom of the pavement. The analysis, however, focused on the reflection amplitudes at the pavement mid-depth to compare sections with and without a bond interface.

The predicted versus actual radar reflection amplitudes at mid-depth are shown in Figure 46. The overall model was statistically significant (p-value < 0.001) and had a moderate adjusted R^2 value of 0.55. The statistical results for each predictor variable are shown in Table 17, and the main effect of *Interface Type* is illustrated in Figure 47. The reflection amplitude was statistically higher when there was a bond interface. This means that the 3D Radar could consistently detect

the presence of the less-compacted lift interface on two-lift sections. In typical construction this interface would not be desirable and should be a uniform layer. The interface was most visible on the DAL-SH 121 Detour project, which had the thickest construction. The roller passes and screed settings did not affect the pavement quality at mid-depth.

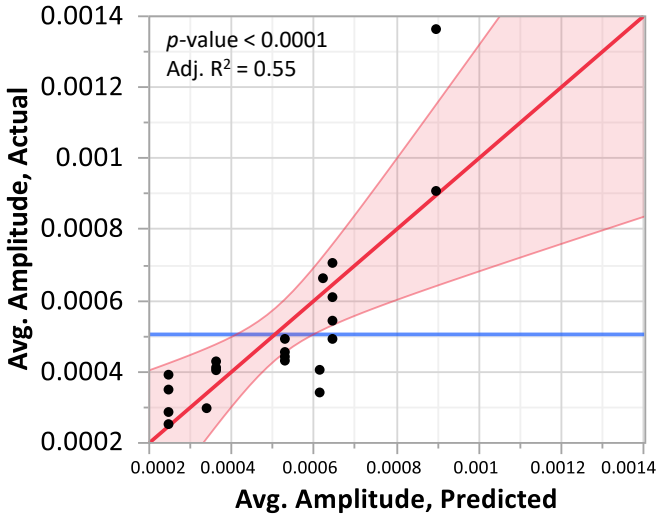

Figure 46. Predicted versus Actual Amplitude (3D Radar, Mid-Depth).

Table 18. Statistical Results of Amplitude Analysis_3D Radar.

Predictor Variable	*p*-value	−log(*p*-value)	Significant
Interface Type	0.0008	3.1	Y
Project	0.0161	1.8	Y
Roller Passes	0.7703	0.11	N (Not included)
Screed Setting	0.8085	0.92	N (Not included)

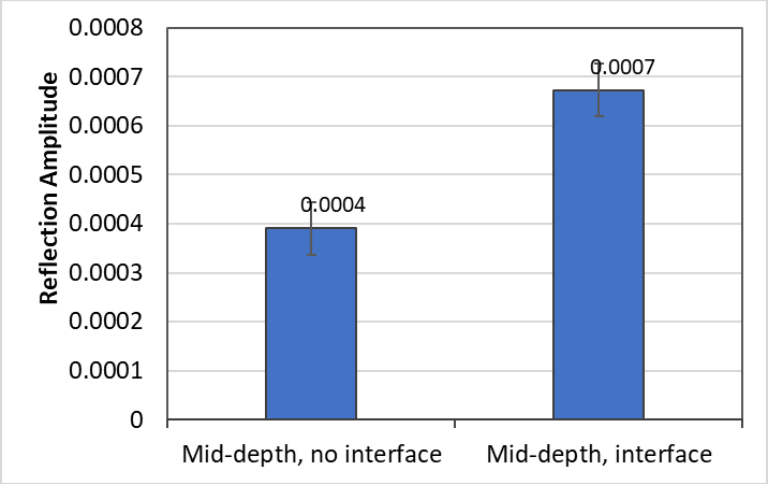

Figure 47. Reflection Amplitude versus Presence of Mid-depth Interface.

ROUGHNESS

The results of the statistical model for roughness are shown in Table 19. The *Project * Number of lifts*, *Project*, and *Project * Screed* factors had the most statistically significant results. This means that there was more variability in roughness from project to project, because of any number of unaccounted for factors, than for the main effects of interest studied, namely *Number of lifts* and *Screed settings*. Roughness by project and number of lifts is shown in Figure 48. In both the ATL and TYL projects, the single-lift test sections had higher roughness. Paving in two lifts decreased the roughness from around 90 to 70 inches/mi on these projects. This is the kind of trend that the researchers expected since the contractor can improve roughness with each subsequent lift. On the DAL project, however, the trend was drastically reversed, and the two-lift section had much higher roughness (i.e., 155 versus 85 inches/mi). The researchers conclude that building research test sections can at times cause greater confusion to the operators, which can lead to mistakes, when they are asked to diverge from their typical paving practices, making frequent changes to the construction plan. The researchers believe that the trends observed in the ATL and TYL projects are typical of what might happen when paving one versus two lifts, but statistically speaking, the data are inconclusive.

Table 19. Statistical Results of Profile Roughness Analysis.

Predictor Variable	*p*-value	−log(*p*-value)	Significant
Project * Lifts	< 0.0001	18.8	Y
Project	< 0.0001	17.3	Y
Project * Screed	0.0002	3.6	Y
Lifts	0.0011	3.0	Y
Screed setting	0.0129	1.9	Y

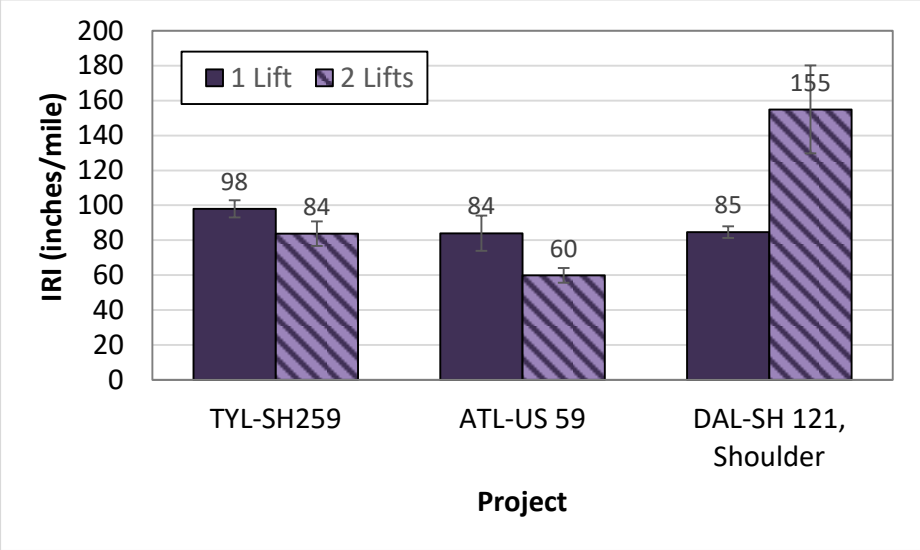

Figure 48. Profile Roughness by Project and Number of Lifts.

The *Number of lifts* and *Screed setting* were significant and are illustrated in Figure 49. In the TYL and ATL projects, the screed with the tamper bar enabled has lower roughness than with the vibratory-only setting. Again, for the DAL project, the trend was reversed. As discussed before, interpreting the effect of screed setting is somewhat difficult because the TYL and ATL projects used a different paver, different screed settings, different mixture, and a different construction crew than the DAL project. There does seem to be evidence, at least, that using a Vögele paver with the tamper bar enabled does improve roughness. This finding also matches observations by the industry.

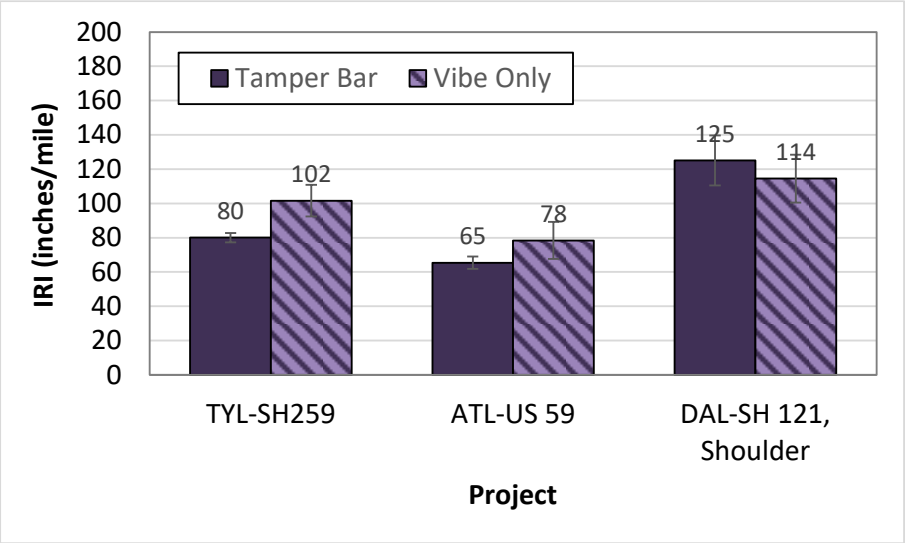

Figure 49. Profile Roughness by Project and Screed Settings.

SUMMARY

Several aspects of thick-lift paving were assessed including mat cooldown time, air voids, and roughness. The take-aways from each study are summarized below:

- **Mat Cooldown Time**
  - The middle or bottom of the mat takes at least 1.5 hours longer to cooldown than the surface.
  - An additional 1 inch of asphalt increases the cooldown time by 0.7 hours.
- **Air Voids (During construction)**
  - The mat air voids directly behind the paver were just under 9 percent.
  - The screed setting had no effect on the air voids content behind the screed. On the DAL-SH 121 projects, using a tamper bar that was actually in good condition might have affected the results.
  - Additional roller passes had the biggest effect on compaction than any other factor. Air voids decreased by 2 percent on the first pass, then by 1 percent on the second pass, and 0.1 percent by the sixth roller pass.

- **Air Voids (Overall)**
    - Roller passes again had the biggest influence on air voids, about 1.5 percent decrease per pass.
    - Two-lift cores had about 1.3 percent more air voids than single-lift cores. Air voids at the bond interface (within 0.25 inches) were very high at around 14 percent, compared to 4 percent in the middle of a single-lift core.
    - Screed settings was not a practically significant factor.
    - As the lift t/NMAS increased, so did the air voids content.
- **Air Voids (By lift)**
    - Once again, the roller passes factor was most significant. Interestingly, the *Lift t/NMAS* factor was not significant.
    - The top lift, on average, had less compaction and 1.8 percent higher air voids than the bottom lift.
- **Air Voids Uniformity**
    - The bottom of the mat was more segregated (i.e., higher air voids) for thicker lifts.
    - Additional compaction effort (i.e., screed settings and roller passes) did not have an effect on the non-uniform area at the bottom of the mat.
- **Air Voids from the PaveScan RDM**
    - The equipment (Pavescan RDM) could only investigate the top lifts.
    - Most of the compaction fell comfortably within the acceptable air voids range.
    - The TYL-SH 259 project was the most uniform and the ATL-US 59 was the least.
    - The most significant factor affecting air voids was *Lift t/NMAS*, especially on ATL-US 59 and DAL-SH 121.
- **Reflection Amplitude from the 3D Radar**
    - The 3D Radar could consistently detect the presence of a less-compacted lift interface on two-lift sections.

- Roller passes and screed settings did not affect the pavement quality at mid-depth.

- **Roughness**
  - There was more variability in roughness from project to project, than from the number of lifts or the screed settings.
  - Interpreting the effects of number of lifts and screed settings was difficult since the trends observed on TYL-SH 259 and ATL-US 59 were opposite than what was observed on DAL-SH 121 Shoulder.
  - Paving with the Vögele paver with the tamper enabled bar did reduce roughness. The Caterpillar tamper bar paver required servicing (tamper bar worn down significantly), so the results on that job are inconclusive.

CHAPTER 5:
CONCLUSION

OVERVIEW

Thick-lift paving is the placement of asphalt concrete in a lift greater than the allowable maximum. With thick-lift paving, a contractor can construct a thick design layer in a single lift instead of two or three separate lifts. This approach can streamline paving operations, eliminate bond interfaces, and save money by eliminating a tack coat. Still, there can be challenges and concerns with thick-lift paving such as potential for inadequate and non-uniform compaction, lower ride quality, and long cooldown times. The purpose of this research was to determine whether a tamper bar paver can effectively place asphalt concrete in thick lifts and to identify the best practices to do so.

Tamper bar pavers were deployed on three paving projects to place thick asphalt layers ranging from 6 to 10 inches thick. On each project, test sections were constructed in one or two lifts, evaluating different lift thicknesses, paver screed settings, and rolling patterns. The research team monitored the asphalt cooldown time after laydown and the mat density throughout compaction. After construction, the in-situ pavement density was tested with 3D Radar and a rolling density meter. Cores were sampled for laboratory testing including CT scanning for air void uniformity and bulk air void testing. Each project was profiled to measure ride quality.

FINDINGS

The following are key findings from the research.

Mat Cooldown Time

- The middle or bottom of a thick mat takes at least 1.5 hours longer to cooldown than the surface.
- An additional 1 inch of asphalt increases the cooldown time by 0.7 hours.

Air Voids

- Overall mat compaction was acceptable for all test sections, even when paving in less-than-ideal circumstances.
- The screed setting (i.e., whether the tamper bar was enabled or disabled) had no effect on the air voids behind the screed. On the DAL-SH 121 projects, using a tamper bar screed that was in better condition may have affected the results.
- Additional roller passes had the biggest effect on compaction than any other factor but with diminishing returns. On average, each pass reduced the air voids by 1.5 percent, but the sixth roller pass reduced the air voids by only 0.1 percent.
- Two-lift cores had about 1.3 percent higher air voids than single-lift cores because the air voids at the bond interface were considerably higher (about 14 percent) compared to the rest of the core (about 4 percent).
- As the ratio of lift thickness to NMAS increased, so did the air voids content.
- The bottom of the mat was more segregated (i.e., higher air voids) for thicker lifts. Additional compaction effort did not improve compaction at the bottom of the mat.

Air Voids from the PaveScan RDM

- The Pavescan RDM could only investigate the top lifts and was unsuitable for testing the full-layer air voids on two-lift sections.
- Most of the compaction fell comfortably within the acceptable range of air voids.
- The most significant factor that affected the air voids was *Lift t/NMAS*, especially on ATL-US 59 and DAL-SH 121.

Reflection Amplitude from the 3D Radar

- The 3D Radar could consistently detect the presence of a less-compacted lift interface on two-lift sections.
- Roller passes and screed settings did not affect the pavement quality at mid-depth.

Roughness

- The evaluation of roughness was inconclusive. There was more variability from project to project than from the number of lifts or the screed settings.
- The trends observed on TYL-SH 259 and ATL-US 59 were opposite than what was observed on DAL-SH 121 Shoulder.
- Still, the research team believes that roughness would generally improve with multiple lifts.

RECOMMENDATIONS

Thick-lift asphalt concrete paving is a valid construction approach. A thick one-lift layer has better overall compaction, and more uniform compaction, than a two-lift layer because the high-air void interface is eliminated. Still, there are constraining factors, such as long cooldown times and potentially increased roughness, that limit the scenarios that are appropriate for thick-lift construction. The scenarios for when and when not to use thick-lift paving are shown in Table 20.

Table 20. Scenarios for Thick-Lift Paving.

When to Use Thick-Lift Paving	When NOT to Use Thick-Lift Paving
• Thick mill-and-fill patches. • To place thick intermediate lifts at one time (e.g., place one 4-inch lift of SP Type C instead of two 2-inch lifts). • Asphaltic concrete base layers. • Perpetual pavement layers. • When there is a concern with bonding of multiple lifts. • When there is a concern with air voids at the lift interface.	• For the final riding surface when optimal ride quality is needed. • Roadway needs to be opened to traffic very quickly. • If mixture delivery will not be consistent. Frequent paver stops will increase roughness. • If milling and construction would leave excessive work zone drop-offs that cannot be adequately protected.

The following are guidelines for the best practices for thick-lift paving, followed by recommendations for future research. The guidelines were also presented in a stand-alone document titled “Thick-Lift Asphalt Concrete Paving Guidelines: Benefits, Scenarios, and Construction.” Draft special provisions were prepared for Item 320, “Equipment for Asphalt

Concrete Pavement;" Item 340, "Dense-Graded Hot-Mix Asphalt (Small Quantity);" Special Specification (SS) 3077, "Superpave Mixtures;" and SS3076, "Dense-Graded Hot-Mix Asphalt."

Paving Equipment

- Use a tamper bar paver to increase compaction behind the screed and improve ride quality in thick-lift paving. During the study, the effect of the tamper bar screed was generally insignificant; however, this may be a result of certain confounding factors with the equipment condition and contractor operations.
- Tamper bar pavers can be used for any type of paving, not just for thick lifts. The equipment is larger than a traditional paver, so it may not be suitable for paving in some confined spaces.
- There are multiple types of tamper bar and other high-compaction screeds on the market. These screeds must be used with a compatible paver model.
- Ensure the tamper bar plate and other screed components are in proper working order. Replace the plate if it is excessively worn.
- The researchers believe that thick-lift paving can also be performed with a lighter, traditional vibratory screed and paver, but this was outside the scope of the study.

Compaction

- Add one or two roller passes (defined as down-and-back) to the rolling pattern. Of all the study factors, this was the most effective way to improve compaction. This is especially important if paving with a traditional vibratory screed.
- Use pneumatic rollers to improve deep compaction when placing base or intermediate layers.
- Be sure to roll unconfined edges of the mat, but monitor for lateral movement of the mat that may cause the roller to sit unevenly.

Opening to Traffic

- Use tools to estimate the cooldown time in the design process to help determine traffic control strategies. (See the MultiCool calculator, hosted by Auburn University: https://www.eng.auburn.edu/users/timmdav/MultiCool/FinalRelease/Main.html.)
- Keep traffic closed until the surface temperature reaches 160°F.
- As needed, apply water to the surface to shorten the cooldown time.
- Keep in mind that lowering the mixing and application temperatures (e.g., using warm mix) does not substantially shorten the cooldown time.

Ride Quality

- Since paving in one lift usually results in a rougher ride, consider providing additional smoothness opportunities such as milling, leveling-up, or placing a final surface course.
- Recognizing that ride quality is affected, use pay schedule 3 in Item 585, "Ride Quality for Pavement Surfaces."
- Ensure the mix delivery is sufficient to minimize paver stops.
- Rolling patterns should be optimized to ensure the compaction operation does not contribute to roughness.

Topics for Future Research

- Evaluating a traditional paver with a vibratory screed in thick-lift paving.
- Evaluating compaction and roughness when using a tamper bar and other high-compaction screed models in a production environment for thick-lift paving.

REFERENCES

1. ForConstructionPros. CONEXPO Video: A Look at the Vogele Tamper Screed. *YouTube*. https://www.youtube.com/watch?v=wGp1_3-VX04. Accessed Feb. 6, 2020.
2. Caterpillar SE50 VT Tamper Bar Screed. https://www.cat.com/en_US/products/new/equipment/asphalt-pavers/screeds/1000001356.html. Accessed Feb. 6, 2020.
3. Vogele Pavers. Dash 3 Paver Super 2100-3i. *For Construction Pros*. https://www.forconstructionpros.com/asphalt/pavers/product/11328712/vogele-wirtgen-group-dash-3-paver-super-21003i. Accessed Feb. 6, 2020.
4. Volvo Construction Equipment | ABG High Compaction Screed. https://www.volvoce.com/united-states/en-us/attachments/abg-tracked-pavers-attachments/. Accessed Feb. 10, 2020.
5. Narsingh, L. and Vogele, Wirtgen Group. *Personal Communication*. Phone interview, 2020.
6. ISO/TC 195/WG 5. *Road Construction and Maintenance Equipment - Asphalt Pavers - Terminology and Commercial Specifications*. ISO/WD 15878. 2014.
7. Lombardo, J. How Screeds Improve Paving Performance. Asphalt Contractor, June/July 2017, May 31, 2017, pp. 44–52.
8. Turner, C. Personal Phone Conversation about Tamper Bar Pavers. May 09, 2019.
9. Scherocman, J. A., T. W. Kennedy, M. Tahmoressi, and R. Holmgreen. *Inspectors' Guide: Mat Problems (from Hot Mix Asphalt Construction Training Program)*. T2-1. Center for Transportation Research, University of Texas at Austin, Austin, TX, 1988, p. 16.
10. Virginia Department of Transportation. Materials Certification School: Asphalt Field Certification Study Guide. , 2012.
11. Wentland, K. A. Roller-Compacted Concrete Pavement, An Industry Perspective. Presented at the International Society for Concrete Pavements, 2005.
12. Abrams, J. M., J. L. Jacksha, R. L. Norton, and D. J. Irvine. Roller-Compacted Concrete Pavement at Portland International Airport. *Transportation Research Record*, No. 1062, 1986.
13. *Vibro-Duo Tamp High-Density Screed Paver*. Bulletin 101.1084. Hameln, Federal Republic of Germany.
14. Madden, D. Tamper Screed Experience: Presentation. , 2018.
15. Roberts, F. L., P. S. Kandhal, E. R. Brown, D.-Y. Lee, and T. W. Kennedy. *Hot Mix Asphalt Materials, Mixture Design & Construction*. National Asphalt Pavement Association, 1996.
16. Lombardo, J. Five Forces Acting on Your Asphalt Paver Screed. *For Construction Pros*. https://www.forconstructionpros.com/asphalt/pavers/article/21110400/five-forces-acting-on-your-asphalt-paver-screed. Accessed Jan. 27, 2020.
17. Kuennen, T. For Perfect Paving, Know the Five Forces of a Floating Screed. p. 2.
18. Cooley Jr, L. A., and K. L. Williams. *Evaluation of Hot Mix Asphalt (HMA) Lift Thickness*. Burns Cooley Dennis, Inc, Jackson, Mississippi, 2009.
19. Hainin, M. R., N. I. M. Yusoff, M. K. I. Mohd Satar, and E. R. Brown. The Effect of Lift Thickness on Permeability and the Time Available for Compaction of Hot Mix Asphalt

Pavements Under Tropical Climate Condition. *Journal of Construction and Building Materials*, No. 48, 2013.
20. Larrain, M. M. *Analytical Modeling Of Rutting Potential Of Asphalt Mixes Using Hamburg Wheel Tracking Device*. Thesis for M.Sc Civil Engineering. Univeristy of New Mexico, Albuquerque, New Mexico, 2015.
21. Chen, Q., and Y. Li. SGC Tests for Influence of Material Composition on Compaction Characteristic of Asphalt Mixtures. *The Scientific World Journal*, Vol. 2013, 2013. https://doi.org/10.1155/2013/735640.
22. Anderson, R. M., and H. U. Bahia. Evaluation and Selection of Aggregate Gradations for Asphalt Mixtures Using Superpave. *Transportation Research Record*, Vol. 1583, No. 1, 1997, pp. 91–97. https://doi.org/10.3141/1583-11.
23. Stakston, A. D., H. U. Bahia, and J. J. Bushek. Effect of Fine Aggregate Angularity on Compaction and Shearing Resistance of Asphalt Mixtures. *Transportation Research Record*, Vol. 1789, No. 1, 2002, pp. 14–24. https://doi.org/10.3141/1789-02.
24. Factors Affecting Compaction. *Pavement Interactive*. https://pavementinteractive.org/reference-desk/construction/compaction/factors-affecting-compaction/. Accessed Feb. 5, 2020.
25. Pavement Manual: Hot-Mix Asphalt Pavement Mixtures. http://onlinemanuals.txdot.gov/txdotmanuals/pdm/hma_p_mix.htm. Accessed Feb. 25, 2020.
26. Brown, E. R., B. Lord, D. Decker, and D. Newcomb. Hot Mix Asphalt Tender Zone. 2000.
27. Hughes, C. S. *NCHRP Synthesis 152: Compaction of Asphalt Pavement*. Virginia Transportation Research Council, Washington, D.C., 1989.
28. QIP 118 Cold Weather Compaction. http://driveasphalt.org/assets/content/resources/QIP-118_Cold_Weather_Compaction.pdf. Accessed Feb. 13, 2020.
29. Scherocman, J. A. *Compacting Hot-Mix Asphalt Pavements: Part I*. 2000.
30. Chadbourn, B. A., D. Newcomb, V. Voller, R. A. Desombre, J. A. Luoma, and D. H. Timm. *An Asphalt Paving Tool for Adverse Conditions*. Mn/DOT 1998-18. University of Minnesota, Minneapolis, MN, 1998.
31. Timm, D. H., V. Voller, E. Lee, and J. Harvey. Calcool: A Multi-Layer Asphalt Pavement Cooling Tool for Temperature Prediction During Construction. *International Journal of Pavement Engineering*, Vol. 2, No. 3, 2001, pp. 169–185.
32. Choubane, B., G. C. Page, and J. A. Musselman. *Investigation of Water Permeability of Coarse Graded Superpave Pavements*. FL/DOT/SMO/97-416. Florida Department of Transportation, State Materials Office, Gainesville, Florida, 1997.
33. Russell, J. *Effect of Pavement Thickness on Superpave Mix Permeability and Density*. Wisconsin Department of Transportation, Madison, Wisconsin, 2005.
34. Brown, E. R., M. R. Hainin, L. A. Cooley Jr, and G. C. Hurley. *Relationship of Air Voids, Lift Thickness, and Permeability in Hot Mix Asphalt Pavements*. NCHRP Report 531. National Center for Asphalt Technolgy, Washington, D.C., 2004.
35. Hand, A., and J. A. Epps. *Factors Affecting Compaction of Asphalt Pavements*. E-C105. 2006.
36. Compaction Pavement Interact. *Pavement Interactive*. https://pavementinteractive.org/reference-desk/construction/compaction/. Accessed Feb. 19, 2020.
37. Caltrans. *Standard Specifications.* Department of Transportation, California, 2018.

38. FDOT. *Standard Specifications for Road and Bridge Construction*. Florida Department of Transportation, Tallahassee, FL, 2010.
39. MnDOT. *Standard Specifications for Construction*. Minnesota Department of Transportation, 2018.
40. TxDOT. *Standard Specifications for Construction and Maintenance of Highways, Streets, and Bridges*. Texas Department of Transportation, Austin, TX, 2014.
41. ODOT. *ODOT 2010 Construction and Material Specifications*. Ohio Department of Transportation, Columbus, OH, 2010.
42. Alaska Department of Transportation and Public Facilities. *Standard Specifications for Highway Construction*. Alaska Department of Transportation and Public Facilities, Juneau, Alaska, 2020.
43. ADOT. *Standard Specifications for Road and Bridge Construction*. Arizona Department of Transportation, Phoenix, Arizona, 2008, p. 1089.
44. GDOT. *Section 400 - Hot Mix Asphaltic Concrete Construction*. Georgia Department of Transportation, Atlanta, GA, 2013, p. 41.
45. IDOT. *Standard Specifications for Road and Bridge Construction*. Illinois Department of Transportation, 2016.
46. KYCT. *Division 400 Asphalt Pavements*. Kentuky Transportation Cabinet, Frankfort, Kentucky, 2019.
47. LDOT. *Standard Specifications For Roads And Bridges*. Louisiana Department of Transportation, Baton Rough, Louisiana, 2016.
48. MDOT. *Standard Specifications for Construction AndMaterials*. 2018.
49. MassDOT. *Supplemental Specifications to the 1988 English Standard Specifications for Highways and Bridges and the 1995 Metric Standard Specifications for Highways and Bridges - April 1, 2019*. Massachusetts Department of Transportation, Massachusetts, 2019, p. 363.
50. NMDOT. *Standard Specifications for Highway and Bridge Construction*. New Mexico Department of Transportation, 2019.
51. NYDOT. *Volume 2 Standard Specifications (US Customary Units)*. New York Department of Transportation, Albany, New York, 2020, p. 448.
52. ODOT. *Oregon Standard Specifications for Construction*. Oregon Department of Transportation, 2018.
53. SCDOT. *2007 Standard Specifications for Highway Construction*. South Carolina Department of Transportation, Columbia, South Carolina, 2007, p. 1080.
54. VDOT. *2016 Road and Bridge Specifcations*. Virginia Department of Transportation.
55. Wisconsin Department of Transportation. Chapter 4, Section 57 - Asphalt Pavers. In *Construction and Materials Manual*, p. 6.
56. Frequently Asked Questions | Asphalt Pavement Construction | "What Is the Proper Nominal Aggregate Size to Use?" *Asphalt Institute*. http://www.asphaltinstitute.org/engineering/frequently-asked-questions-faqs/asphalt-pavement-construction/. Accessed Feb. 26, 2020.
57. Rebbechi, J., and L. Petho. *Guide to Pavement Technology Part 4B: Asphalt*. Austroads, Sydney, Australia, 2014, p. 139.

APPENDIX A:
VALUE OF RESEARCH

Table 21 is a summary of the qualitative value of the research. Figure 50 is a summary of the value of research based on the cost of research and potential future savings.

Table 21. Qualitative Value of Research.

Project Number: 0-7064							
Project Title: "Use of Tamper Bar Paver to Place Thick Lift Asphalt Concrete Pavement"							
Qualitative Value							
Benefit Area	**Qualitative**	**Economic**	**Both**	**TxDOT**	**State**	**Both**	**Definition in context with the Project Statement and Value**
Traffic and Congestion Reduction		X			X		Providing flexibility in construction processes can lead to innovative design improvements that can reduce delays during construction.
Reduced Construction, Operations, and Maintenance Cost		X			X		Cost saving opportunity by allowing flexibility of the contractors' operations. Placing thicker lifts also reduces the need for tack coat to help ensure bond, which is a cost savings. Construction of layers that have uniform air voids can lead to more durable pavements resulting in reduced operation and maintenance costs.
Materials and Pavements		X			X		The characteristics and factors that affect long-term durability of asphaltic concrete pavement can be improved through this construction process.

VoR

Project #	0-7064			
Project Name:	Use of Tamper Bar Paver to Place Thick Lift Asphalt Concrete Pavement			
Agency:	TTI	Project Budget	$	412,634
Project Duration	3	Exp. Value (per Yr)	$	1,421,193
Expected Value Duration (Yrs)	10	Discount Rate	2%	

Economic Value

Total Savings:	$ 12,181,123	Net Present Value (NPV):	$	12,593,757
Payback Period (Yrs):	2.2	Cost Benefit Ratio (CBR, $1 : $___):	$	31
		Return on Investment (ROI, $1 : ___):	$	33.44

Years	Expected Value
0	$0
1	$1,421,193
2	$1,421,193
3	$1,421,193
4	$1,421,193
5	$1,421,193
6	$1,421,193
7	$1,421,193
8	$1,421,193
9	$1,421,193
10	$1,421,193

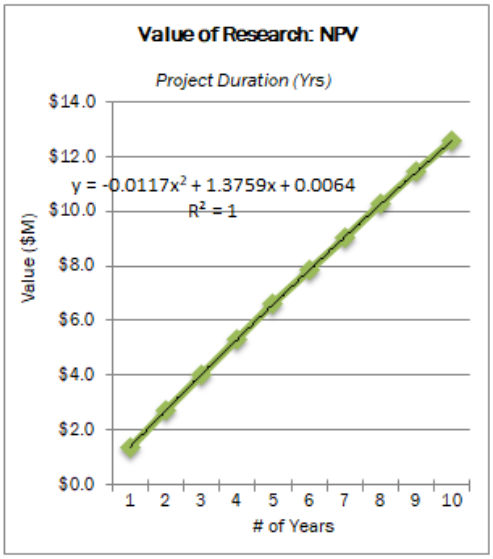

Variable Justification

Placing thicker lifts will reduce the need for tack coat which is used between multiple lifts. In the last 12 months, TxDOT has contracted with ITEMS 340, 3076 and 3077 $10,956,009.08 for tack coat. If assume that 25% of the projects place thick lifts then the savings in tack coat alone would be $1,421,193 (Cost * 25% projects* half of tack coat needed).

May 2022 statewide low bid

			Construction Contracts		Maintenance Contracts		
ITEM CODE	ITEM DESCRIPTION	ITEM UNIT	STATEWIDE 12M QUANTITY	STATEWIDE 12M AVG	STATEWIDE 12M QUANTITY	STATEWIDE 12M AVG	Total
03406272	TACK COAT	GAL	88,427.51	$3.47	29,931.00	$3.42	$409,207.48
30766066	TACK COAT	GAL	1,205,355.32	$3.30	36,114.20	$2.94	$4,083,848.30
30776075	TACK COAT	GAL	1,827,806.32	$3.65	66,129.27	$3.10	$6,876,493.81
						Total	$11,369,549.59
						25% projects	$2,842,387.40
						use 1/2 the tack	$1,421,193.70

Figure 50. Value of Research.

APPENDIX B:

LITERATURE REVIEW DETAILS

The review of thick-lift paving practices by 19 states, the Asphalt Institute, and Austroads is presented in Table 22.

Table 22. Specifications and Guidance for Thick-Lift Paving.

State/ Agency	Item Number	Item Title	Mixture Type	Nominal Max. Agg. Size (inch)	Max. Lift Thickness (inch)	Max. t/NMAS Ratio
Texas	340/341	Dense-graded[1]	Type A	1.5	6	4.0
			Type B	1	5	5.0
			Type C	0.75	4	5.3
	344	Superpave[1]	Type A	1.5	5	3.3
			Type B	1	4	4.0
			Type C	0.75	3	4.0
Alaska	401	Hot Mix Asphalt Pavement	Type I to V and SP	0.5 to 1.0	3	3 to 6
Arizona	409	Asphaltic Concrete (Miscellaneous Structural)	—	0.5	2	4.0
			—	0.75	No limit[2]	No limit[2]
Asphalt Institute	NA	FAQ: What is the proper nominal aggregate size to use?[3]	NA	NA	NA	NA
Australia	NA	Austroads Pavement Guide[4]	10 mm	0.4	1.6–2.0	4 to 5
			14 mm	0.5	2.2–2.8	4 to 5
			20 mm	0.8	3.1–3.9	4 to 5
			28 mm	1.1	4.4–5.5	4 to 5
California	39 2.02	Type A HMA[5]	—	0.75	No limit	No limit
			—	1	No limit	No limit
Florida	330	Hot Mix Asphalt—General Construction Requirements[6]	—	NA	NA	NA
	334	Superpave[6]	Type SP-12.5 (fine)	0.5	2.5	5.0
			Type SP-19.0 (fine)	0.75	3	4.0
			Type SP-12.5 (coarse)	0.5	3	6.0
			Type SP-19.0 (coarse)	0.75	3.5	4.7
	234	Superpave Asphalt Base[6]	Type B-12.5	0.5	3	6.0

Note: — = not defined; NA = not applicable.

1. On lifts > 2.5 inches, the amplitude setting on the vibratory roller compactors should be increased.
2. Not explicit in the specification.
3. With static rollers, limited to 3-inch thickness. With vibratory or pneumatic rollers, there is no practical limit to lift thickness, but still thickness generally limited to 6 or 8 inches.
4. General maximum limits, but not a hard-specified rule. When going to a ratio > 4, may be more economical to use a larger sized mixture.
5. When pavement thickness is 4 inches or greater, contractor may place in multiple lifts. Minimum ambient and surface temperatures are 10°F lower for lifts ≥ 1.8 inches.
6. When > 1 inch thick, minimum ambient temperature is 45°F for PG76+ mixtures and 40°F for < PG76 mixtures.

Table 22. Specifications and Guidance for Thick-Lift Paving. (continued)

State/ Agency	Item Number	Item Title	Mixture Type	Nominal Max. Agg. Size (inch)	Max. Lift Thickness (inch)	Max. t/NMAS Ratio
Georgia	400	Hot Mix Asphalt Concrete Construction[7]	25-mm Superpave	1	5	5.0
			19-mm Superpave	0.75	3	4.0
			12.5-mm Superpave	0.5	2.5	5.0
Illinois	406	Hot Mix Asphalt Binder and Surface Course	—	NA	No limit	No limit
Kentucky	403	Production and Placement of Asphalt Mixtures	19	0.75	3.5	4.7
			25	1	4.5	4.5
			37.5	1.5	5	3.3
Louisiana	502	Asphalt Concrete Mixtures	12.5 Wearing Course or Incidental Paving	0.5	2	4.0
			19.0 Wearing Course	0.75	2	2.7
			19.0 Binder Course	0.75	3	4.0
			25.0 Binder Course	1	4	4.0
			25.0 Base Course and ATB	1	No limit	No limit
			37.5 Base Course	1.5	No limit	No limit
			SMA Wearing	0.5	2	4.0
Maryland	505	Asphalt Patches	12.5	0.5	3	6.0
			19	0.75	4	5.3
			25	1	5	5.0
			37.5	1.5	6	4.0
Massachusetts	450	Hot Mix Asphalt Pavement[8]	—	NA	NA	4.0

Note: — = not defined; NA = not applicable.

7. Maximum total thickness of a 12.5-mm mixture restricted to 8 inches. No restriction on 25-mm or 19-mm mixtures. Allow up to 6 inches per lift on trench widening. Place 12.5-mm Superpave up to 4 inches thick for driveway and side road transition. For lift thicknesses between 4.1 to 8 inches, no specified minimum air temperature. Left to the contractor's discretion.
8. Specific for patching mixture.

Table 22. Specifications and Guidance for Thick-Lift Paving. (continued)

State/ Agency	Item Number	Item Title	Mixture Type	Nominal Max. Agg. Size (inch)	Max. Lift Thickness (inch)	Max. t/NMAS Ratio
Minnesota	2360	Plant Mixed Asphalt Pavement[9]	SPNWA	0.5	No limit	No limit
			SPNWB	0.75	No limit	No limit
			SPNWC	1	No limit	No limit
New Mexico	416	Minor Paving	SP-III	0.75	3.5	4.7
			SP-IV	0.5	3	6.0
			SP-V	0.375	1.5	4.0
New York	402	Hot Mix Asphalt (HMA) Pavement	12.5 Top Course	0.5	2	4.0
			19.0 Binder Course	0.75	3	4.0
			25.0 Binder Course	1	3	3.0
			25.0 Base Course	1	5	5.0
			37.5 Base Course	1.5	5	3.3
Ohio	442	Superpave Asphalt Concrete	Surface, 12.5 mm	0.5	2.5	5.0
			Intermediate, 19 mm	0.75	3	4.0
	301	Asphalt Concrete Base	Base	1.5	6	4.0
	302	Asphalt Concrete Base	Base	2	7.75	3.9
Oregon	00745	Asphalt Concrete Pavement - Statistical Acceptance	3/8" ACP	0.375	4	10.7
South Carolina	401	Hot Mixed Asphalt (HMA) Pavement	HMA Aggregate Base Course	NA	4.5	NA
			HMA Sand Base Course	NA	3	NA
			HMA Intermediate Course	0.375	3	8.0
			HMA Surface Course	0.187 to 0.375	2	5.3 to 10.7
Virginia	315	Asphalt Concrete Placement	Superpave	NA	NA	4.0
Wisconsin	460	Hot Mix Asphalt Pavement	—	1.5	6	4.0
			—	1	6	6.0
			—	0.75	5	6.7
			—	0.5	4	8.0

Note: — = not defined; NA = not applicable.

9. For patch work (no specification on patch size), perform "ordinary compaction." Minimum mixture temperature varies based on lift thickness and air temperature. Between 225 and 250°F for thickness ≥ 3 inches. Thicker lifts improves density, while multiple thinner lifts improve rideability (especially one lift to two).

APPENDIX C:
TESTING MECHANICAL PROPERTIES OF CORES

Select cores were used to test stiffness and cracking resistance (Figure 51). The resilient modulus test has simple sample preparation procedures and is performed very quickly. The test is also non-destructive allowing further testing of cracking performance with the same samples. The cores were then tested for their resistance to cracking using the indirect tensile asphalt cracking test (IDEAL-CT). The output of the IDEAL-CT test is the Cracking Tolerance (CT) Index, which is a mechanistic-based parameter.

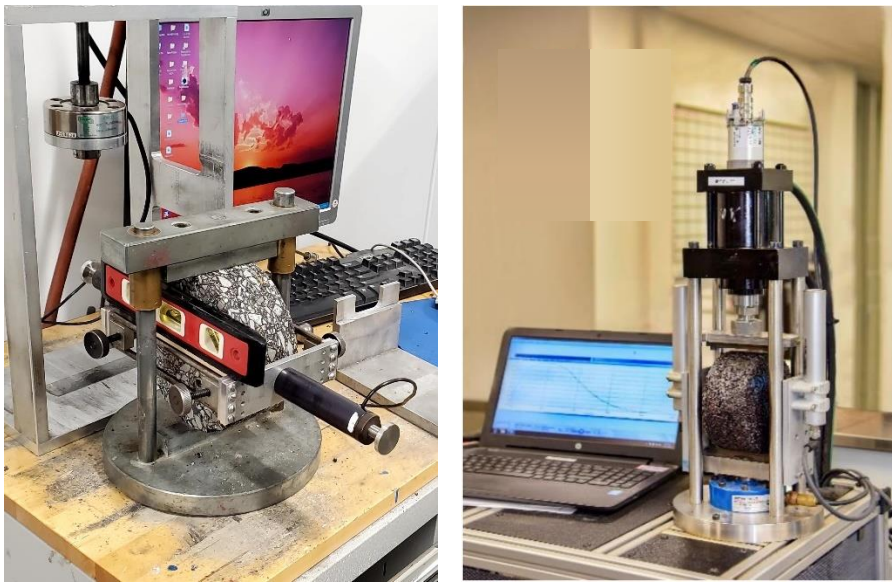

Figure 51. Test Equipment for Resilience Modulus (left) and IDEAL-CT (right).

The effect of air voids on the layer stiffness (i.e., modulus of resilience) is shown in Figure 52, and the statistical summary is in Table 23. The DAL-SH 121 SP Type B mixture was very sensitive to changes in air voids content, where increased air voids decreased the stiffness. The TYL-SH 259 and ATL-US 59 mixture, which was the same SP Type C design, showed practically no change with air voids. The SP Type B mixture was a little less than twice as stiff as the SP Type C mixture.

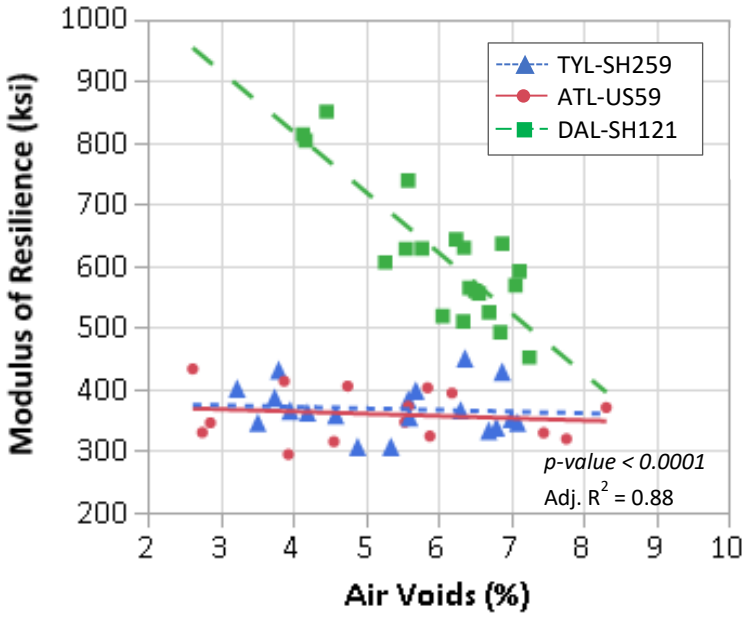

Figure 52. Modulus of Resilience versus Air Voids.

Table 23. Statistical Results of Resilient Modulus Analyses.

Predictor Variable	*p*-value	−log(*p*-value)	Significant
Project	< 0.0001	23.0	Y
Project *Air Voids	< 0.0001	7.6	Y
Air Voids	< 0.0001	7.0	Y

The effect of air voids on cracking susceptibility (i.e., CT index) is shown in Figure 53, and the statistical summary is in Table 24. The CT index increased linearly with air voids. The SP Type C mixture had higher stiffness than the SP Type B mixture.

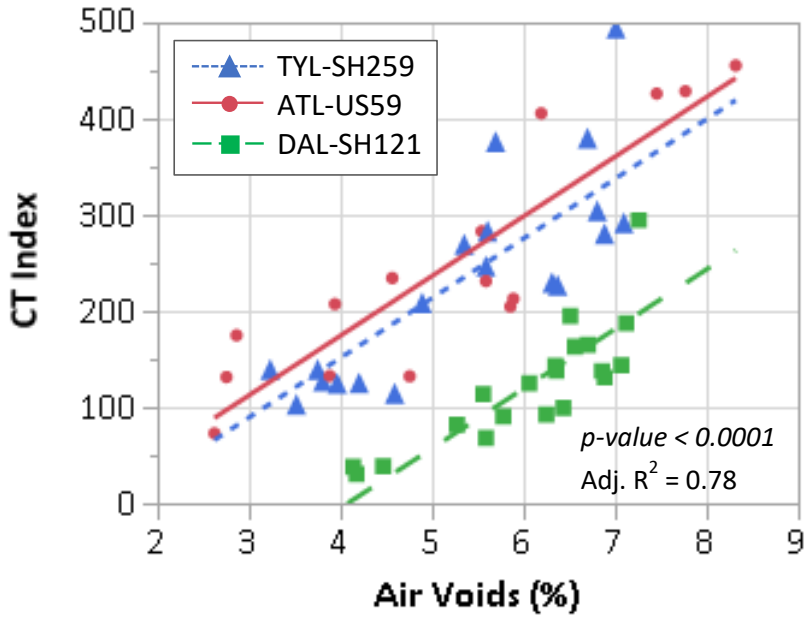

Figure 53. CT Index versus Air Voids.

Table 24. Statistical Results of CT Index Analyses.

Predictor Variable	*p*-value	−log(*p*-value)	Significant
Air Voids	< 0.0001	14.9	Y
Project	< 0.0001	13.2	Y

APPENDIX D:
STATISTICAL ANALYSIS FORMULATION

This appendix provides the details of how each analysis was formulated and defines the response variable, predictor variables, data set, and sample size. As needed, information about unique modeling approaches are also presented.

MAT COOLDOWN TIME

The effect of lift thickness on cooldown time was evaluated using a multivariate analysis of variance. The data analysis parameters and defined data set are detailed in Table 25.

Table 25. Inputs for Cooldown Time Analysis.

Response Variable	Predictor Variables	Factor Levels/Ranges
Time until 160°F (hr)	Project	• TYL-US 259 • DAL-SH 121, Detour • DAL-SH 121, Shoulder
	Thickness	• 4.5 to 10 inches
	Laydown temperature	• 301 to 323°F
	Sensor location	• Surface (IR) • Top of lift • Middle of lift • Bottom of lift

Sample Size: 16

AIR VOIDS DURING CONSTRUCTION

The effect of several project variables on the in-situ air voids, measured with the PQI, was evaluated with a multivariate analysis of covariance (MANCOVA) and later with non-linear regression analysis. The variables and the defined data set of 473 measurements is described in Table 26. For this analysis, the number of roller passes was transformed with a log(X+1) operation since the effect of passes was strongly non-linear when considering passes from 0 through 7. The model was then built using linear regression, evaluating only the variables as main effects.

Table 26. Inputs for Air Voids during Construction Analysis.

Response Variable	Predictor Variables	Factor Levels/Ranges
Air Voids from PQI (%)	Project	• TYL-SH 259 • ATL-US 59 • DAL-SH 121, Detour • DAL-SH 121, Shoulder
	Lift Thickness	• 3 to 10 inches
	Lift	• Bottom • Top
	Screed Setting	• Tamper bar • Vibratory only
	log(Breakdown Roller Passes + 1)	• 0 through 7 passes

Sample Size: 473

An alternative non-linear model was created to illustrate the change in air voids during compaction. The model is in the form of an exponential decay function which defines the initial value, a terminal value represented as a horizontal asymptote, and a decay rate. Models with this form were developed for each test section (27 total), and both the high and low roller pass sections were combined into one. The overall model was created by averaging the model parameters for the 27 section-level models.

Using the non-linear models, the team further investigated the effect of screed type on the mat density directly behind the paver before any roller passes were applied. The analysis factors and sample size are shown in Table 27.

Table 27. Inputs for Air Voids behind the Screed Analysis.

Response Variable	Predictor Variables	Factor Levels/Ranges
Air voids from PQI (%) but only directly behind the paver (0 passes)	Project	• TYL-SH 259 • ATL-US 59 • DAL-SH 121, Detour • DAL-SH 121, Shoulder
	Lift thickness	• 3 to 10 inches
	Lift	• Bottom, Top
	Screed setting	• Tamper bar, • Vibratory only

Sample Size: 473

AIR VOIDS FROM CORES

This section describes the different statistical analyses of air voids from the core samples. The first analysis was the overall air voids from the bulk saturated surface-dry (SSD) testing. Next was the analysis of air voids by lift, still based on bulk SSD data. Last was the analysis of air voids uniformity based on the computed tomography (CT) scan data.

Overall Air Voids

The effect of several project variables on the core air voids, measured with the bulk SSD method, was evaluated with a MANCOVA. The variables used in this analysis, and the defined data set of 152 samples, is described in Table 28. While lift thickness and pavement thickness itself wasn't used directly as a variable, the ratio of lift thickness to the NMAS was included. This term captures both the paving thickness and mixture properties in a single term. For this analysis, and throughout the project, the actual lift thickness, as measured from the cores, was used in the ratio calculation.

Table 28. Analysis of Core Air Voids (Overall).

Response Variable	Predictor Variables	Factor Levels/Ranges
Overall air voids, bulk SSD (%)	Project	• TYL-US 259 • ATL-US 59 • DAL-SH 121, Detour • DAL-SH 121, Shoulder
	Number of lifts	• 1 lift, 2 lifts
	Lift thickness* /NMAS	• 4.7 to 13.7
	Screed setting	• Tamper bar • Vibratory only
	Breakdown roller passes	• 3 to 6

Sample Size: 152
** Used actual core thickness.*

A statistical model was built using stepwise regression. The possible model parameters included the variables in Table 28 as main effects and all two-way interactions. Both a forward

and backward stepwise approach was used, adding or subtracting parameters until the minimum BIC was achieved. Main effects were always included when an interaction term was significant.

Air Voids by Lift

Rather than analyzing the data for the overall core, this analysis focused on the air voids for each core lift. The variables used in this analysis, and the defined data set of 233 samples, is described in Table 29. The air voids in the analysis were measured from each core lift with the bulk SSD method (as opposed to using the CT scan data). The model was built considering all main effects and two-way interactions. All main effects were kept in the model, but insignificant interactions were removed.

Table 29. Analysis of Core Air Voids (By Lift).

Response Variable	Predictor Variables	Factor Levels/Range
Lift air voids, bulk SSD (%)	Project	• TYL-US 259 • ATL-US 59 • DAL-SH 121, Detour • DAL-SH 121, Shoulder
	Lift thickness*/NMAS	• 4.7 to 13.7
	Screed setting	• Tamper bar • Vibratory only
	Breakdown roller passes	• 3 to 6

Sample Size: 233
** Used actual core thickness.*

Air Voids Uniformity

One concern about placing thick lifts is whether the contractor can achieve adequate compaction at the bottom of the lift. An analysis of the air voids at the bottom of the lift versus the lift thickness was performed. Specifically, the response variable was the ratio of the air voids at the bottom of the lift to the overall air voids of the core. A ratio of 2, for example, means that the air voids at the bottom are twice as high as the overall average, and a ratio of 1 means the bottom air voids are the same as the overall average. The predictor variables and the defined data

set of 235 samples are shown in Table 30. The model was built considering predictor and main variables and all two-way interactions.

Table 30. Analysis of Core Air Voids Uniformity.

Response Variable	Predictor Variables	Factor Levels/Range
Ratio of air voids at bottom to overall	Project	• TYL-US 259 • ATL-US 59 • DAL-SH 121, Detour • DAL-SH 121, Shoulder
	Lift thickness	• 3 to 10 inches
	Lift	• Top • Bottom
	Screed setting	• Tamper bar • Vibratory only
	Breakdown roller passes	• 3 to 6

Sample Size: 235

AIR VOIDS FROM THE PAVESCAN RDM

A MANCOVA was done to determine the influence of key factors on air void content predicted with the PaveScan SCM and calibration equations. The predictor variables and the defined data set of 193,032 samples are shown in Table 31. The model was built considering predictor variables as main effects and all two-way interactions using stepwise regression.

Table 31. Analysis of Air Voids from the PaveScan RDM.

Response Variable	Predictor Variables	Factor Levels/Range
Air voids of the top layer, predicted by PaveScan RDM.	Project	• TYL-US 259 • ATL-US 59 • DAL-SH 121, Detour • DAL-SH 121, Shoulder
	Lift t/NMAS	• 4.7 to 13.7
	Screed setting	• Tamper bar • Vibratory only
	Breakdown roller passes	• 3 to 6

Sample Size: 193,032

REFLECTION AMPLITUDE FROM THE 3D RADAR

A MANCOVA was performed on the reflection amplitudes at mid-depth. The analysis would show if the bond interface was significantly different than the middle of the single-lift layer. The predictor variables and the defined data set of 22 samples are shown in Table 32. The model was built with predictor variables as main effects with no interactions.

Table 32. Analysis of Reflection Amplitude from the 3D Radar.

Response Variable	Predictor Variables	Factor Levels/Range
Average reflection amplitude at mid-depth	Project	• TYL-US 259 • ATL-US 59 • DAL-SH 121, Detour • DAL-SH 121, Shoulder
	Interface type	• Middle, no interface • Middle, interface
	Screed setting	• Tamper bar • Vibratory only
	Breakdown roller passes	• 3 to 6

Sample Size: 22

MECHANICAL PROPERTIES FROM CORES

A MANCOVA was performed on the resilient modulus and cracking (CT) index of the sampled cores. The analysis would show the relationship of these mechanical properties and the air voids. The predictor variables and the defined data set of 54 cores are shown in Table 33. The model was built with predictor variables as main effects and the *Project * Air Voids* interaction effect.

Table 33. Analysis of Core Mechanical Properties.

Response Variables	Predictor Variables	Factor Levels/Range
Resilient Modulus (ksi) and CT Index	Project	• TYL-US 259 • ATL-US 59 • DAL-SH 121, Shoulder
	Air Voids (%)	• 2.6 to 8.3

Sample Size: 22

ROUGHNESS

The effect of lift thickness and paver type on profile roughness was analyzed. Data from three projects (excluding DAL-SH 121 Detour) were collected over each section. The predictor variables and the defined data set of 12 samples are shown in Table 34. The model was built considering predictor and main variables and all two-way interactions.

Table 34. Analysis of Profile Roughness.

Response Variable	Predictor Variables	Factor Levels/Range
International roughness index	Project	• TYL-US 259 • ATL-US 59 • DAL-SH 121, Shoulder
	Number of lifts	• 1 lift • 2 lifts
	Screed setting	• Tamper bar • Vibratory only

Sample Size: 12

APPENDIX E:

DETAILED STATISTICAL ANALYSIS RESULTS

COOLDOWN TIME

Actual by Predicted Plot

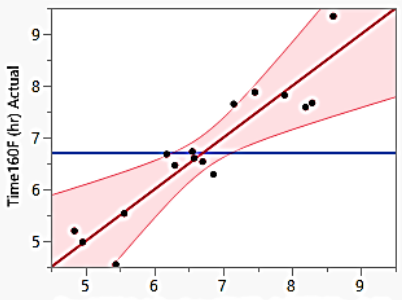

Effect Summary

Source	LogWorth	PValue
Location	2.763	0.00173
Lift Thickness (in)	2.406	0.00393
Project2	1.843	0.01434
MaxTemp_Pred (F)	0.409	0.39014

Remove Add Edit Undo FDR

Residual by Predicted Plot

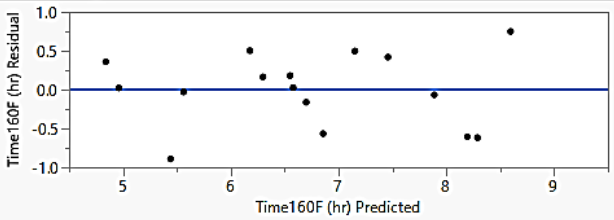

Summary of Fit

RSquare	0.859868
RSquare Adj	0.766447
Root Mean Square Error	0.607748
Mean of Response	6.72077
Observations (or Sum Wgts)	16

Analysis of Variance

Source	DF	Sum of Squares	Mean Square	F Ratio
Model	6	20.397825	3.39964	9.2042
Error	9	3.324215	0.36936	Prob > F
C. Total	15	23.722040		0.0020*

Parameter Estimates

Term	Estimate	Std Error	t Ratio	Prob>|t|
Intercept	7.2841952	6.155711	1.18	0.2670
Lift Thickness (in)	0.7840304	0.203851	3.85	0.0039*
MaxTemp_Pred (F)	-0.019832	0.021966	-0.90	0.3901
Location[Bottom of Lift]	0.7483516	0.263162	2.84	0.0193*
Location[Middle of Lift]	1.0549452	0.263162	4.01	0.0031*
Location[Surface]	-0.841232	0.263162	-3.20	0.0109*
Project2[DAL-SH121]	-1.167765	0.385923	-3.03	0.0143*

Effect Tests

Source	Nparm	DF	Sum of Squares	F Ratio	Prob > F
Lift Thickness (in)	1	1	5.463694	14.7924	0.0039*
MaxTemp_Pred (F)	1	1	0.301070	0.8151	0.3901
Location	3	3	13.224718	11.9349	0.0017*
Project2	1	1	3.381866	9.1561	0.0143*

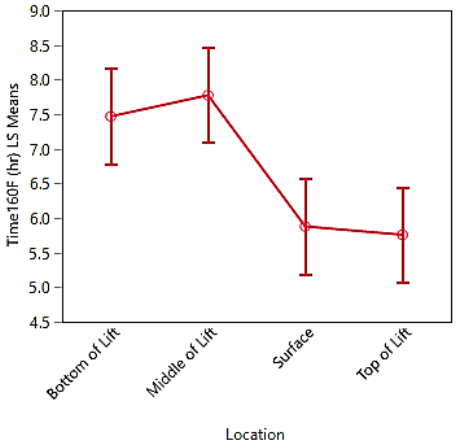

AIR VOIDS DURING CONSTRUCTION

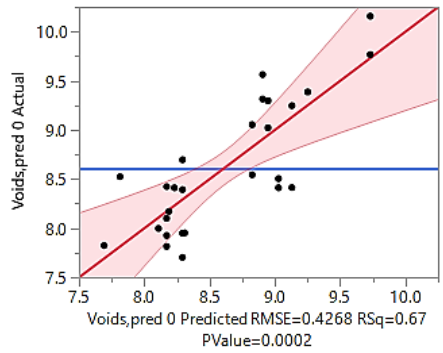

Effect Summary

Source	LogWorth	PValue
Project	4.244	0.00006
Lift Thickness	2.491	0.00323
Screed Setting	0.326	0.47247

Residual by Predicted Plot

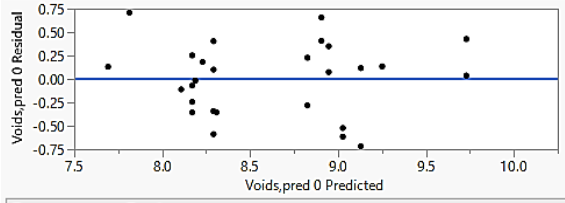

Parameter Estimates

Term	Estimate	Std Error	t Ratio	Prob>|t|
Intercept	9.5364435	0.259601	36.73	<.0001*
Project[ATL-US59]	0.6111837	0.160455	3.81	0.0010*
Project[DAL-SH121 Dtr]	0.2276129	0.16732	1.36	0.1881
Project[DAL-SH121 Shldr]	-0.012075	0.150062	-0.08	0.9366
Lift Thickness	-0.159538	0.048012	-3.32	0.0032*
Screed Setting[Tamper Bar]	0.0606411	0.082882	0.73	0.4725

Summary of Fit

RSquare	0.415919
RSquare Adj	0.365495
Root Mean Square Error	0.856882
Mean of Response	5.908917
Observations (or Sum Wgts)	152

Lift Thickness

Leverage Plot

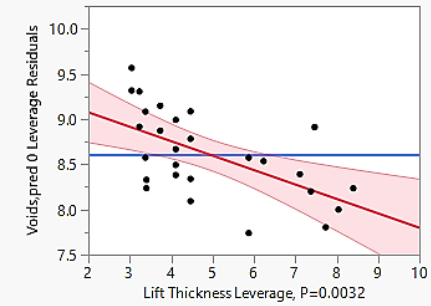

Project

Leverage Plot

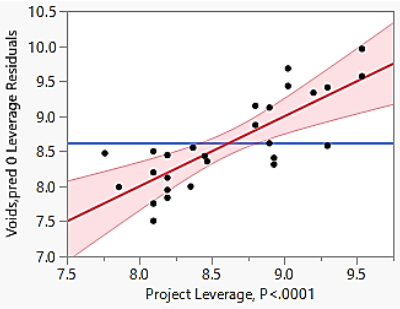

Least Squares Means Table

Level	Least Sq Mean	Std Error	Mean
ATL-US59	9.3676616	0.19157870	9.39397
DAL-SH121 Dtr	8.9840908	0.19400701	8.70047
DAL-SH121 Shldr	8.7444026	0.17552418	8.67350
TYL-SH259	7.9297564	0.14846342	8.13538

Screed Setting

Leverage Plot

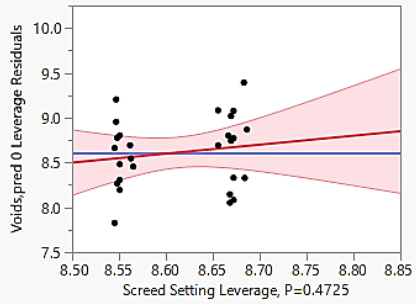

Least Squares Means Table

Level	Least Sq Mean	Std Error	Mean
Tamper Bar	8.8171190	0.11552392	8.72687
Vibratory	8.6958367	0.12275303	8.49164

OVERALL AIR VOIDS

Actual by Predicted Plot

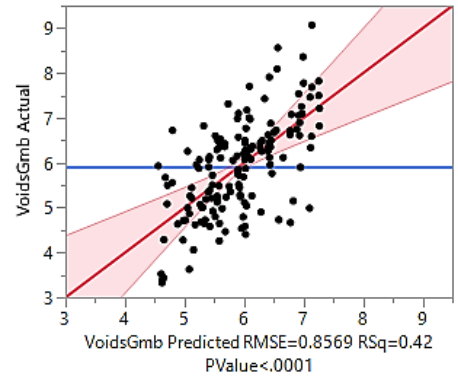

Residual by Predicted Plot

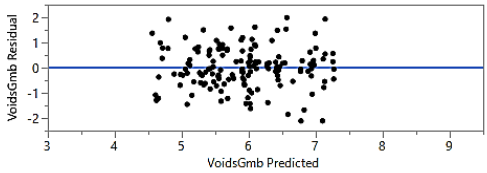

Summary of Fit

RSquare	0.665903
RSquare Adj	0.586356
Root Mean Square Error	0.426756
Mean of Response	8.61361
Observations (or Sum Wgts)	27

Effect Summary

Source	LogWorth	PValue
RollerPasses	8.556	0.00000
Project{ATL-US59-DAL-SH121 Shldr}	5.112	0.00001
NumLifts*RollerPasses	4.449	0.00004
T_LiftActual_NMAS_Ratio*Project{DAL-SH121 Dtr-TYL-SH259}	4.210	0.00006
RollerPasses*T_LiftActual_NMAS_Ratio	3.368	0.00043
RollerPasses*Project{ATL-US59-DAL-SH121 Shldr}	3.094	0.00081
ScreedSetting	3.084	0.00082
T_LiftActual_NMAS_Ratio	1.932	0.01170 ^
NumLifts*Project{ATL-US59-DAL-SH121 Shldr}	1.866	0.01361
NumLifts	1.844	0.01432 ^
Project{DAL-SH121 Dtr-TYL-SH259}	1.296	0.05053 ^
Project{DAL-SH121 Dtr&TYL-SH259-ATL-US59&DAL-SH121 Shldr}	0.840	0.14451

Parameter Estimates

Term	Estimate	Std Error	t Ratio	Prob>|t|
Intercept	8.9370338	1.232033	7.25	<.0001*
Project{DAL-SH121 Dtr&TYL-SH259-ATL-US59&DAL-SH121 Shldr}	-0.135535	0.09236	-1.47	0.1445
Project{DAL-SH121 Dtr-TYL-SH259}	0.2569072	0.130239	1.97	0.0505
Project{ATL-US59-DAL-SH121 Shldr}	-0.727991	0.156652	-4.65	<.0001*
NumLifts[2-1]	1.2412484	0.500433	2.48	0.0143*
ScreedSetting[Tamper Bar]	0.2422993	0.070856	3.42	0.0008*
RollerPasses	-1.316396	0.20714	-6.36	<.0001*
T_LiftActual_NMAS_Ratio	0.2346416	0.091843	2.55	0.0117*
NumLifts[2-1]*(RollerPasses-4.39474)	1.5832918	0.370506	4.27	<.0001*
(RollerPasses-4.39474)*(T_LiftActual_NMAS_Ratio-8.74531)	0.2470012	0.068453	3.61	0.0004*
(T_LiftActual_NMAS_Ratio-8.74531)*(Project{DAL-SH121 Dtr-TYL-SH259}+0.15789)	-0.194842	0.047144	-4.13	<.0001*
(RollerPasses-4.39474)*(Project{ATL-US59-DAL-SH121 Shldr}+0.10526)	-0.35817	0.104539	-3.43	0.0008*
NumLifts[2-1]*(Project{ATL-US59-DAL-SH121 Shldr}+0.10526)	0.5291717	0.211735	2.50	0.0136*

AICc	BIC
401.8788	441.1474

RollerPasses

Leverage Plot

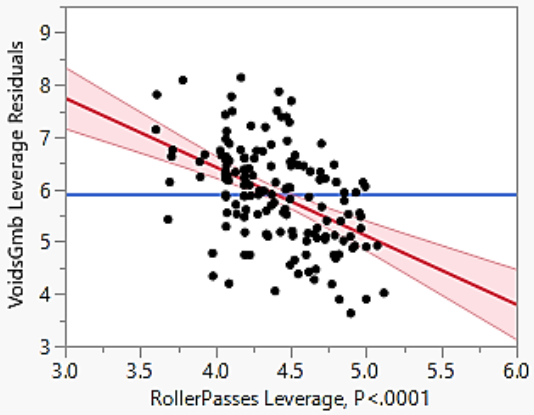

NumLifts*RollerPasses

Leverage Plot

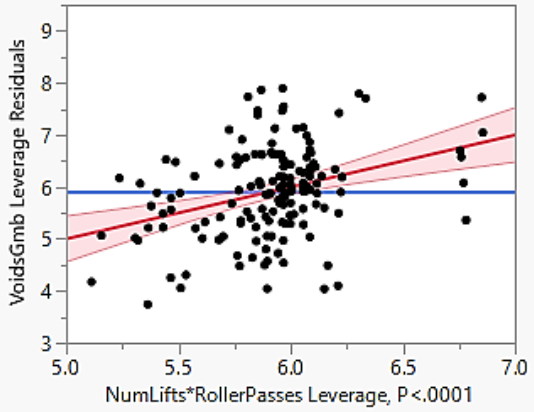

RollerPasses*T_LiftActual_NMAS_Ratio

Leverage Plot

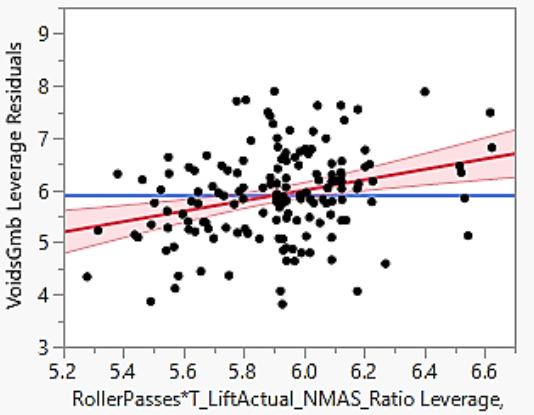

Project{ATL-US59-DAL-SH121 Shldr}

Leverage Plot

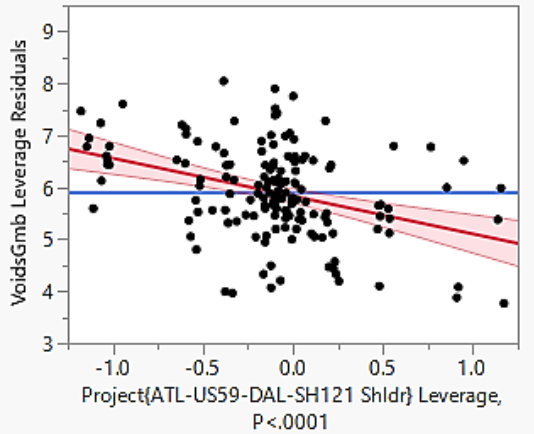

T_LiftActual_NMAS_Ratio*Project{DAL-SH121

Leverage Plot

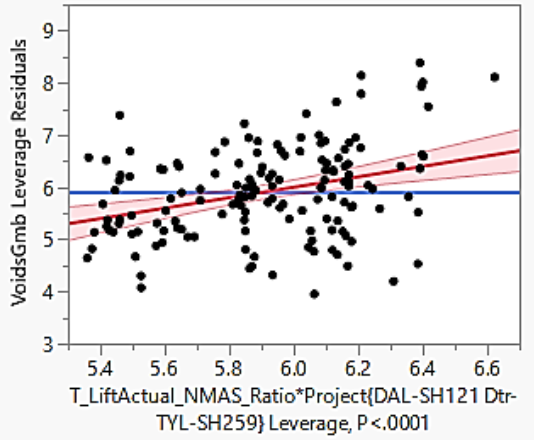

RollerPasses*Project{ATL-US59-DAL-SH121 Shldr}

Leverage Plot

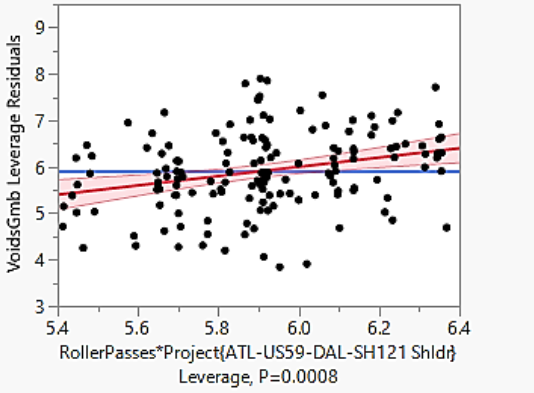

ScreedSetting

Leverage Plot

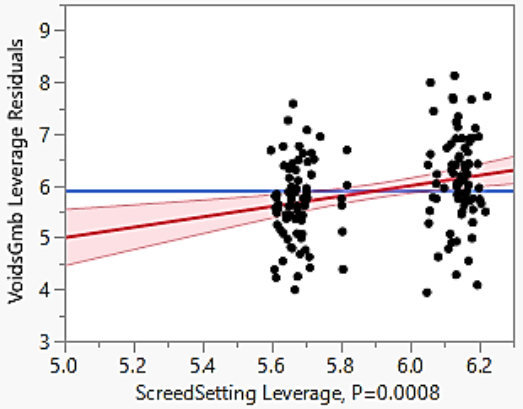

Least Squares Means Table

Level	Least Sq Mean	Std Error	Mean
Tamper Bar	5.4893324	0.27859160	6.18228
Vibratory	5.0047338	0.29753797	5.63556

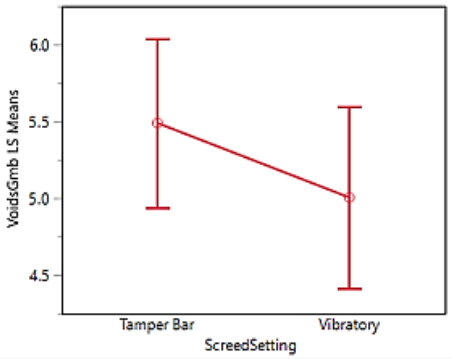

T_LiftActual_NMAS_Ratio

Leverage Plot

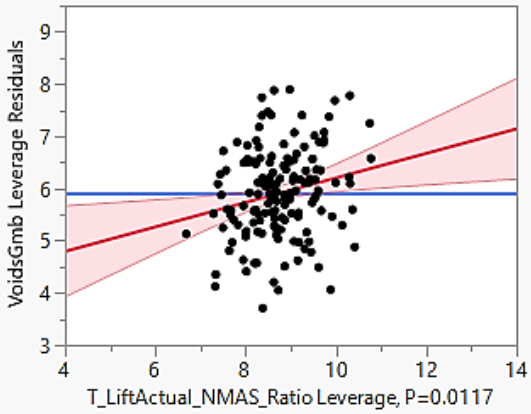

NumLifts*Project{ATL-US59-DAL-SH121 Shldr}

Leverage Plot

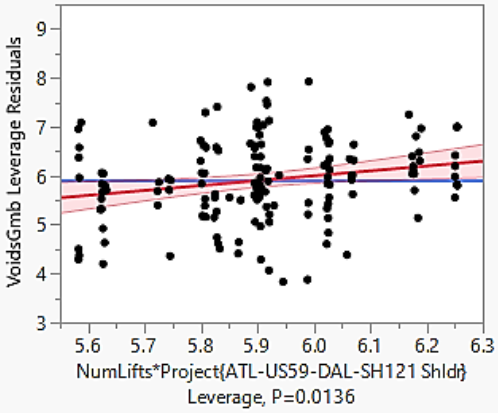

NumLifts

Leverage Plot

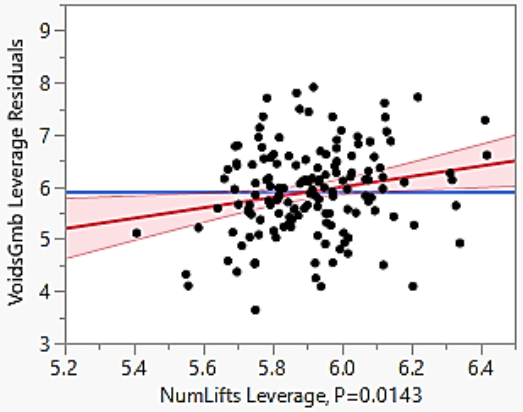

Least Squares Means Table

Level	Least Sq Mean	Std Error	Mean
1	5.2470331	0.27937514	5.82268
2	6.4882815	0.24440151	5.98254

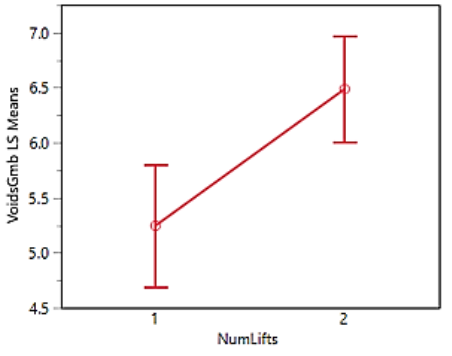

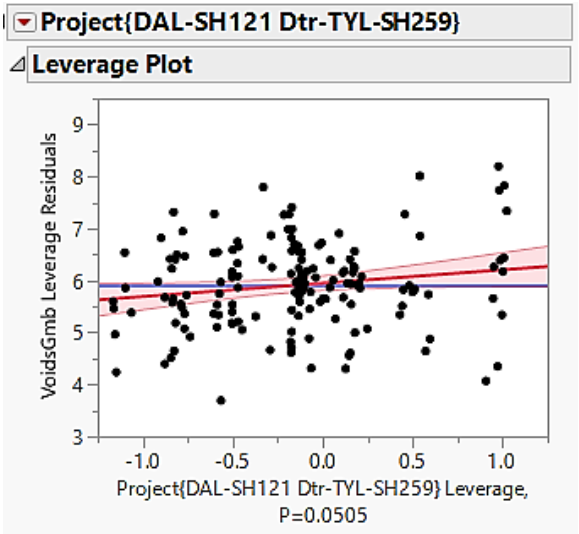

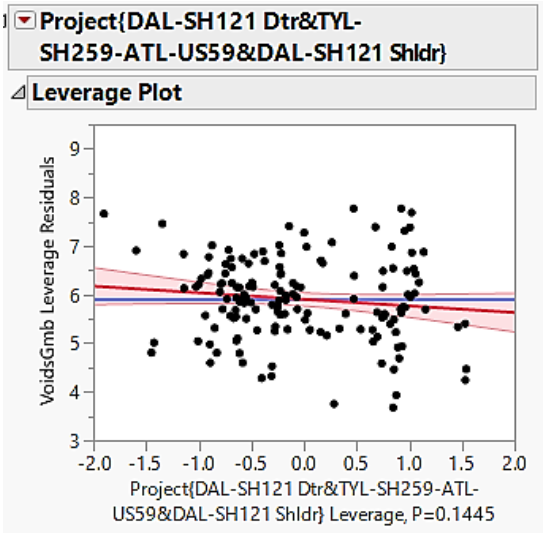

AIR VOID UNIFORMITY ANALYSIS

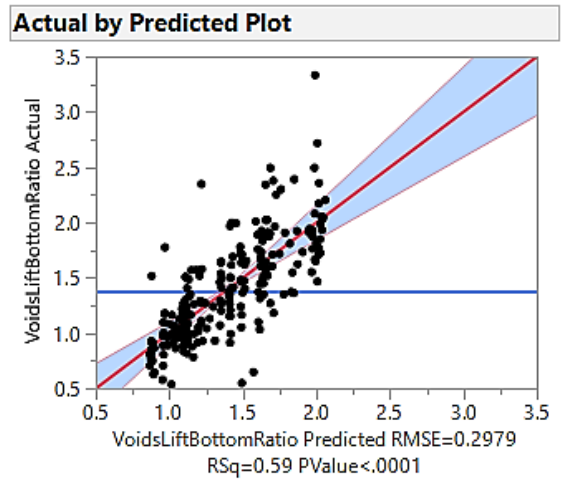

Effect Summary

Source	LogWorth	PValue
ThicknessLift	14.446	0.00000
Lift	5.620	0.00000
Project	5.251	0.00001
Project*Lift	4.017	0.00010
Project*ThicknessLift	3.909	0.00012

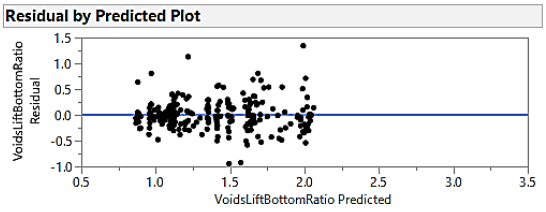

Summary of Fit	
RSquare	0.588995
RSquare Adj	0.568721
Root Mean Square Error	0.297907
Mean of Response	1.382151
Observations (or Sum Wgts)	235

Parameter Estimates

Term	Estimate	Std Error	t Ratio	Prob>|t|
Intercept	0.7488408	0.06763	11.07	<.0001*
ThicknessLift	0.1251345	0.014794	8.46	<.0001*
Project[ATL-US59]	0.18619	0.047864	3.89	0.0001*
Project[DAL-SH121 Dtr]	-0.203712	0.054209	-3.76	0.0002*
Project[DAL-SH121 Shldr]	0.1070595	0.038361	2.79	0.0057*
Lift[Bottom]	-0.127176	0.026264	-4.84	<.0001*
Project[ATL-US59]*Lift[Bottom]	0.1677705	0.044326	3.78	0.0002*
Project[DAL-SH121 Dtr]*Lift[Bottom]	0.028642	0.049072	0.58	0.5600
Project[DAL-SH121 Shldr]*Lift[Bottom]	-0.135076	0.040075	-3.37	0.0009*
Project[ATL-US59]*(ThicknessLift-4.66468)	0.1323378	0.028765	4.60	<.0001*
Project[DAL-SH121 Dtr]*(ThicknessLift-4.66468)	-0.025646	0.023393	-1.10	0.2741
Project[DAL-SH121 Shldr]*(ThicknessLift-4.66468)	-0.035079	0.020569	-1.71	0.0895

Lift Thickness

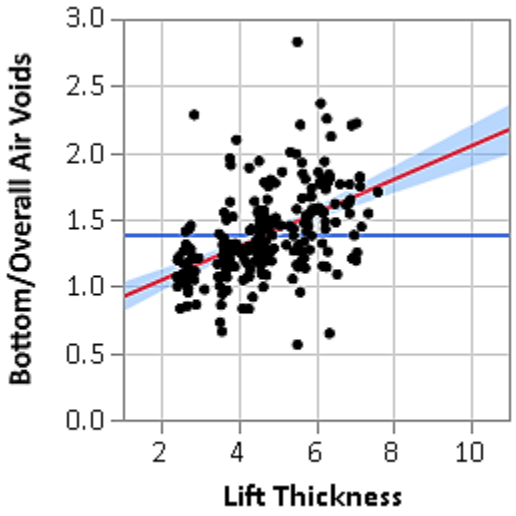

Lift

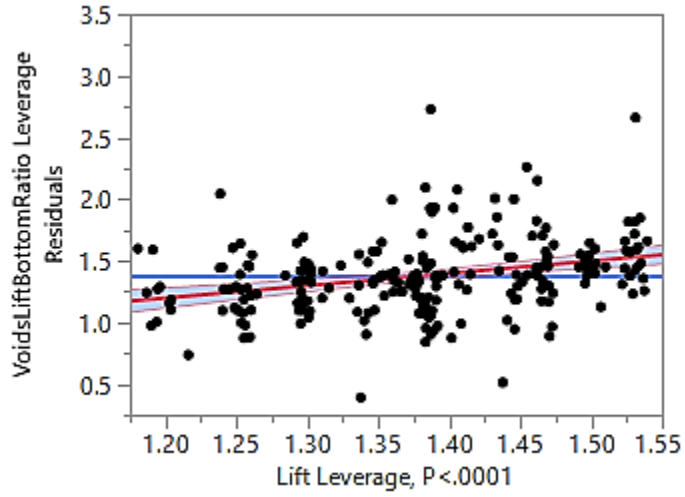

Least Squares Means Table

Level	Least Sq Mean	Std Error	Mean
Bottom	1.2053765	0.04470604	1.04658
Top	1.4597287	0.03016844	1.55865

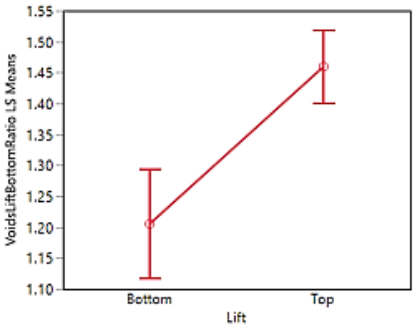

Project

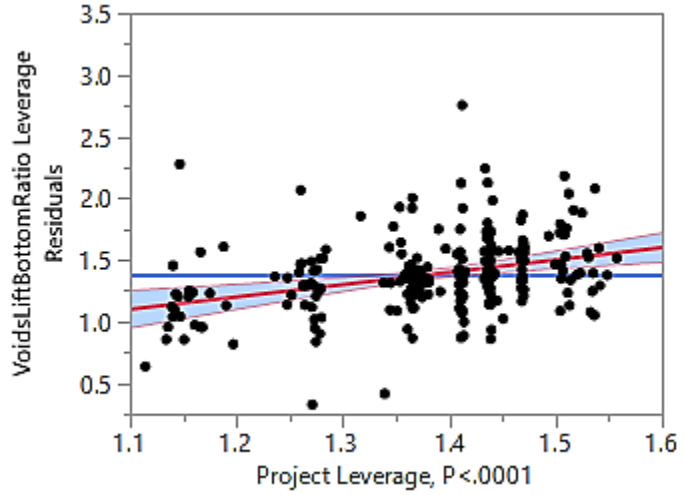

Least Squares Means Table

Level	Least Sq Mean	Std Error	Mean
ATL-US59	1.5187426	0.05525223	1.32836
DAL-SH121 Dtr	1.1288404	0.06593945	1.34311
DAL-SH121 Shldr	1.4396122	0.03760295	1.59563
TYL-SH259	1.2430154	0.05846740	1.23024

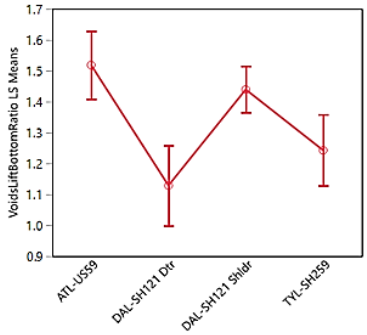

Project*Lift

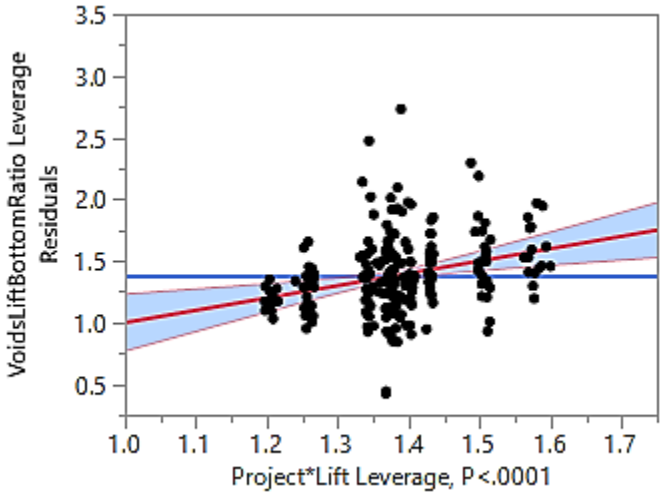

Level	Least Sq Mean	Std Error
ATL-US59,Bottom	1.5593370	0.09133251
ATL-US59,Top	1.4781483	0.05351520
DAL-SH121 Dtr,Bottom	1.0303062	0.09110888
DAL-SH121 Dtr,Top	1.2273745	0.08525271
DAL-SH121 Shldr,Bottom	1.1773599	0.06258077
DAL-SH121 Shldr,Top	1.7018645	0.05075997
TYL-SH259,Bottom	1.0545030	0.10686098
TYL-SH259,Top	1.4315277	0.04305436

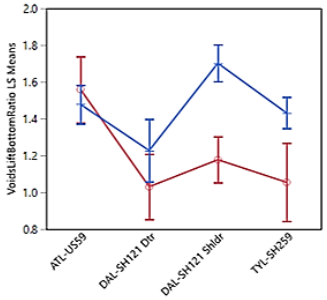

Project*Lift Thickness

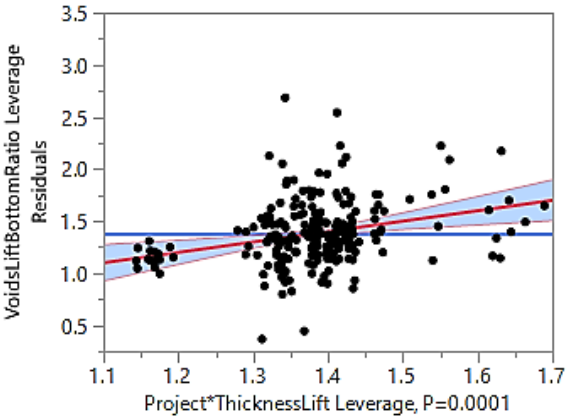

PAVESCAN RDM AIR VOIDS ANALYSIS

Actual by Predicted Plot

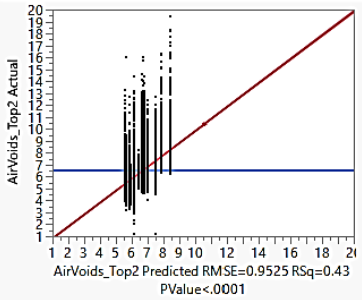

Effect Summary

Source	LogWorth	PValue
T-Lift_NMAS_Ratio	14581.59	0.00000
Project	3882.771	0.00000
RollerPasses	639.575	0.00000
T-Lift_NMAS_Ratio*RollerPasses	487.396	0.00000
ScreedSetting	6.775	0.00000

Remove Add Edit Undo FDR

Residual by Predicted Plot

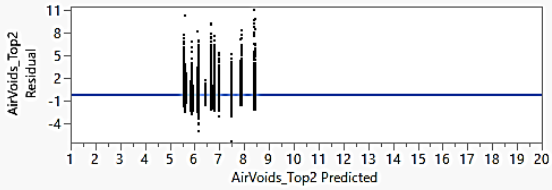

Summary of Fit

RSquare	0.432657
RSquare Adj	0.432636
Root Mean Square Error	0.952534
Mean of Response	6.641706
Observations (or Sum Wgts)	193030

Analysis of Variance

Source	DF	Sum of Squares	Mean Square	F Ratio
Model	7	133556.52	19079.5	21028.41
Error	193022	175132.80	0.90732	Prob > F
C. Total	193029	308689.32		<.0001*

Parameter Estimates

Term	Estimate	Std Error	t Ratio	Prob>|t|
Intercept	8.4255816	0.012986	648.83	<.0001*
T-Lift_NMAS_Ratio	-0.239845	0.000846	-283.4	<.0001*
Project[ATL-US59]	-0.203509	0.004191	-48.56	<.0001*
Project[DAL-SH121 Dtr]	0.3922151	0.007444	52.69	<.0001*
Project[DAL-SH121 Shldr]	0.2859853	0.004553	62.81	<.0001*
RollerPasses	0.1248267	0.002295	54.40	<.0001*
(T-Lift_NMAS_Ratio-9.18508)*(RollerPasses-4.36633)	-0.038158	0.000805	-47.43	<.0001*
ScreedSetting[Tamper Bar]	-0.011512	0.0022	-5.23	<.0001*

Effect Tests

Source	Nparm	DF	Sum of Squares	F Ratio	Prob > F
T-Lift_NMAS_Ratio	1	1	72854.337	80296.15	<.0001*
Project	3	3	17008.083	6248.466	<.0001*
RollerPasses	1	1	2685.105	2959.379	<.0001*
T-Lift_NMAS_Ratio*RollerPasses	1	1	2040.914	2249.386	<.0001*
ScreedSetting	1	1	24.836	27.3732	<.0001*

T-Lift_NMAS_Ratio

Leverage Plot

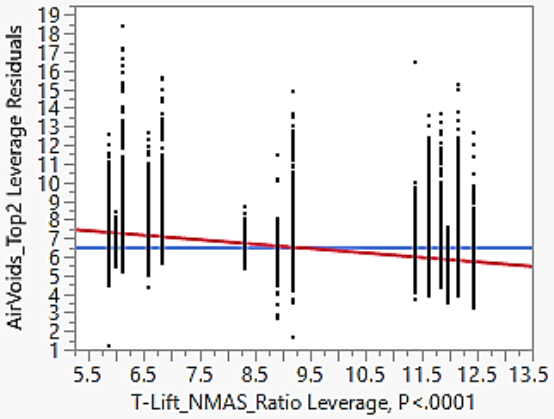

Project

Leverage Plot

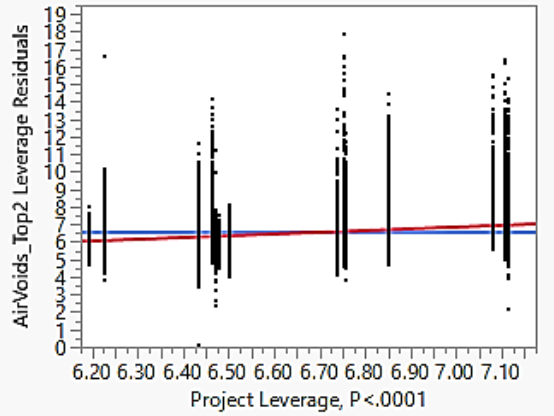

Least Squares Means Table

Level	Least Sq Mean	Std Error	Mean
ATL-US59	6.5647880	0.00405623	6.60337
DAL-SH121 Dtr	7.1586551	0.00954520	6.14389
DAL-SH121 Shldr	7.0535260	0.00443447	7.44120
TYL-SH259	6.2913793	0.00394212	6.10803

RollerPasses

Leverage Plot

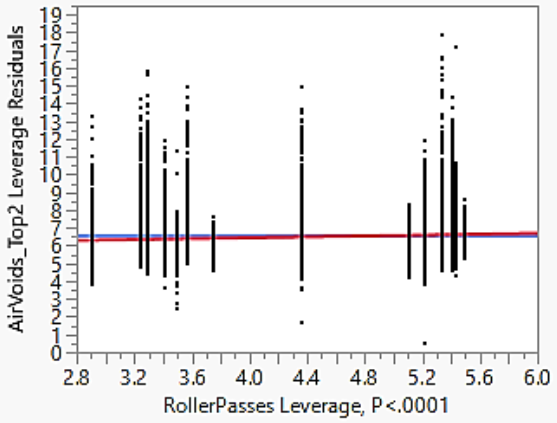

ScreedSetting

Leverage Plot

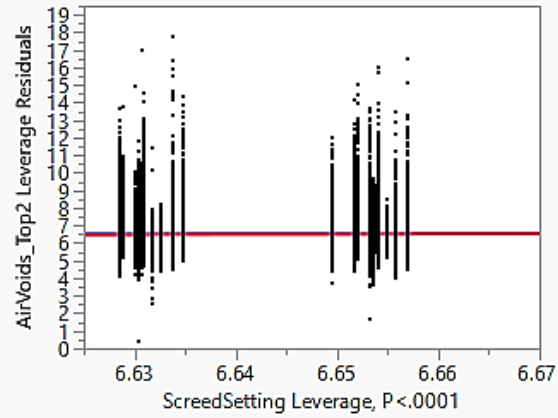

Least Squares Means Table

Level	Least Sq Mean	Std Error	Mean
Tamper Bar	6.7561128	0.00354566	6.62352
Vibratory	6.7791367	0.00367098	6.66096

T-Lift_NMAS_Ratio*RollerPasses

Leverage Plot

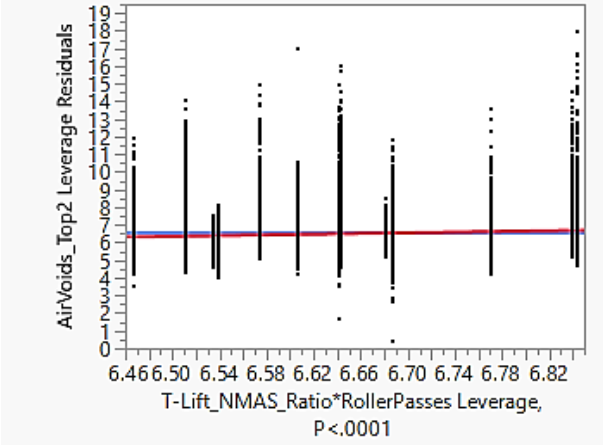

3D RADAR AMPLITUDE ANALYSIS

Actual by Predicted Plot

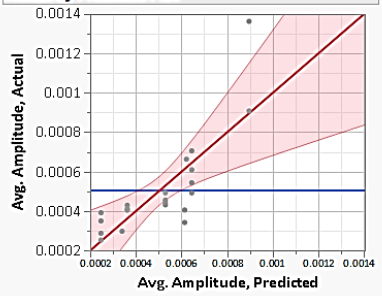

Effect Summary

Source	LogWorth	PValue
Interface Type 2	3.109	0.00078
Project of By Interface No Formulas	1.793	0.01610

Remove Add Edit Undo FDR

Residual by Predicted Plot

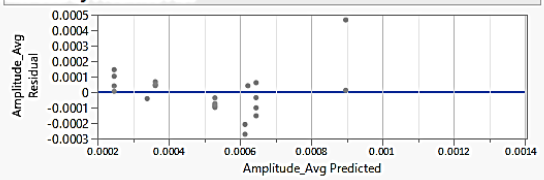

Summary of Fit

RSquare	0.640838
RSquare Adj	0.556329
Root Mean Square Error	0.000162
Mean of Response	0.000505
Observations (or Sum Wgts)	22

Analysis of Variance

Source	DF	Sum of Squares	Mean Square	F Ratio
Model	4	8.00012e-7	0.0000002	7.5831
Error	17	4.48372e-7	2.6375e-8	Prob > F
C. Total	21	1.24838e-6		0.0011*

Parameter Estimates

Term	Estimate	Std Error	t Ratio	Prob>|t|
Intercept	0.0005318	4.06e-5	13.10	<.0001*
Project of By Interface No Formulas[SH 121]	-2.823e-5	5.742e-5	-0.49	0.6292
Project of By Interface No Formulas[SH 121_10]	0.0002233	7.032e-5	3.18	0.0055*
Project of By Interface No Formulas[US 59]	-0.000144	5.742e-5	-2.50	0.0228*
Interface Type 2[Interface]	0.0001413	3.462e-5	4.08	0.0008*

Effect Tests

Source	Nparm	DF	Sum of Squares	F Ratio	Prob > F
Project of By Interface No Formulas	3	3	3.60822e-7	4.5602	0.0161*
Interface Type 2	1	1	4.3919e-7	16.6518	0.0008*

Project of By Interface No Formulas

Leverage Plot

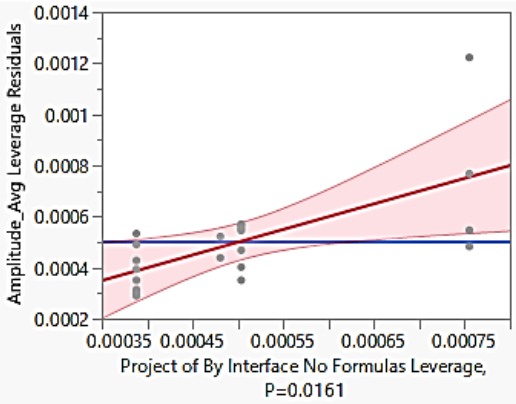

Least Squares Means Table

Level	Least Sq Mean	Std Error	Mean
SH 121	0.00050358	0.00005742	0.000504
SH 121_10	0.00075509	0.00008120	0.000755
US 59	0.00038804	0.00005742	0.000388
US 259	0.00048053	0.00011484	0.000481

Interface Type 2

Leverage Plot

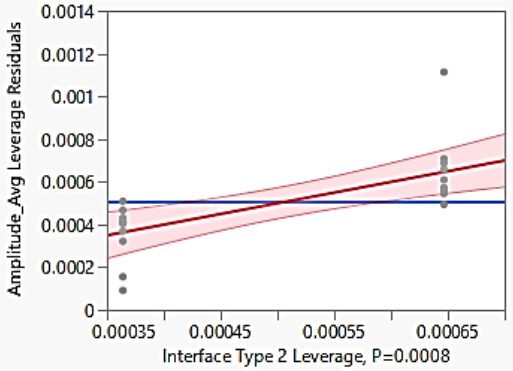

Least Squares Means Table

Level	Least Sq Mean	Std Error	Mean
Interface	0.00067310	0.00005336	0.000646
Middle	0.00039052	0.00005336	0.000364

MECHANICAL PROPERTIES—RESILIENT MODULUS

Actual by Predicted Plot

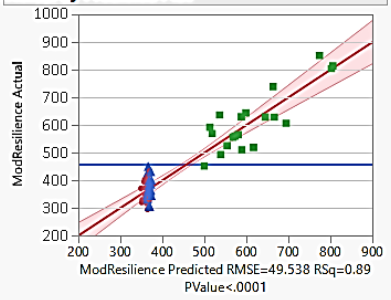

Effect Summary

Source	LogWorth	PValue
Project	23.027	0.00000
Project*VoidsMechGmb	7.582	0.00000
VoidsMechGmb	7.024	0.00000 ^

Remove Add Edit ☐ FDR ('^' denotes effects with containing effects above them)

Residual by Predicted Plot

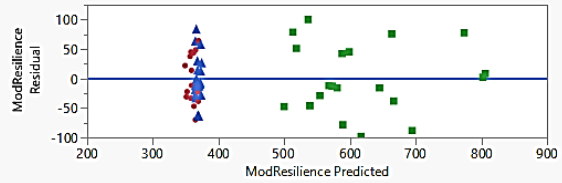

Summary of Fit

RSquare	0.890916
RSquare Adj	0.879553
Root Mean Square Error	49.53836
Mean of Response	458.0089
Observations (or Sum Wgts)	54

Analysis of Variance

Source	DF	Sum of Squares	Mean Square	F Ratio
Model	5	962057.8	192412	78.4057
Error	48	1177944	2454	Prob > F
C. Total	53	1079852.1		<.0001*

Parameter Estimates

Term	Estimate	Std Error	t Ratio	Prob>|t|
Intercept	657.83803	32.33539	20.34	<.0001*
VoidsMechGmb	-34.78916	5.542462	-6.28	<.0001*
Project[ATL-US59]	-105.264	10.4149	-10.11	<.0001*
Project[DAL-SH121 Shldr]	201.37306	10.21682	19.71	<.0001*
Project[ATL-US59]*(VoidsMechGmb-5.56877)	31.194525	6.976047	4.47	<.0001*
Project[DAL-SH121 Shldr]*(VoidsMechGmb-5.56877)	-63.38776	8.867345	-7.15	<.0001*

Effect Tests

Source	Nparm	DF	Sum of Squares	F Ratio	Prob > F
VoidsMechGmb	1	1	96686.44	39.3987	<.0001*
Project	2	2	955167.27	194.6105	<.0001*
Project*VoidsMechGmb	2	2	126014.88	25.6749	<.0001*

VoidsMechGmb

Leverage Plot

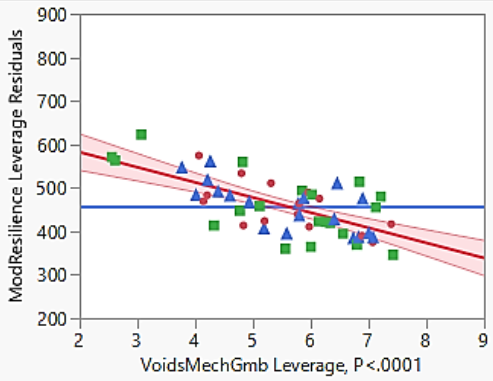

Project

Leverage Plot

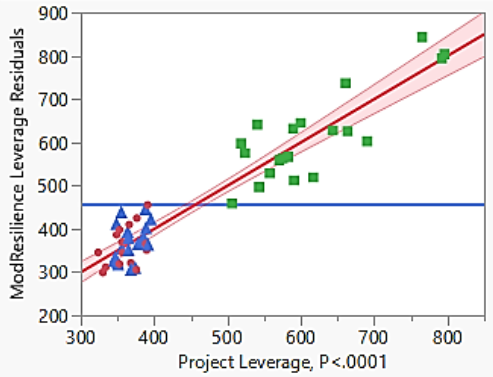

Least Squares Means Table

Level	Least Sq Mean	Std Error	Mean
ATL-US59	358.84106	13.076655	360.173
DAL-SH121 Shldr	665.47816	12.599147	616.320
TYL-SH259	367.99608	11.554129	368.605

Project*VoidsMechGmb

Leverage Plot

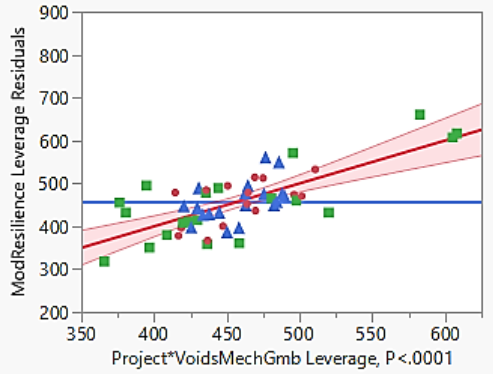

MECHANICAL PROPERTIES—CT INDEX

Actual by Predicted Plot

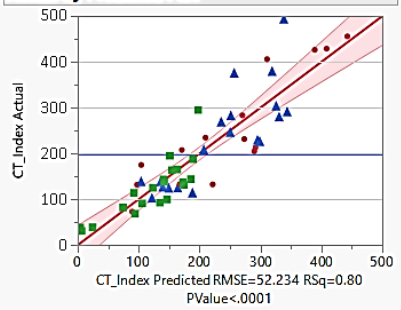

Effect Summary

Source	LogWorth	PValue
VoidsMechGmb	14.930	0.00000
Project	13.228	0.00000

Remove Add Edit Undo FDR

Residual by Predicted Plot

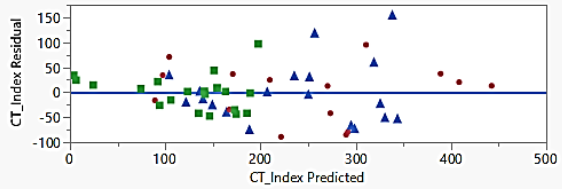

Summary of Fit

RSquare	0.796905
RSquare Adj	0.784719
Root Mean Square Error	52.23375
Mean of Response	197.5255
Observations (or Sum Wgts)	54

Analysis of Variance

Source	DF	Sum of Squares	Mean Square	F Ratio
Model	3	535277.95	178426	65.3967
Error	50	136418.22	2728	Prob > F
C. Total	53	671696.17		<.0001*

Parameter Estimates

Term	Estimate	Std Error	t Ratio	Prob>|t|
Intercept	-140.9696	30.7002	-4.59	<.0001*
Project[ATL-US59]	67.438391	10.73477	6.28	<.0001*
Project[DAL-SH121 Shldr]	-111.8209	10.25381	-10.91	<.0001*
VoidsMechGmb	62.053393	5.394422	11.50	<.0001*

Effect Tests

Source	Nparm	DF	Sum of Squares	F Ratio	Prob > F
Project	2	2	324911.47	59.5433	<.0001*
VoidsMechGmb	1	1	361030.32	132.3248	<.0001*

Project

Leverage Plot

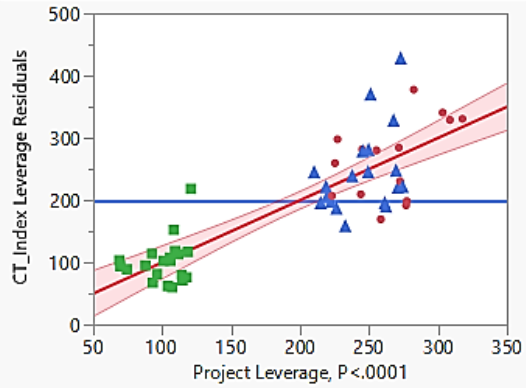

Least Squares Means Table

Level	Least Sq Mean	Std Error	Mean
ATL-US59	272.03008	13.634085	249.031
DAL-SH121 Shldr	92.77084	11.988077	123.842
TYL-SH259	248.97415	12.049808	234.425

VoidsMechGmb

Leverage Plot

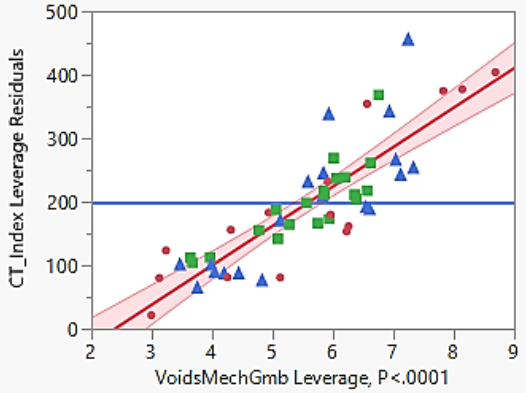

PROFILE ROUGHNESS ANALYSIS

Actual by Predicted Plot

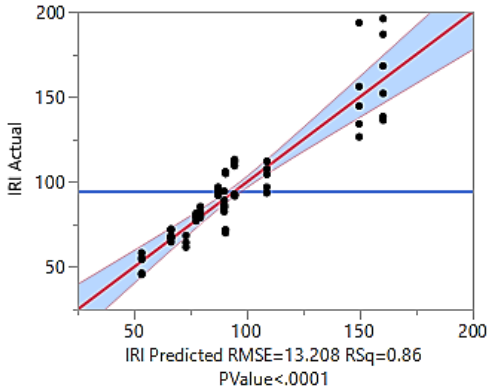

Analysis of Variance

Source	DF	Sum of Squares	Mean Square	F Ratio
Model	8	66768.229	8346.03	47.8398
Error	63	10990.849	174.46	Prob > F
C. Total	71	77759.078		<.0001*

Summary of Fit

RSquare	0.858655
RSquare Adj	0.840707
Root Mean Square Error	13.20825
Mean of Response	94.18979
Observations (or Sum Wgts)	72

Level	Least Sq Mean	Std Error
ATL-US59,Bottom	1.5593370	0.09133251
ATL-US59,Top	1.4781483	0.05351520
DAL-SH121 Dtr,Bottom	1.0303062	0.09110888
DAL-SH121 Dtr,Top	1.2273745	0.08525271
DAL-SH121 Shldr,Bottom	1.1773599	0.06258077
DAL-SH121 Shldr,Top	1.7018645	0.05075997
TYL-SH259,Bottom	1.0545030	0.10686098
TYL-SH259,Top	1.4315277	0.04305436

Effect Summary

Source	LogWorth	PValue
Project*Lifts	18.771	0.00000
Project	17.290	0.00000 ^
Project*Screed	3.615	0.00024
Lifts	2.955	0.00111 ^
Screed	1.892	0.01283 ^

Residual by Predicted Plot

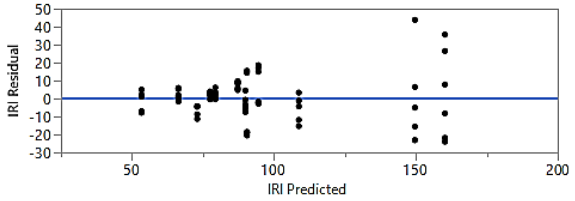

Parameter Estimates

Term	Estimate	Std Error	t Ratio	Prob>|t|
Intercept	94.189792	1.556607	60.51	<.0001*
Screed[Tamper Bar]	-3.98709	1.556607	-2.56	0.0128*
Lifts[1]	-5.321459	1.556607	-3.42	0.0011*
Project[ATL-US 59]	-22.27438	2.201375	-10.12	<.0001*
Project[DAL-SH 121]	25.603379	2.201375	11.63	<.0001*
Project[ATL-US 59]*Lifts[1]	17.393543	2.201375	7.90	<.0001*
Project[DAL-SH 121]*Lifts[1]	-29.84247	2.201375	-13.56	<.0001*
Project[ATL-US 59]*Screed[Tamper Bar]	-2.50666	2.201375	-1.14	0.2591
Project[DAL-SH 121]*Screed[Tamper Bar]	9.2874104	2.201375	4.22	<.0001*

Project*Lifts

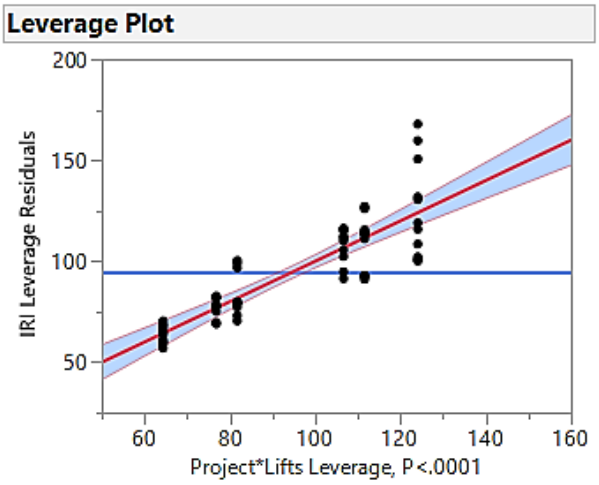

Level	Least Sq Mean	Std Error
ATL-US 59,1	83.98750	3.8128940
ATL-US 59,2	59.84333	3.8128940
DAL-SH 121,1	84.62924	3.8128940
DAL-SH 121,2	154.95710	3.8128940
TYL-SH259,1	97.98826	3.8128940
TYL-SH259,2	83.73332	3.8128940

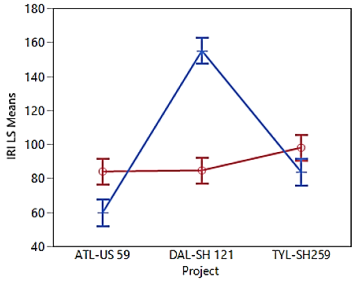

Project

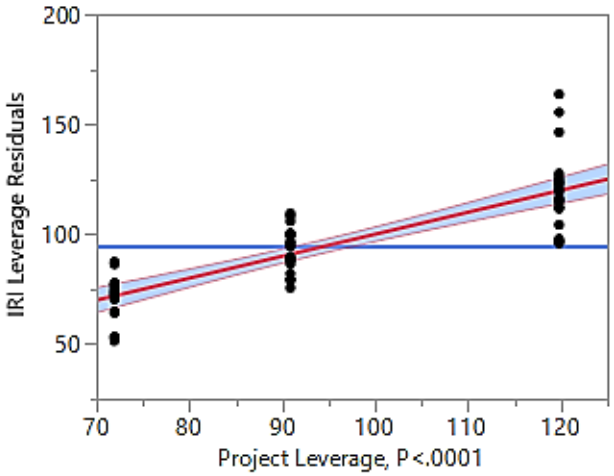

Level	Least Sq Mean	Std Error	Mean
ATL-US 59	71.91542	2.6961232	71.915
DAL-SH 121	119.79317	2.6961232	119.793
TYL-SH259	90.86079	2.6961232	90.861

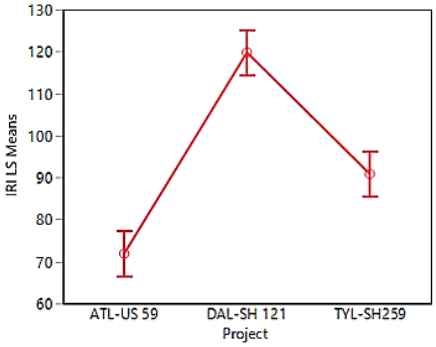

Project*Screed

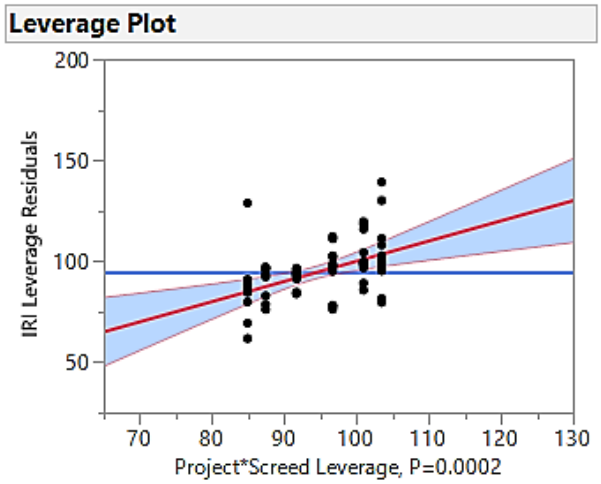

Level	Least Sq Mean	Std Error
ATL-US 59,Tamper Bar	65.42167	3.8128940
ATL-US 59,Vibe Only	78.40917	3.8128940
DAL-SH 121,Tamper Bar	125.09349	3.8128940
DAL-SH 121,Vibe Only	114.49285	3.8128940
TYL-SH259,Tamper Bar	80.09295	3.8128940
TYL-SH259,Vibe Only	101.62863	3.8128940

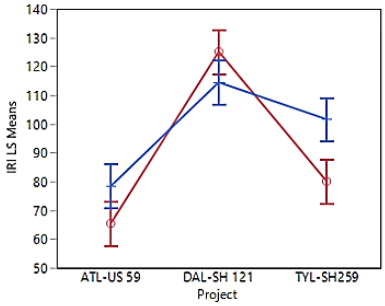

Lifts

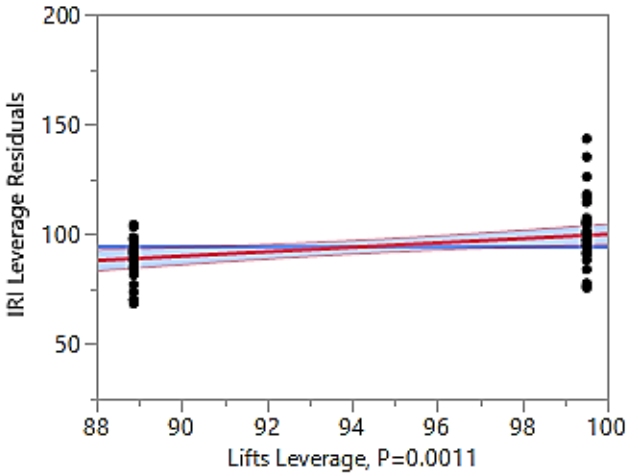

Level	Least Sq Mean	Std Error	Mean
1	88.868333	2.2013754	88.8683
2	99.511251	2.2013754	99.5113

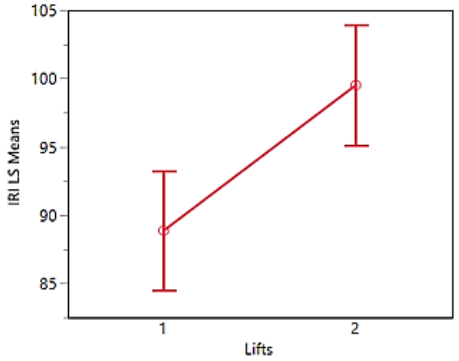

Screed Setting

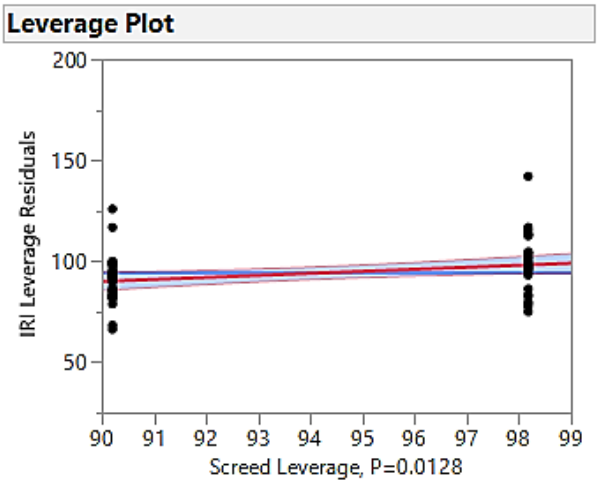

Level	Least Sq Mean	Std Error	Mean
Tamper Bar	90.202702	2.2013754	90.2027
Vibe Only	98.176882	2.2013754	98.1769